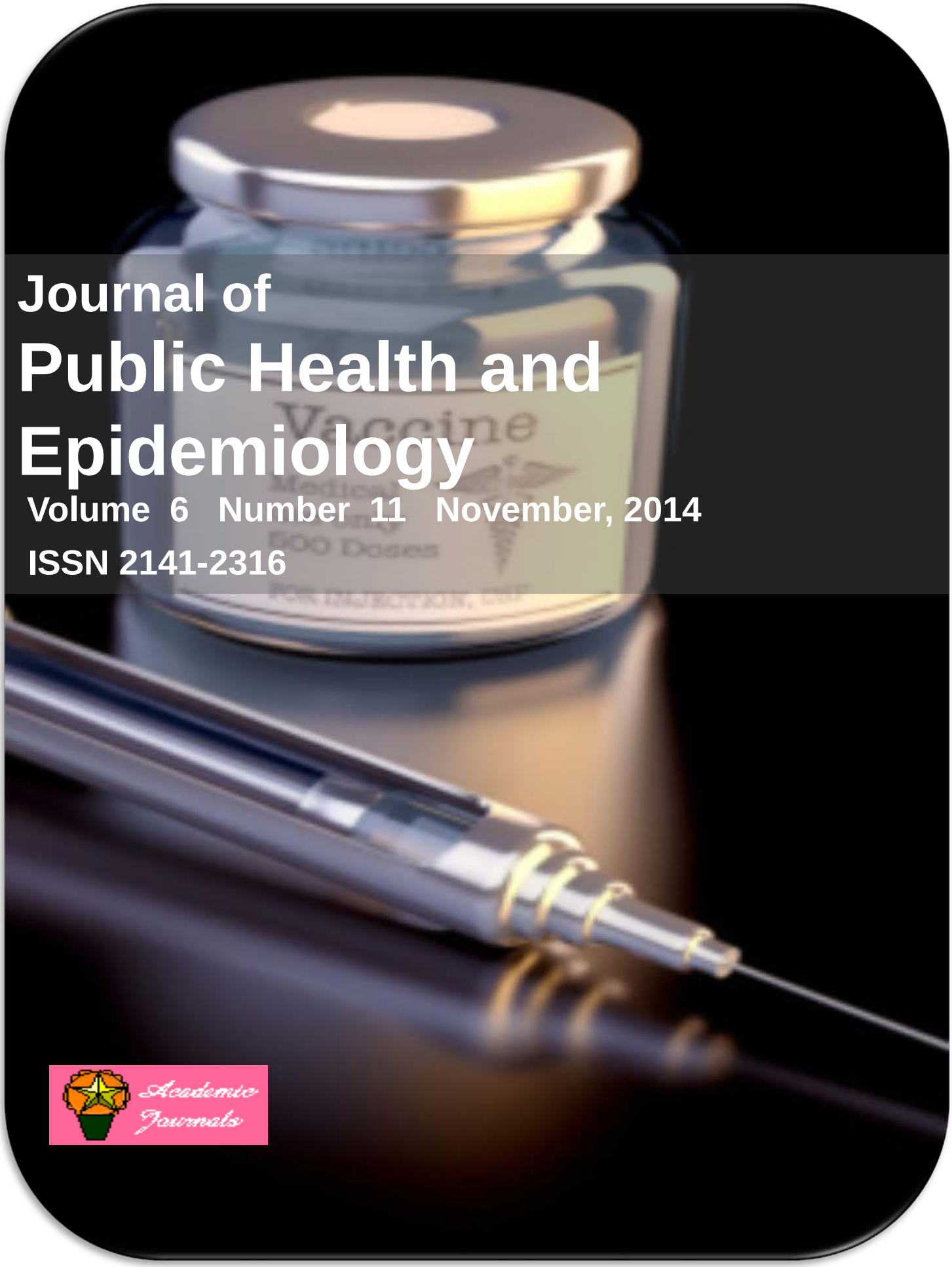

Journal of Public Health and Epidemiology

Volume 6 Number 11 November, 2014

ISSN 2141-2316

Academic Journals

ABOUT JPHE

The **Journal of Public Health and Epidemiology (JPHE)** is published monthly (one volume per year) by Academic Journals.

Journal of Public Health and Epidemiology (JPHE) is an open access journal that provides rapid publication (monthly) of articles in all areas of the subject such as health observatory, biostatistics, occupational health, behavioral medicine etc. The Journal welcomes the submission of manuscripts that meet the general criteria of significance and scientific excellence. Papers will be published shortly after acceptance. All articles published in JPHE are peer-reviewed.

Submission of Manuscript

Submit manuscripts as e-mail attachment to the Editorial Office at: jphe@academicjournals.org. A manuscript number will be mailed to the corresponding author shortly after submission.

The Journal of Public Health and Epidemiology will only accept manuscripts submitted as e-mail attachments.

Please read the **Instructions for Authors** before submitting your manuscript. The manuscript files should be given the last name of the first author.

Editors

Professor Mostafa A. Abolfotouh
Professor of Family & Community Medicine
Head of Medical Team - Biobanking Section.
King Abdullah International Medical Research CEnter, King Saud Bin-Abdulaziz University for Health Sciences, National Guard Health Affairs, Saudi Arabia

Editorial Board

Instructions for Author

Electronic submission of manuscripts is strongly encouraged, provided that the text, tables, and figures are included in a single Microsoft Word file (preferably in Arial font).

The **cover letter** should include the corresponding author's full address and telephone/fax numbers and should be in an e-mail message sent to the Editor, with the file, whose name should begin with the first author's surname, as an attachment.

Article Types

Three types of manuscripts may be submitted:

Regular articles: These should describe new and carefully confirmed findings, and experimental procedures should be given in sufficient detail for others to verify the work. The length of a full paper should be the minimum required to describe and interpret the work clearly.

Short Communications: A Short Communication is suitable for recording the results of complete small investigations or giving details of new models or hypotheses, innovative methods, techniques or apparatus. The style of main sections need not conform to that of full-length papers. Short communications are 2 to 4 printed pages (about 6 to 12 manuscript pages) in length.

Reviews: Submissions of reviews and perspectives covering topics of current interest are welcome and encouraged. Reviews should be concise and no longer than 4-6 printed pages (about 12 to 18 manuscript pages). Reviews are also peer-reviewed.

Review Process

All manuscripts are reviewed by an editor and members of the Editorial Board or qualified outside reviewers. Authors cannot nominate reviewers. Only reviewers randomly selected from our database with specialization in the subject area will be contacted to evaluate the manuscripts. The process will be blind review.

Decisions will be made as rapidly as possible, and the journal strives to return reviewers' comments to authors as fast as possible. The editorial board will re-review manuscripts that are accepted pending revision. It is the goal of the JPHE to publish manuscripts within weeks after submission.

Regular articles

All portions of the manuscript must be typed double-spaced and all pages numbered starting from the title page.

The Title should be a brief phrase describing the contents of the paper. The Title Page should include the authors' full names and affiliations, the name of the corresponding author along with phone, fax and E-mail information. Present addresses of authors should appear as a footnote.

The Abstract should be informative and completely self-explanatory, briefly present the topic, state the scope of the experiments, indicate significant data, and point out major findings and conclusions. The Abstract should be 100 to 200 words in length.. Complete sentences, active verbs, and the third person should be used, and the abstract should be written in the past tense. Standard nomenclature should be used and abbreviations should be avoided. No literature should be cited.

Following the abstract, about 3 to 10 key words that will provide indexing references should be listed.

A list of non-standard **Abbreviations** should be added. In general, non-standard abbreviations should be used only when the full term is very long and used often. Each abbreviation should be spelled out and introduced in parentheses the first time it is used in the text. Only recommended SI units should be used. Authors should use the solidus presentation (mg/ml). Standard abbreviations (such as ATP and DNA) need not be defined.

The Introduction should provide a clear statement of the problem, the relevant literature on the subject, and the proposed approach or solution. It should be understandable to colleagues from a broad range of scientific disciplines.

Materials and methods should be complete enough to allow experiments to be reproduced. However, only truly new procedures should be described in detail; previously published procedures should be cited, and important modifications of published procedures should be mentioned briefly. Capitalize trade names and include the manufacturer's name and address. Subheadings should be used. Methods in general use need not be described in detail.

Results should be presented with clarity and precision. The results should be written in the past tense when describing findings in the authors' experiments. Previously published findings should be written in the present tense. Results should be explained, but largely without referring to the literature. Discussion, speculation and detailed interpretation of data should not be included in the Results but should be put into the Discussion section.

The Discussion should interpret the findings in view of the results obtained in this and in past studies on this topic. State the conclusions in a few sentences at the end of the paper. The Results and Discussion sections can include subheadings, and when appropriate, both sections can be combined.

The Acknowledgments of people, grants, funds, etc should be brief.

Tables should be kept to a minimum and be designed to be as simple as possible. Tables are to be typed double-spaced throughout, including headings and footnotes. Each table should be on a separate page, numbered consecutively in Arabic numerals and supplied with a heading and a legend. Tables should be self-explanatory without reference to the text. The details of the methods used in the experiments should preferably be described in the legend instead of in the text. The same data should not be presented in both table and graph form or repeated in the text.

Figure legends should be typed in numerical order on a separate sheet. Graphics should be prepared using applications capable of generating high resolution GIF, TIFF, JPEG or Powerpoint before pasting in the Microsoft Word manuscript file. Tables should be prepared in Microsoft Word. Use Arabic numerals to designate figures and upper case letters for their parts (Figure 1). Begin each legend with a title and include sufficient description so that the figure is understandable without reading the text of the manuscript. Information given in legends should not be repeated in the text.

References: In the text, a reference identified by means of an author‘s name should be followed by the date of the reference in parentheses. When there are more than two authors, only the first author‘s name should be mentioned, followed by ’et al‘. In the event that an author cited has had two or more works published during the same year, the reference, both in the text and in the reference list, should be identified by a lower case letter like ’a‘ and ’b‘ after the date to distinguish the works.

Examples:

Abayomi (2000), Agindotan et al. (2003), (Kelebeni, 1987a,b; Tijani, 1993,1995), (Kumasi et al., 2001)
References should be listed at the end of the paper in alphabetical order. Articles in preparation or articles submitted for publication, unpublished observations, personal communications, etc. should not be included in the reference list but should only be mentioned in the article text (e.g., A. Kingori, University of Nairobi, Kenya, personal communication). Journal names are abbreviated according to Chemical Abstracts. Authors are fully responsible for the accuracy of the references.

Examples:

Chikere CB, Omoni VT and Chikere BO (2008). Distribution of potential nosocomial pathogens in a hospital environment. Afr. J. Biotechnol. 7: 3535-3539.

Moran GJ, Amii RN, Abrahamian FM, Talan DA (2005). Methicillinresistant Staphylococcus aureus in community-acquired skin infections. Emerg. Infect. Dis. 11: 928-930.

Pitout JDD, Church DL, Gregson DB, Chow BL, McCracken M, Mulvey M, Laupland KB (2007). Molecular epidemiology of CTXM-producing Escherichia coli in the Calgary Health Region: emergence of CTX-M-15-producing isolates. Antimicrob. Agents Chemother. 51: 1281-1286.

Pelczar JR, Harley JP, Klein DA (1993). Microbiology: Concepts and Applications. McGraw-Hill Inc., New York, pp. 591-603.

Short Communications

Short Communications are limited to a maximum of two figures and one table. They should present a complete study that is more limited in scope than is found in full-length papers. The items of manuscript preparation listed above apply to Short Communications with the following differences: (1) Abstracts are limited to 100 words; (2) instead of a separate Materials and Methods section, experimental procedures may be incorporated into Figure Legends and Table footnotes; (3) Results and Discussion should be combined into a single section. Proofs and Reprints: Electronic proofs will be sent (e-mail attachment) to the corresponding author as a PDF file. Page proofs are considered to be the final version of the manuscript. With the exception of typographical or minor clerical errors, no changes will be made in the manuscript at the proof stage.

Fees and Charges: Authors are required to pay a $650 handling fee. Publication of an article in the Journal of Public Health and Epidemiology is not contingent upon the author's ability to pay the charges. Neither is acceptance to pay the handling fee a guarantee that the paper will be accepted for publication. Authors may still request (in advance) that the editorial office waive some of the handling fee under special circumstances.

Submission of a manuscript implies: that the work described has not been published before (except in the form of an abstract or as part of a published lecture, or thesis) that it is not under consideration for publication elsewhere; that if and when the manuscript is accepted for publication, the authors agree to automatic transfer of the copyright to the publisher.

Journal of Public Health and Epidemiology

Table of Content: Volume 6 Number 11 November 2014

ARTICLES

Research Articles

Social determinants of health and inequity among people with disabilities: A Brazilian experience 326
Regina C. Fiorati and Valeria M. C. Elui

Heath Care in the rural areas in Chad: Accessibility and catch of load (case study of the sub-prefecture of Donon Manga in East Tandjilé) 338
Ndoutorlengar Médard, Djimouko Sabine and Mbairo Pascal

Denoising a model employing automated bandwidth selection procedures and pre-whitened Euclidean-based quadratic surrogates in PROC ARIMA for optimizing asymptotic expansions and simulations of onchocerciasis endemic transmission zones in Burkina Faso 347
Benjamin G. Jacob, Robert J. Novak, Laurent Toe, Moussas S. Sanfo, Rose Tibgueria, Alain Pare, Mounkaila Noma, Daniel Griffith and Thomas R. Unnasch

Epidemiology of malaria among children aged 1 to 15 years in Southeast Nigeria 390
Oko N. F, Odikamnoro O. O, Uhuo C. A, Okereke C. N, Azi S. O. and Ogiji E. D.

Prevalence of malnutrition among preschool children (6-59 months) in Western Province, Kenya 398
Isaac Kisiangani, Charles Mbakaya, Anzelimo Makokha and Dennis Magu

Evaluation of measles surveillance systems in Afghanistan-2010 407
Jawad Mofleh and Jamil Ansari

academicJournals

Vol. 6(11), pp. 326-337, November 2014
DOI: 10.5897/JPHE2014.0645
ISSN 2006-9723
Article Number: A4AAEDE47907

http://www.academicjournals.org/JPHE

Journal of Public Health and Epidemiology

Full Length Research Paper

Social determinants of health and inequity among people with disabilities: A Brazilian experience

Regina C. Fiorati* and Valeria M. C. Elui

Department of Neurosciences and Behavioral Sciences, Undergraduate Program in Occupational Therapy, University of São Paulo at Ribeirão Preto, Medical School, Ribeirão Preto, SP, Brazil

Received 03 May, 2014; Accepted 12 September, 2014

This paper presents a discussion concerning the results of research conducted between 2011 and 2012 in the city of Ribeirão Preto, SP, Brazil, in which the general objectives were to understand the socio-familial inclusion of people with disabilities and their daily living needs. The methodological approach was qualitative and the data collection techniques were open life history interviews. The research subjects were ten people with acquired or congenital disabilities who were residents of the region enrolled at Primary Health Care Service of Ribeirão Preto city. Analysis of data was based on interpretation in light of dialectical hermeneutics. Our results showed that the socio-familial inclusion of individuals depends on their socioeconomic conditions, with significant indices of socially vulnerable families who have difficulty accessing primary health care and rehabilitation services, and presented indicators of social inequity. Their daily lives were marked by social isolation and not being adequately occupied with social determinants that cause negative health impacts. Due to indices of vulnerability and social inequity presented by population studied, we conclude that the creation of social vulnerability reduction programs coordinated with primary health care services is required.

Key words: Disability/disabled persons, health care primary, rehabilitation, social determinants of health, social inequity.

INTRODUCTION

Disabilities have been defined as human existential states related to certain conditions, in which the affected subjects are unable to perform some activities necessary for daily living and social interaction. There is, however, no consensus regarding a definition of disability, and the concept involves historical and cultural variations (Phelan, 2011). Despite the variations and fluctuations of specific contexts, the perceptions and treatments of disability show one historical constant: social segregation.

Historical investigation reveals that in antiquity and the Middle Ages, disability was understood within a model of divine fatalism or demonic possession. With the onset of the scientific revolution in the 16th century and its

*Corresponding author. E-mail: reginacf@fmrp.usp.br.

expansion beginning in the 18th century, a new model appeared, in which disability was understood according to the rationale of biosciences and medical models of treatment and was defined as a lesion, within which its manifestations consisted of corporal irregularities and biomechanical propellants of states characterized by abnormalities (Clapton and Fitzgerald, 1997).

According to Clapton and Fitzgerald, during the 20th century, the biomedical model was modified, such that after abandoning total institutionalization, a model of intervention that focused on services was adopted. However, this new practice of rehabilitation did not modify the central axis of understanding and treatment of disability as a deviation from normality. Thus, based on a notion of adaptation, systematic knowledge and technically qualified professionals, forms of action against disability remained focused on the normalization of people with disabilities, imprisoned within an individual and pathological dimension, founded on the logic of corporal correction of the lesion and pressure on the individual to adapt to physical, mental and sensorial normativity by any means possible.

A biopsychosocial model of disability gains relevance and recognition, beginning in 2001 when the World Health Organization (WHO) presented a review of the International Classification of Impairment, Disabilities and Handicaps (ICIDH), overcoming the purely biomedical approach adopted so far and acknowledging the social and political nature of disability based on the publication of the International Classification of Functioning, Disability and Health (ICF) (WHO, 2001; Bampi et al., 2010).

The social model of disability emerges as an alternative to the biomedical model, which, as it shifts from a concept of disability defined solely as biological fact, proposes a definition of disability based on its relationship with the political, economic, cultural and social spheres as important generators of barriers to the development of people with disabilities. Accordingly, disabilities are not understood as enclosed within the individual sphere of the subject, but as generated within the sociocultural sphere, such that environmental and psychosocial barriers to the vital development of people with disabilities generate important social inequalities in relation to the means of accessibility for individual to collective opportunities and social participation (Tregaskis, 2002; Levasseur et al., 2007).

Recognition of a biopsychosocial model of disability gained relevance and developed into a central concern beginning in 2001, when the World Health Organization (WHO) presented a review of the International Classification of Impairment, Disabilities and Handicaps (ICIDH), superseding the purely biomedical approach that had marked the ICIDH. At this point, the WHO recognized the social and political nature of disability. In 2001, the WHO published the International Classification of Functioning, Disability and Health (ICF), which superseded the purely biomedical model by defining disadvantages not as the result of lesions, but as belonging to the social sphere and the difficulties imposed by a form of sociopolitical organization that excludes and stigmatizes those who are disabled. Exclusion and stigmatization occurs through the imposition of geographic, cultural, economic, political and social barriers that prevent the autonomy and self-determination of people with disabilities, limiting their freedom of movement and access to diverse environments, services and equipment present within the collective area (Farrell et al., 2007; WHO, 2001).

The framework used in this study was the social approach to disability; that is, disability is seen as a socially constructed condition and the role of society is to reorganize itself to ensure these people universal access to all public spaces, devices, services, organizations and resources available to the community, in general. Therefore, once the idea of the normalization of individuals is overcome, rehabilitation services need to provide alternatives that facilitates the full participation of individuals with disabilities in society (Tregaskis, 2002; Gannon and Nolan, 2007). Thus, understanding disability as a social construct, an adjustment in the whole of society is needed to ensure universal access for people with disabilities to all spaces, equipment, services, organizations and resources publicly available to the community. Having overcome the concept of the normalization of the individual, rehabilitation services are now required to offer alternatives to facilitate the full social participation of people with disabilities (Barnes et al., 2002).

Inserted into a new paradigm that advocates a social approach to disability, certain organized social movements formed by people with disabilities initiated the process of demanding social rights and universal accessibility. It was in this manner that an extension of the protection of human rights of people with disabilities occurred. In 1975, the United Nations (UN) published the Declaration on the Rights of Disabled Persons, culminating with the legislative framework currently in force, the 2006 Convention on the Rights of Persons with Disabilities of the United Nations (UN CRPD) (ONU, 2006; D'Aubin, 2003).

The UN CRPD is innovative in the context of international treaties ratified up to the present because it explicitly recognizes that physical, economic and social environments constitute factors that compounds the effects of disabilities and acknowledges environmental and psychosocial barriers as central obstacles to full social participation and equal opportunities with the remaining members of society.

Even though there have been advances in Brazil in regard

to the work directed to the inclusion of individuals with disabilities in the sociocultural sphere, and occupational therapy has developed technologies to support this inclusion through implementing actions within communities with the direct participation of the community itself, many individuals with disabilities remain deprived of basic rehabilitation services with no equalitarian access to education, professional qualification, work opportunities, leisure, or other activities in the community and society. Moreover, many are isolated and confined to their domestic environment, ignoring the availability of assistive and healthcare devices (Phillips et al., 2013).

In some cases, people with disabilities lose membership in their own families and have no defined place within the family association, which decreases their autonomy and self-determination. This situation repeats itself within the community, as these individuals are sometimes unable to be included in the shared world of communication and remain excluded from the material and symbolic production process of social life (Barnes et al., 2002). The social inclusion of people with disabilities is a key for promoting health and improving the quality of life of this population. For that, they need to become involved and participate in basic and general activities that compose the human existential universe. For these individuals to be effectively included and fully participate and circulate freely in social life, they need to develop occupations and become involved in daily life and social activities, acquiring autonomy and independence (AOTA, 2010; WHO, 2012a).

In Brazil, the Federal Constitution of 1988 (*CF/88*) provides for care, public assistance, protection and social integration and guarantees the rights of people with disabilities within the joint competence of the three spheres of government. Thus, the CF/88 guarantees the defense of inclusive and integral human rights under the rule of law, including the obligation to provide health care for people with disabilities through the Brazilian Public Health System (Sistema Único de Saúde - SUS), coordinating among municipal, state and federal governments, at all three levels of care: primary, secondary and tertiary (Brasil, 2006). According to this perspective, one of the founding principles of the *SUS*, integrality, is highlighted as an important demarcation in the health care of people with disabilities. In the process of consolidating the expanded concept of health as a complex human existential condition that is interconnected with various sociocultural, political and economic factors, all of which are more significant than simply being in a dichotomous relationship with disease, comprehensiveness amplifies the possibilities of offering health care as an interconnected and continuous set of actions and health services, in which practices are communicated and integrated continuously, with the main objective of achieving comprehensive, complex and humanizing care (Campos, 2000; MacLachlan et al., 2012).

Once the concept of disability as socially shared responsibility is established, comprehensive health care for people with disabilities is defined within the framework of attention and care, ranging from preventative health care actions and health promotion to rehabilitation, with access to both Primary Health Care (PHC) and specialized services and equipment, ensuring connected and extended health care for people with disabilities that covers all sociocultural, historical, political and economic bases that are determinant in the health-disease continuum, without neglecting the accumulation of knowledge and technologies in the biomedical field (Brasil, 2008; Maclachlan et al., 2012).

Thus, for the social group under discussion, interconnections among health promotion, disease prevention, early diagnosis of disabilities and primary care and specialized rehabilitation networks would be expected. What can be attested to, however, is that the delivery of integral healthcare to people with disabilities remains far from what is envisioned under the National Health Policy (NHP). Observation confirms that the central focus remains on disability from an organic perspective, on the rehabilitation process and on actions centered around specialized, highly technological services that are difficult to access for a significant portion of people with disabilities, especially those who find themselves in situations of social vulnerability (Brasil, 2008; Evans et al., 2001).

People with disabilities are among those who are vulnerable to social determinants of health. Social determinants of Health are understood as social, economic, cultural, ethnic/racial, psychological and behavioral factors that influence the occurrence of health problems and their risk factors in the population. Studies show that high rates of social inequity present in the population with disabilities, within which there is a lack of access to employment and income, education, adequate transportation and public utilities and health services (Bus and Pellegrini, 2006; Chappell and Johannsmeier, 2009). This discussion is consonant with observations obtained from a survey conducted in 2011 and 2012 in Ribeirão Preto, SP, Brazil involving people with disabilities living in the region enrolled in a Family Health Unit (FHU) associated with the School Health Center (Centro de Saúde Escola, CSE) of the Medical School (Faculdade de Medicina de Ribeirão Preto, FMRP) of the University of São Paulo at Ribeirao Preto (USP).

The assumptions guiding this study include the following: There are still a considerable number of individuals with disabilities who lack access to social opportunities, material and non-material goods that are part of society's system of patrimony, and who have

difficulty accessing the most basic forms of social inclusion, which effectively mean inclusion in family and community dynamics and structures. This is so even though there are public policies and constitutional provisions in Brazil that focus on the care provided to individuals with disabilities within the healthcare and welfare spheres, both to provide socioeconomic protection and enable universal access to healthcare services. There is a lack of coordination among the various levels of healthcare (for example, at the primary, secondary and tertiary levels) delivered to individuals with disabilities, compromising the integrality of healthcare actions. Additionally, there are immense geographical and psychosocial barriers hindering the access of people with disabilities and their social mobility. Concomitantly, people with disabilities belong to the poorest segments of the population, with poor access to education, work opportunities and activities that generate income, transportation, housing and a sustainable environment; thus, they are socially vulnerable as a result of social inequality. From this perspective, the social determinants existing in Brazil have more strongly impacted the conditions of life and health of individuals with disabilities than have conditions that are linked to physiological, anatomic-morphological or clinical factors. Given these objectives and the hypothesis, we seek to reflect on the results presented in the research.

METHODOLOGICAL APPROACH

An interpretive and reconstructive approach to the data

It is a field research that makes an investigation into the natural environment of the subjects and it is characterized by a descriptive exploratory study. The method followed a qualitative approach consistent with the elements involved in this investigation, which are in the symbolic dimension of human existence and include the interpersonal relationships present in the families and individuals studied, their values and the meanings that mark their health status and living conditions, cultural understanding and social representations. Therefore, as it is a qualitative methodology, statistical analysis do not apply. The instrument for data collections were open interviews of life stories (Minayo, 2008; Johnson and Barach, 2008). The study subjects were ten people with congenital or acquired disabilities, who were 16 years old or older and had sufficient cognitive abilities to narrate their life histories and living in the area covered by the city's Family Health Unit. The type of disability did not constitute a criterion for selection, that is, any variable among the manifestations of disability were accepted: physical, motor, sensorial, mental and/or multiple disabilities, because this study sought to understand the nature of the condition of disability, regardless of the specific clinical implications related to the disability. The selection of subjects was made from information from medical charts of families served by the Family Health Unit according to the selection criteria mentioned earlier.

The research locations were the homes of each subject, residents of the Western region of the city of Ribeirão Preto who were enrolled in FHU associated with the CSE-FMRP-USP. Data were collected through open interviews regarding life stories. The interviews were based on open-ended questions concerning the life histories narrated by the subjects. During the interviews, we noted the residence, relationships and family dynamics of the survey participants. Since the interviews were conducted in the subject's home, family members were always present, which allowed contact with the family dynamics existing in each situation studied. We interviewed ten subjects at home and they were asked to narrate their lives from birth to that moment. Twenty people with disabilities were identified in the territory encompassed by the study, and the population served by the Family Health Service reference was estimated at approximately 250 families. Of these 20 subjects, four declined to participate, two had no cognitive condition to make a story of life and three were not found in their homes. Therefore the subjects selected were ten people who agreed to participate and fit the criteria laid.

We sought to allow a free narrative, but we interjected with prompts to provide some narrative linearity when necessary. The interviews were recorded with the permission of the subjects and transcribed later. The textual contents from the narratives were intersected in the analysis of the data and interpreted in light of dialectical hermeneutics (Habermas, 1989), which provided a reconstructive, rather than a descriptive interpretation of the data during our analysis: from the ordering of the data, we have developed a thorough and extensive reading of the stories of life and a link between the information and reports of the historical and cultural factors that have conditioned the telling of the stories. Additionally, we connected the perceptions of the subjects studied to reveal their expectations regarding their autonomy, the health actions of health services and their life projects, to previous information (Bauer and Gaskel, 2002). The stages of the data analysis were as follows:

a) Reading and rereading of the interviews repeatedly and carrying out a data analysis of the printed material from the interviews according to the thematic content analysis method.
b) Identification of emerging themes that outlined certain symbolic universes shared between the participants in the research and a crossover with data in the literature.
c) Establishment of relations with the field of fundamental determinants, such as: cultural, political, economic and social conjunctures in which the statements find reference for their construction.
d) Establishment of relations between the thematic axes and the historical constitution process of the social group being researched and why they build such conceptions about the phenomenon under study.

The research project was submitted to the Research Ethics Committee of the CSE-FMRP-USP and approved under protocol no. 468/CEP/CSE-FMRP-USP on the 27th of December, 2011. Ethical procedures were followed at all stages of the research as set out in the approval document Committee on Ethics in Research.

RESULTS

Search results are presented and arranged through the table (Table 1). In regard to access to health services, the study participants reported difficulty accessing primary and secondary healthcare services, with no access to rehabilitation, due to two sets of factors: socioeconomic

Table 1. Results and thematic axes.

Thematic Axes	Results	Number of participants/families
Social family inclusion of the study participants	The social family inclusion of individuals with disabilities addressed in the study is related to the degree of social inclusion/integration the family itself experiences in society.	-
Participants and their families are included	Families with better socioeconomic, cultural and educational conditions have greater access to social resources and these individuals: have stronger social support and occupy a personalized position within the family; perform an articulated role in family dynamics; and have an important degree of autonomy with the ability to make decisions in regard to personal and family events. Therefore, their social participation becomes more effective as they have greater access to cultural and social resources in the community, which is important for human development	Two participants and their families presented this condition
Participants and their families who are socially vulnerable	Limited socioeconomic and cultural resources, low levels of education and social support, which generate weakened family ties. Three families presented social vulnerability characterized by indicators of social inequality: (a) Low education; (b) Lack of access to work; (c) Lack of access to education; (d) Lack of access to transportation; (e) Difficult access to housing; (f) Lack of access to a sustainable environment Poor hygiene conditions were found both in regard to domestic environments and to the study participants; lack of information on the part of the family members and participants in regard to the study participant's disability and care it requires, lack of material resources such as assistive technology and transportation, and lack of financial resources to acquire basic necessities	Eight of the interviewed people do not perform significant tasks in their routine, do not have effective social participation, do not work, and do not have any source of income. Four interviewees remain restricted to their homes, with difficulty accessing services, public places, and opportunities that are available to the entire collectivity. Eight individuals have difficult access to transportation, have no access to assistive technology, have economic difficulties commuting to places or accessing services, and social and cultural equipment. They also report geographical, psychosocial and cultural barriers. Economic difficulties are due to their exclusion from the job market

and cultural factors and those related to the organization and coordination of healthcare services, as described in the table (Table 2).

DISCUSSION

Analysis of the data obtained led to the identification of four thematic axes, which encompassed and organized the predominant themes in the narratives and systematic observations, representative of situations often experienced in the daily lives of the subjects studied, together with their families and community, as well as sets of characteristics and common health care and social needs presented by the people with disabilities being studied. The thematic axes are: (a) the inclusion of people with disabilities in familial and community contexts and the relevant proportion of social vulnerability present; (b) the daily lives of people with disabilities and existential emptiness; (c) participation in and access to PHC and specialized rehabilitation services for people with disabilities, and (d) social and health care needs. The presentation and discussion of these four thematic axes are as follows:

Table 2. Access to healthcare services.

Access and the lack of access to healthcare services	Nature of the problem
Socioeconomic and cultural factors	Lack of transportation to commute to the services, and the conditions of urban mobility
	Lack of technical information and information concerning social rights or how to access such rights
	Absence of assistive technology to facilitate mobility and the presence of geographical barriers
	Poor economic conditions leading to a lack of private transportation or any other paid transportation
Factors intrinsic to the healthcare services and management	The set of healthcare actions provided by the healthcare services to the community and at home, which would promote universal access to those with disabilities, is limited
	There is a lack of cooperation within the healthcare network, which hinders the coordination and integrality of healthcare delivery

Socio-familial inclusion of people with disabilities

Familial belonging to the people with disabilities analyzed in this study is related to the degree of social integration that the family itself occupies in society. The quality of care and attention dispensed by the family to the family member with a disability depends on the socioeconomic status of the family in question and the social and community resources available. Middle class families and those with more education provide more care resources, the individual being cared for has more powerful social support and occupies a personalized place in the family, that is, they occupy a connected role in family dynamics and present an important degree of autonomy, with the capacity for decision-making regarding personal and family events:

Subject 1 (S1): *If it's not my brother, it's my father; when I need something, my mother picks it up; she closes that there and we go by bus, car, whatever works best. In my mother's small living room, over there, I do my crafts; I sell clothes, lingerie, Avon. My cousin made a proposal to me for us to set up a shop. I'm thinking about it before I give him an answer.*

However, this reality is not observed in families whose social condition is more vulnerable, those with limited socioeconomic and cultural resources, a low level of education and poor social support, or in families with weakened ties. In one case, violence against the family member with disabilities was observed. In three family nuclei, we identified characteristics of social vulnerability, and in these cases significant problems were observed, including: poor hygiene conditions in the domestic space and for the study subjects; a lack of information among family members and the subjects concerning disability and care needs; lack of material resources, such as assistive technology and transportation; and lack of financial resources for the acquisition of basic materials. In addition, the individual with the disability does not always occupy an autonomous place within the family dynamics; they are cared for by one family member, usually the mother or wife, and only in accordance with what is possible for this single caregiver to accomplish. Subject 6 (S6) is a 70-year-old man who, like his wife, did not complete the final year of elementary school. A former farm worker, who became a bricklayer when he moved to the city, he is an alcoholic. He remains bedridden following a fall, in which he fractured his lower limbs (LL), and a stroke. He does not have a wheelchair, presents poor hygiene and his wife is the only caregiver. She reported:

I do everything, though sometimes our youngest helps me, but the others leave early and get home late. I try to do things like they taught me at the hospital, but I've also got back pain, I've got a lot of leg pain, so he doesn't get out of bed; I wash him right here. The guy from the ambulance says a ramp is needed here, but we don't have a wheelchair; whenever necessary, my son-in-law has to carry me. I'm hoping to go to (mentions a popular TV show). I've seen him give wheelchairs to others.

The condition of social vulnerability is frequently associated with the reality of people with disabilities. They are among the poorest individuals, with the lowest

level of education and income in Brazil and worldwide. The development of disabilities is directly related to poor conditions of nutrition, housing, sanitation, access to health services and social facilities, and low income. These, in turn, are determinant living conditions in areas of poverty incidence (WHO, 2012b; Braveman and Gruskin, 2003).

Social inequality and poverty influence and, in certain cases, make it impossible to access the equipment of social support networks, basic information regarding social rights and the resources available in society. In addition, people with disabilities compose a social segment that is among the most excluded from the labour market and income generation mechanisms. The closest caregivers often have to abandon their own work activities and means of income generation, further increasing the conditions of vulnerability of the family nucleus. Caregivers frequently present problems of worsening health due to care activities (Marmot, 2005; Cooper et al., 2012). Conditions of social and economic vulnerability of people with disabilities impede the satisfaction of their needs, the guarantee of their independence and quality of life, and public policies have proven insufficient in responding to the problematic situations indicated (Cooper et al., 2012).

The severity of poverty and misery in Brazil constitutes an ongoing preoccupation and demands reflection concerning their social influence, particularly in the area of actuation involving the family, in which public policies still lack more expressive action. The state should ensure the rights of the disabled and provide the conditions necessary for the effective participation of the family in the development of their children, particularly for families that include individuals with disabilities; however, Brazilian public investment in the social sector is increasingly linked to economic performance (Gomes and Pereira, 2005; Prince, 2010).

It is not possible to assign a single meaning to poverty, but it becomes evident when part of the population is unable to generate enough income to maintain sustainable access to basic resources to ensure their quality of life. Moreover, the high levels of poverty that affect Brazilian society are the main determinant in the structure of perverse social inequalities in income distribution and economic inclusion. This highlights the need to revitalize the constitutionally established social rights of people with disabilities and to seek to connect sectors of society to develop and implement public policies designed to solve the prevailing conditions of social vulnerability among this population.

The daily lives of people with disabilities: The need to aggregate the value of existential meaning

Our research shows that majority of respondents do not develop activities that are structured, productive, related to leisure or, in some cases, self-care activities in their daily lives. S6 is the most serious case, remaining bedridden the entire time. However, others, even though they can move around within their domestic spaces, are isolated from social participation:

Subject 3 (S3): Going back to where I was, to my job, was bad, but I worked with the public, I worked with people, so, it was great. It had its problems, but it was good. Now, I don't leave the house.

Subject 5 (S5): I don't walk or drive, because everything hurts. It's difficult for me to go out; I don't even go to my kids' homes anymore. You miss working, miss making things, cooking, but I can't do it anymore. S5 is a 75-year-old woman who used to be a seamstress and was very active in maintaining her family's income. When she lost her sight, she developed depressive symptoms and attempted suicide twice.

In addition, there is the prejudice generated in the field of social stigmas that genuinely affects the disposition of these individuals to engage public environments, affecting their self-esteem and body image:

S3: I'm ashamed. I don't like it. I don't like myself. I comb my hair and don't look in the mirror. That's why I don't like being around other people.

Subject 2 (S2): I was slower than the others, and like it or not, we're less than a normal person, we want to give the best of ourselves, but we'll never be like a normal person, it's very difficult.

Daily existence is the territory in which human potential encounters its subjective inscription of achievement. It is the field of the human actions of creation and recreation of the world and social living. Human daily living activities range from those concerned with the maintenance of daily living and self-care to those concerned with the ongoing recreation of social living. Thus, the individual is perceived in their daily reality, inserted in an intersubjective world, whose existence only attains meaning in participation and conjunction with other people. It is here, in the terrain of exchanges and human relationships, that daily living forms and is produced. Daily existence is the context in which the subject moves, observes the passage of time, constitutes their existential experience and recreates their uniqueness (Clair et al., 2011; Lefebvre, 2002).

Arendt (1998) alludes to human action as the fundamental condition of human life in the world. The activities in which people engage involve the dimension of the biological reproduction of life, work as an activity of

construction, the instrumentalization of life, the production of objects that shape humans as producers and modifiers of nature, of mundanity, as the author called it; human action is the terrain on which individual existence is transcended. Furthermore, humans involve themselves in praxis, the political dimension of human existence, action intersubjectively mediated among people, by which they may inhabit the shared world. Engaging in activities therefore ensures an individual the condition of singularity and plurality at the same time: every person is plural, since they share the same condition with all others; however, no person in the world is exactly like any other who exists or has existed.

According to the perspective of the field of occupational therapy, occupations and activities have the potential to structure an individual's subjectivity and external reality, establishing internal mechanisms and restoring the unity of an individual in their biological and cultural conditions and in their biographical and collective experiential fields. While in the field of health production, occupations can, for this reason, occupy the centralizing and guiding element of the construction of a quality life (Pierce, 2001; AOTA, 2008). What we perceived from the research is that the daily lives of the subjects studied were clearly impoverished, void of existential meaning, mainly due to the minimal or lack of involvement in a routine and creative occupations.

The daily life of an individual is revealed at the intersection of the dimensions of subjective life and external reality. Thus, this interface between subjectivity and the social sphere has the possibility of being realized in the cultural sphere of human life in which individuals exercise all their creative potential, inscribing their subjectivity into culture and ensuring their social participation in the world, a condition that is central to occupational therapy (Larivière, 2008). Thus, an existential emptiness can be perceived in the lives of the subjects, a barely-filled void, since they are maintained without the creative exercise provided by involvement with and in occupations. This existential emptiness directly interferes in and influences the global health processes of these individuals. It interferes both in physical health, leading to becoming overweight or to obesity, and in mental health, such as depressive states, and can lead to extremes, such as the suicide attempts identified in the case of *S5*.

Inclusion in and access to PHC and specialized rehabilitation services for people with disabilities

The individuals studied encountered difficulty accessing health care services, both primary and secondary care. This is due to several factors: lack of transport of people to accompany them, of technical information and concerning social rights, and a lack of assistive technology. Even among those who are capable of walking, they were unable to get to these services due to the poor conditions of sidewalks and public roads. Thus, we observed that the majority of the subjects remained without rehabilitation. There is also, on the part of health care services, a lack of attention and care conducted within the community and within the home. Primary health care services focus on maintaining general health and do little to impact the condition of disability because they consider this to be the responsibility of specialized rehabilitation services, that is, secondary and tertiary levels of health care. Specialized rehabilitation services are located far from the subjects' residences and do not provide attention and care centered in the community or within the home. Thus, the subjects reported that, faced with the immense difficulties of getting to rehabilitation services, they eventually abandon their use. In addition, some stated that the rehabilitation services discharged them, including one individual who was extremely dependent.

S1: It's tiring, because you go by van early and stay till late, until they come to pick you up. You can't lie down, you can only sit on the seats. There, they discharged me and the psychologist gave me a piece of paper saying that to continue, I needed another referral.

S3: You use a wheelchair and need your things, it's getting difficult, with the diapers and the medication... not everyone is willing to help you, not everyone can help you. My brother-in-law takes me, but he has to leave me there, take the kids to school, pick up my sister and then come back and get me. Feels like you're causing a lot of trouble. Physiotherapy ended, seems that it might start here at the local Unit; I'm waiting. My sister said that the equipment arrived, and she would talk to the lady at the Unit and leave my name.

This lack of interconnection within the health service network that affects people with disabilities can only be broached and resolved within the field of the integrality of health, that is, the axis by which the right to and access to health care is guaranteed to people with disabilities and by which the weaknesses of the system caused by the discontinuity of the same are overcome (Sullivan et al., 2011). Integrality, understood as the scope of providing appropriate care from a minimum list of services and actions that respond to the needs of the population, is the basis of the Brazilian Public Health System (SUS), which guarantees knowledge and attendance to the health care needs of people not only as they relate to disease, but within their sociocultural contexts (Junior et al., 2012).

However, in the case of people with disabilities, intergra-

lity is not being fulfilled and the subjects of this study encountered difficulty accessing health care services, especially those providing rehabilitation services. A condition of fragility and discontinuity exists regarding care delivered to people with disabilities. According to the WHO, only 2% of people with disabilities have access to rehabilitation; however, in developing countries, this drops to 1 to 2 individuals in 10,000. In Brazil, tertiary care predominates in the case of people with disabilities, in direct contravention of the National Policy for Persons with Disabilities, which advocates integrated care among all three levels of complexity for this social segment (OMS, 2003; Brasil, 2008). There is also a problem regarding comprehension that specialized in rehabilitation services present in relation to disability. The vast majority of these services continue to work with an excessively organicist conception of disability, guided solely by a morpho-anatomical and biological point of reference. Without a social conception of disability, specialized services fail to understand that actions promoting the social inclusion of people with disabilities and the restoration of their autonomy and independence in their practical and social lives are the services' responsibility. When a given medical condition stabilizes and large gains in functional outcome are not verifiable, the service discharges the patient without considering the social dimensions of disability (Lancet, 2009). This clearly deviates from what is advocated by the principle of integrality, which provides for not only the continuity of care, but also, and above all else, extended care to the user, necessitating the consideration of the totality of their needs (Campos, 2000).

Therefore, people with disabilities require attention and care centered within the community and the home. We highlight the importance of programs aimed at eradicating poverty, and reducing social inequities in the territories and community-based. The Primary Health should co-ordinate activities and programs that minimize the negative effects of social determinants of health prioritizing human special groups such as people with disabilities (Hartley et al., 2009; (Wood et al., 2013).

Social and health care needs of people with disabilities

The social and healthcare needs (see Table 1) presented by the study subjects are:

1) Adequate public transport - the majority of the subjects emphasized the lack of adequate public transport available that is adapted to people with special needs. There is one local public service available for transporting people with special needs; however, the subjects say that this is a limited service and access is difficult because few vehicles are available, the timetable is limited and the individual wastes the whole day when they depend on this form of transportation. The remaining vehicles are not adapted to the needs of people with disabilities;
2) Universal access - the subjects indicated difficulties accessing services, equipment and private and public environments, all of which are regularly accessed by the collective. People with disabilities start by highlighting the terrible condition in which the streets are maintained, which makes movement around the city and within the region they inhabit unviable. Conditions for wheelchair users are equally bad. In addition to these factors, the geographic, cultural and psychosocial obstacles are immense and hinder or prevent social integration, as well as deny those with disabilities equal opportunities within common and social environments;
3) Rehabilitation - the vast majority of the subjects emphasize the difficulty of accessing rehabilitation services, indicating the need for the existence of services closer to their homes, while requiring rehabilitation within the home. This topic was discussed in detail;
4) Directly related to the preceding item, the subjects presented the need for assistive technology (AT), information concerning their rights to obtain AT and access to the dispensation of the same;
5) Social support - considering the significant number of subjects experiencing social vulnerability, the need for social support is evident. Some subjects live in poor socioeconomic conditions and have basic social needs that are unmet, which consequently results in a lack of resources and instrumentalization for the caregiver, wherein the individual being cared for lives in an extremely precarious situation and domestic space;
6) Social spaces for coexistence and social participation - some subjects highlighted the need for spaces for coexistence and social participation in their region. Some presented personal situations of social isolation due to biased attitudes and physical, cultural, political, economic and psychosocial barriers resulting from the lack of attention that society devotes to this segment of the population. Other factors include a lack of AT and rehabilitation programs that facilitate social participation and work;
7) In addition, some subjects presented the need for mental health treatment. However, they lack information and the guidance required to seek this form of treatment, since the prevailing perception is that the physical dimension is more important and more urgent when searching for health care treatment (Tomlinson et al., 2009).

The social and health care needs presented by the subjects are highly interconnected to the social determinants of health and presented indicators of social inequity. Although the SUS provides care in three levels

of care system, integrality of the system and the network of health services and access to rehabilitation services, free distribution of assistive technology and equity there are still people with disabilities without access to basic health services and other public services. Although the Federal Constitution ensure the access of persons with disabilities to public spaces and public services, free transport special, at the local level these public policies have not been implemented. These data show that in Brazil significant social inequalities still persist.

From this study, it is observed that social determinants of health predominate over all other determinants health in relation to people with disabilities studied. Data analysis showed that subjects who participated in the study have difficulty accessing health services (rehabilitation and primary care), as well as wrapping other essential public services: employment and income, education, transportation, sustainable environment and quality of life. This fact shows the existence of social inequality because one of the principles of the Brazilian Unified Health is the equity, in which people who have special needs should be met with priority and this does not happen. Instead, it is observed that these people are not living their needs met in unjust inequalities of access, configuring a reality of social inequities, although there are laws which provide for the social rights of persons with disabilities.

The social determinants of health are defined, with a few differences among the existing references, as the social, economic, cultural, ethical/racial, psychological and behavioral factors that influence the occurrence of health problems and their risk factors in the population. According to the WHO model on the Social Determinants of Health (CDSH), the social determinants of health (DSS) are defined on three levels: structural and intermediate determinants; sociopolitical context; and the contexts in which it is possible to deal with social inequities. In turn, all of these factors are conditioned by the political macro-determinant linked to the globalization of the economy and its effects on National economies, resulting in political organizations that are focused on economic development to the detriment of social policies (CSDH, 2008; Starfield, 2011).

The model of CDSH establishes the social determinants of health (SDH) in three spheres: the structural and intermediary determinants; the sociopolitical context; and the contexts in which one can deal with social inequality. The structural determinants are those linked to social stratification, which generates the stratification, and include traditional factors of income and education. They also include: gender, ethnicity and sexuality as social stratifiers and social cohesion related to social capital. The intermediate determinants emerge from the configuration of subliminal social stratification and determine differences in the exposure to and vulnerability to conditions that compromise health. These include: life conditions, work conditions, availability of food, behaviors within the population, and barriers to adopting a healthier lifestyle. This model considers the social and political contexts as determinant factors that influence the health and disease continuum in certain population segments. Social contexts include rapid urban growth with settlements and housing areas with poor sanitation and life conditions, child development that influences development, and working conditions and processes, the healthcare system and access to public services. All these factors are conditioned by a political macro-determinant linked to the globalization of the economy and its effects on nations' economies, resulting in a political organization that focuses on economic development at the expense of social policies (WHO, 2012b). Although the SDH also include the ways that people, groups and populations work, their cultural manifestations and their conceptions about health, disease and means of treatment, the iniquitous conditions in which many social segments are inserted have most impacted and determined the persistence of diseases, conditions and status that could be eradicated. In other words, there is technology and knowledge for this, but an effective resolution cannot be achieved, thus configuring an avoidable, unfair and unnecessary reality experienced by this group of populations in their social vulnerability (Moene and Wallerstein, 2001).

However, the presence of a reality that is strongly marked by social injustice and inequalities is also noted. Thus, taking into account the social determinants of health and the eradication of social inequities, it is necessary to meet the local contexts, which are still marked by difficulties in accessibility to material and non-material goods and social opportunities, such as people with disability. For this, it is necessary, the creation of comprehensive care programs that are articulated in networks in a multiprofessional and intersectoral manner, uniting the health care, social assistance, and public administration sectors with civil society to seek policies and programs to eradicate poverty and social inequities. Therefore, it is believed that it is necessary for the creation of vulnerability reduction and social inequities in community-based interface with the Primary Health Care programs.

Final considerations

Perceptions of the existential condition of disability have changed historically and culturally. The perception and social comprehension of disability are advocated by current public health policies concerning people with disabilities and sanctioned by associations, councils and organizations working to guarantee the social rights of

this social segment. The social understanding of disability also seems to be more consistent with the principle of integrality in health, by contemplating all the dimensions related to the health and social needs of people with disabilities, ranging from the needs of functional rehabilitation, to actions intended to eliminate physical, geographic, cultural, political and social barriers, to the free and full mobility and social integration of people with disabilities, enabling their universal accessibility.

In Brazil, the democratization of health as a result of the implementation of the SUS drew attention to the segment of people with disabilities within public policy. Thus, beginning with the National Health Policy of Persons with Disabilities, published in 2002, directives for States and Municipalities to organize their actions to assist people with disabilities have been established, advocating an expanded conception of health care for people with disabilities, by contemplating interconnected and continuous care at all three levels of complexity, encompassing health-related prevention and promotion, as well as rehabilitation, seeking the integrality of actions and the individual. However, a social organization also built based on large social inequalities continues to determining a lack of access to decent living conditions.

Despite that and other progress made in recent decades, evidenced by improvement in some indices of social development and the creation of a National Health System, based on the principles of solidarity and universality of care, large portions of the population still suffer from problems that produce important health inequities, such as unemployment, lack of access to decent housing, the sanitation system, health services and quality education and an environment protected.

So it is necessary to create programs for the eradication of poverty and act on social inequities from the Primary Health Care. Monitoring these inequities and systematic study of its determinants should help identify vulnerable points to the impact of public policies that seek to combat them.

Conflict of interest

The author declared he has no conflict of interest.

REFERENCES

American Occupational Therapy Association (AOTA) (2008). The occupational therapy practice framework: Domain and process (2nd ed.). Am. J. Occup. Ther. 62(6):625-683.

Arendt H (1998). The Human Condition (2nd ed.). Chicago: University of Chicago Press.

Bampi LNS, Guilhem D, Alves ED (2010). Social Model: A New Approach of Disability Theme. Rev. Lat. Am. Enfermagem. 18(4):816-823.

Barnes C, Oliver M, Barton L (2002). Disability studies today. Cambridge, UK: Policy Press in association with Blackwell Publishers.

Bauer MW, Gaskel G (2000). Qualitative Researching with Text, Image and Sound: A Practical Handbook for Social Research (1st ed.). Thousand Oaks, CA:SAGE Publications.

Brasil (2006). Ministério da Saúde. Secretaria de Atenção à Saúde. Departamento de Ações Programáticas Estratégicas. Manual de legislação em saúde da pessoa com deficiência. 2 ed. Ver. Atual. Brasília.

Brasil (2008). Ministério da Saúde. Secretaria de Atenção à Saúde. Política Nacional da Pessoa Portadora de Deficiência. Brasília.

Bus PM, Pellegrini Filho A (2006). Iniqüidades em saúde no Brasil, nossa mais grave doença: comentários sobre o documento de referência e os trabalhos da Comissão Nacional sobre Determinantes Sociais da Saúde. Cad. Saúde Pública, Rio de Janeiro 22(9):2005-2008.

Campos GWS (2000). Saúde Pública e Saúde Coletiva: campo e núcleo de saberes e práticas. Ciência & Saúde Coletiva. 5:219-230.

Chappell P, Johannsmeier C (2009). The impact of community based rehabilitation as implemented by community rehabilitation facilitators on people with disabilities, their families and communities within South Africa. Disabil. Rehabil. 31(1):7-13.

Clair VA, W-St Kelse N, Smithe E (2011). Doing everyday occupations both conceals and reveals the phenomenon of being aged. Aust. Occup. Ther. J. 58:88-94.

Clapton J, Fitzgerald J (1997). The History of Disability: A History of 'Otherness'. New Renaissance. Available at: http://www.ru.org/human-rights/the-history-of-disability-a-history-of-otherness.html

Cooper RA, Cooper MA, McGinley EL, Fan X, Rosenthal JT (2012). Poverty, Wealth and Health Care Utilization: A geographic assessment. J. Urban Health 89:828-847.

CSDH (2008). Closing the gap in a generation: Health equity through action on the social determinants of health. Final Report of the Commission on Social Determinants of Health. Geneva, World Health Organization.

D'Aubin A (2003). "Nothing about us without us": CCD's struggle for the recognition of a human rights approach to disability issues. In: Enns, H. Neufeldt, A.H. (Eds), In pursuit of equal participation: Canada and disability at home and abroad. Concord, ON: Captus Press pp. 111-136.

Evans PJ, Zinkina P, Harphamb T, Chaudury G (2001). Evaluation of medical rehabilitation in community-based rehabilitation. Soc. Sci. Med. 53:333-348.

Farrell J, Anderson S, Hewitt K, Livingston MH, Stewart D (2007). A Survey of Occupational Therapists in Canada about Their Knowledge and Use of the ICF. Can J. Occup. Ther. 74:221-232.

Gannon B, Nolan B (2007). The impact of disability transitions on social inclusion. Soc. Sci. Med. 64:1425-1437.

Gomes MA, Pereira MLD (2005). Família em situação de vulnerabilidade social: uma questão de políticas públicas. Ciência & Saúde Coletiva. 10:357-363.

Habermas J (1989). The Transformation of the Public Sphere. Cambridge: Polity Press.

Hartley S, Finkenflugel H, Kuipers P, Thomas M (2009). Community-based rehabilitation: opportunity and challenge. The Lancet 374:1803-1804.

Johnson JK, Barach P (2008). The role of qualitative methods in designing health care organizations. Environ. Behav. 40:191-214.

Junior RM, Coimbra M, Matos YAPS (2012). *Direito Sanitário*. São Paulo: Ministério Público, Centro de Apoio Operacional das Promotorias de Justiça Cível e de Tutela Coletiva.

Lancet (2009). Disability: beyond the medical model. The Lancet, 374: 1793 editorial.

Larivière N (2008). Analyse du concept de la participation sociale: définitions, cas d'illustration, dimensions de l'activité et indicateurs. Can. J. Occup. Ther. 75:114-127.

Lefebvre H (2002). Critique of everyday life. Foundations for a sociology

of the everyday. London/New-York: Verso.
Levasseur M, Desrosiers J, St-Cyr Tribble D (2007). Comparing the Disability Creation Process and International Classification of Functioning, Disability and Health Models. Can. J. Occup. Ther. 74:233-242.
Maclachlan M, Khasnabis C, Mannan H (2012). Inclusive health. J. Trop. Med. Int. Health 17:139-141.
Marmot M (2005). Social determinants of health inequalities. Lancet 365:1099-104.
Minayo MCS (Ed.). (2008). O desafio do conhecimento: pesquisa qualitativa em saúde (11th ed.). São Paulo: Hucitec.
Moene KO, Wallerstein M (2001). Inequality, social insurance and redistribution. Am. Polit. Sci. Rev. 95(4):859-74.
Organização Mundial da Saúde (OMS) (2003). Centro colaborador da Organização Mundial da Saúde para a Família de Classificações Internacionais. CIF: Classificação Internacional de funcionalidade e Saúde. EdUSP: São Paulo.
Phelan SK (2011). Constructions of Disability: A Call for Critical Reflexivity in Occupational Therapy. Can. J. Occup. Ther. 78:164-172.
Phillips RL, Olds T, Boshoff K, Lane AE (2013). Measuring activity and participation in children and adolescents with disabilities: A literature review of available instruments. Aust. Occup. Ther. J. 60:288-300.
Pierce D (2001). Untangling Occupational and Activity. Am. J. Occup. Ther. 50:138-146.
Prince MJ (2010). What about a Disability Rights Act for Canada?: Practice and Lessons from America, Australia and the United Kingdom. Can Public Policy 36:199-214.
Starfield B (2011). The hidden inequity in health care. Int. J. Equity Health 10(15):2-3.
Sullivan WF, Berg JM, Bradley E, Cheetan T, Denton R, Heng J, Hennen B, Joyce D, Kelly M, Korossy M, Lunsky Y, McMillan S (2011). Primary care of adults with developmental disabilities: Canadian consensus guidelines. Can. Fam. Physician 57:541-553.
Tomlinson M, Swart L, Officer A, Chan KY, Rudan I, Saxena S (2009). Research priorities for health of people with disabilities: an expert opinion exercise. Lancet 374:1857-1862.
Tregaskis C (2002). Social model theory: The story so far...Disability and Society 17(4):457-470.
Wood R, Fortune T, McKinstry C (2013). Perspectives of occupational therapists working in primary health promotion. Aust. Occup. Ther. J. 60:161-170.
World Health Organization (2001). International classification of functioning, disability and health. Geneva.
World Health Organization (2012a). World report on disability. Geneva.
World Health Organization (2012b). Social Determinanats of Health. Report by the Secretariat. 132nd session. 23 November.

academicJournals

Vol. 6(11), pp. 338-346, November 2014
DOI: 10.5897/JPHE2014.0626
ISSN 2006-9723
Article Number: AA0576E47910

http://www.academicjournals.org/JPHE

Journal of Public Health and Epidemiology

Full Length Research Paper

Heath Care in the rural areas in Chad: Accessibility and catch of load (case study of the sub-prefecture of Donon Manga in East Tandjilé)

Ndoutorlengar Médard[1], Djimouko Sabine[1] and Mbairo Pascal[2]

[1]UniversitY of Moundou, Chad.
[2]European Open-Source Humanitarian Aid corps (EUROSHA), Chad.

Received 09 February, 2014; Accepted 26 May, 2014

The Health sector occupies the 2nd of those which have profited from the financings of the oil incomes after education and agriculture for one decade. But in spite of this attention particularly given to the sector, the future remains dark. The average distance between the medical households and structures is 14 km at the national level against 26 km in the rural mediums which concentrate 80% of the population living with a minimal vital below 250 Currency of the African Financial Community. Poverty and the inaccessibility are thus the first factors of morbidity and mortality in the Chadian rural areas. The sub-prefecture of Donon Manga is an example. This article proposes to analyze the accessibility to medical care and the catch of load of the rural world through the case of Donon Manga in connection with the plans and project of company for a decision-making. The study is carried out starting from the investigations and the direct observations. Investigations were made near the populations, the looking after personnel and the patients of whom people living with human immunodeficiency virus (HIV) in the hospital complex of the sub-prefecture. Results of the investments are not with the height of the place to which the sector has been hoisted for one decade. The perpetuation of the problems with which people are confronted opens the door to the emergence of new actors who daily cause damage.

Key words: Rural, population, health, accessibility.

INTRODUCTION

The millenium objectives declaration is adopted when Chad started its entry in the oil economy. That is what enabled it to pledge among which the Health sector occupies a significant place. There is, inter alia, the reduction of the infant mortality and youth to 2/3, that related to maternity of 3/4 and the stop of the propagation of the acquired immune deficiency syndrome (AIDS), with an inversion of the tendency during a period of 15 years (ONU, 2002).

Plans and strategies were undertaken and

*Corresponding author. E-mail: mbairopascal@yahoo.fr. Tel: +23566080344.

implemented into Chad to achieve these goals which the United Nations laid down. They aim all to improve public health by equipping the country with a coherent health system, powerful and accessible to all (MSP, 2008). The results awaited through the development plans of the sector are summarized in the decentralization of the health system, equity in the access and the integration of the health care activities. But it is advisable to ask to know, what are the states of places before the expiry day? Such is the apprehension that tries to appreciate this work through the case study of the sub-prefecture of Donon Manga. The right to health is a promulgation which can be made by all the countries without exception. But the decentralization of the health system in order to give equitable access to the populations of a nation to health care, as it is concerned, is an element which can be disturbed by many parameters. It engages the financial, material and human resources which can vary from a country to another. It results from our investigations that the results awaited by the millennium objectives are not for today when poverty and illiteracy come to tangle up the insufficiencies and the errors of the ones and others. The first problems to what the population is confronted are the difficult access to the health services. The relating data of the distance between the functional agglomerations and health structures post varied proportions (PAM, 2005). From more than 10 km to the national level, this distance practically passed almost to the double in the provinces in general and the sub-prefecture in question in particular.

The difficulties of access to the health care and the proportion of doctors per inhabitant which is the weakest one of the world (0.04%) contributed to produce new actors of health care of several natures and levels. The diffusion of the latter is encouraged and facilitated by the weak purchasing power of the population on one hand and the lack of control and reprisals by the authorities in load of the ministry on the other hand.

MATERIALS AND METHODS

The methodology of data acquisition for the realization of this work is based on the investigations, direct observations and talks. On the whole 200 people divided into two distinct groups, were the target of these investigations. The first category is made up of the personnel of the various health centers as well as public and private and the unauthorized actors of the health care of the sub-prefecture. It is about the complex hospital of Donon Manga, the Protestant private health integrated centers of Ter-Mission and Ter-village for the first case and then illegal and clandestine looking after and/or tradesmen of the pharmaceutical products of the principal agglomerations and the weekly markets of Kimré (every Monday) of Ter-village (every Wednesday) and of Donon Manga (every Sunday). The principal sought background information nearby these actors are the capacity of reception structures, the type of their training, the level of study and the statute of holding to understand the quality of the care, the origin and the mode of conservations of the products. The second category of the people to which the investigations were managed is made up of the people randomly catched without taking in account their state of morbidity. Nearby the nonsick people, the sought objective information is to appreciate their comprehension of hygiene and to study accessibility, its mode and the limiting factors. Beside patients, on the other hand, we were in search of information concerning the mechanism of assumption of responsibility of the patients and their follow-up in the health centers. The direct observations provided necessary data making it possible to fill insufficiencies of the investigations through our stays in the surrounding villages of Donon Manga.

RESULTS AND DISCUSSION

The rural area in Chad, like those of other countries of sub-Saharan Africa, is characterized by poverty in spite of the decade of the passage of the country to the row of the oil producers. This situation has effects enormously on the people's life quality by the difficulties of access to drinking water, to health care, knowledge, instruction and improvement of the incomes without which one cannot speak about the human development.

Rurality and poverty

Rurality and poverty are appreciated in the context of this study on the basis of geographical accessibility of the area and of services availability and offered to the populations. The first elements determine the distribution of the goods and services while the second determines their access mode and quality. Donon Manga is the chief town of one of the five sub-prefectures which counts the department of East-Tandjilé (Figure 1). Located at the South-eastern of the latter, it is accessible by tracks built and arranged by COTONTCHAD Company liking which is, itself, in financial difficulties to normal function since the Eighties. This makes the zone difficult to reach during the rainy season from Laï, the chief town of the area and Doba, a close town of the area of East-Logone in the south. Only the South-eastern axis, starting from Koumra in the area of Mandoul, is practicable in any season. It is in the canton Donon Manga, chief town of the sub-prefecture which is built a hospital complex located at the western entry of the village. Indicated by "Saint Michel" from the name of a French monk having been useful a long time in the area, it was built in 2004 to function in 2006. It is a realization of the Catholic Church with the support of the Chadian state.

Donon Manga is separated from the chief towns of the close areas and Laï where the reference hospitals are on an average distance of 80 km. At the interior of the area, it is of a distance of 50 km against 35 in the department.

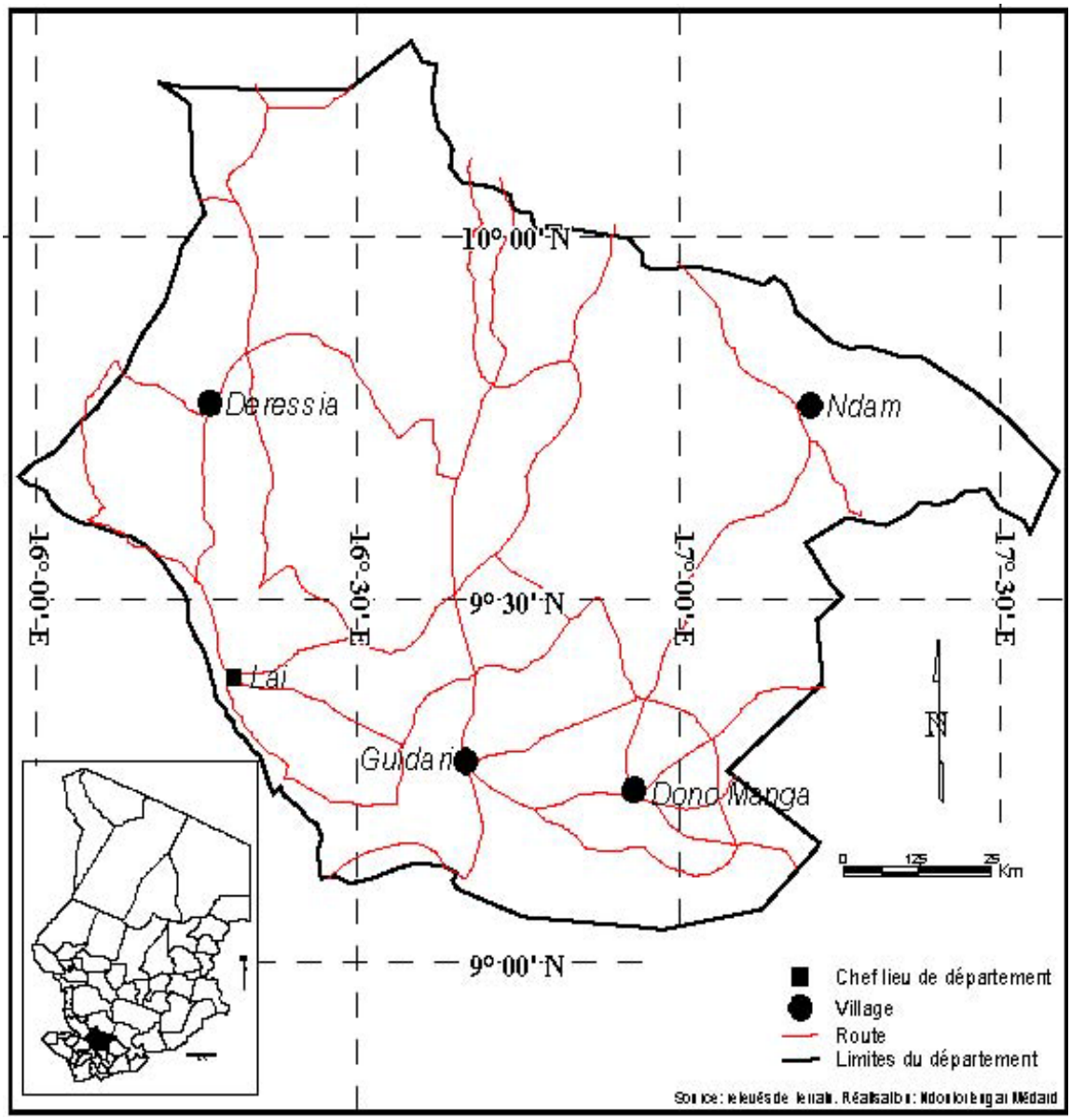

Figure 1. Localization of the sub-prefecture of Donon Manga.

The average distance between the villages and the center of Donon Manga is 26 km in the neighborhoods. The impracticability of the transportation roads weighs down, according to season, the time and the cost of access to the zone. These average costs represent those of the cars. But they vary when they are the motor taxis or carts. Except the market days where one can see the cars going and coming for the goods and the people, the average frequency of passage of the cars observed in the zone,all confused categories, is 0.25 car per hour. It leads the peasants to choose the motor taxis in the event of urgency. Then, in this case, the price of the way goes from simple to the double. The carts of attachment are sometimes also used for displacements to reduce the cost. For this option, one earns money but not on time. Also, the risks to lose the patient during the way from one to two days of road which the cart can take are very high.

The presence of the center of Donon Manga is salutary for the sub-prefecture and the department in general. But its distance and the transport charges related to this one, in time and space, limit the access to the health care and open the door to the improvisation and the maintenance of abstract in this sector of very significant health. Indeed, one of the factors which limit the access to the health

care is the distance which separates the residences from the patients of the center of health from Donon Manga and the latter from regional centers of the closest references. This difficulty of access to the level of the sub-prefecture is one of the causes of mortality: Time put to reach it, because of the distance and the defective condition the ways exacerbates the patient's health or cause death before arriving there. For example, on the 352 cases of cholera recorded in 2011, 22 of 33 deaths are recognized to take place in residence or on the road of the hospital. The false-layers and maternal mortality are mainly related to this problem. Sometimes, the women at the end of the pregnancy, in the absence of means of displacement or of the adequacy of those to cross the distance, are traumatized during hours by the traditional obstetrician ones. In fact, only the cases exceed these latter which arrived at the health centers whereas the victims are already exhausted to have a force to push in order to expel the baby. It follows the loss of the babies, the mothers or sometimes of both. 14 cases of death were recorded during the year 2012 in the hospital complex among which 8 were still-born children, at the same time, two were still-born children and two mothers and two mothers alone, respectively. There is also the case of the 8 people infected with HIV of the sub-prefecture which agreed to testify with disclosed face. Although weak, they met with difficulties of making tens of kilometers to reach the center in the search for their monthly catch of anti-retrovirus (ARV). They often face the rupture for the reason that the one charged with the follow-up of patients meet with difficulties of reaching the center of supply of the southern sector and south-west which is Moundou.

The access problem to the health care in relation to the other centers of references is also crucial. With the two general practitioners and six male nurses, the transfer in complicated case of diseases is imperative. But often, one over three referred cases carries out displacement for bound reasons, not only at the distance, but also with poverty. The transfer implies the assumption of responsibility of the medical expenses and the sick guards. That is, not often of reach to the peasants. The illustrative examples are numerous. Ndeng in the village of Kagama suffers from renal calculi which require an operation. But referred to a qualified center, he has waited for two years to join together the means being able to deal with the medical expenses and sickness before making the displacement to Koumra in Mandoul for its care. Neltongar with Mawa, operated at the "Sémour" hospital of Koumra, is unable to go back there for control after one year that his hernia operation lasted. The access to the health care in the rural medium is not only justified by the geographical distances, distance-cost and distance-time, it is also closely dependent on poverty, the educational level and of the beliefs of the rural populations. The vital minimum of expenditure reached by anybody and per day at the national level is 376 F CFA (Inseed, 2009). This threshold is lower than 250 F CFA in the rural mediums and particularly in the sub-prefecture of Donon Manga whose incomes depend on the production of cotton, a sector which beats wing since more than one decade of years and whose company in load develops increasingly protectionist strategies. With the new system of market said "gone self-managed market", the money from cotton arrives a few months, if not one year later with the peasants, and exceeds hardly 100,000 F CFA for an average producer (Ndoutorlengar, 2012).

In ratio with the low incomes, the peasants are often unable to pay the 12,000 F CFA which request the hospital complex of Donon Manga for the treatment. This amount which represents the hospital expenses, whatever the duration of this one, is approximately 12% of the annual incomes of the rural agricultural producers. It is fixed in a contractual way to facilitate the access to the medical care to the stripped peasants. But in truth, it constitutes an obstacle for all and sundry. It is not only in the case of disease which asks for a short period of hospitalization that the peasants choose to go there. In this amount, for care of short duration, peasants prefer to direct themselves towards looking after abstract or pains clandestine calming. The incomes of cotton are often dragging. In the event of urgency, even if the peasant in question has goods to put on the market to pay the expenses of care, it is necessary to wait the day of this one which is weekly in all the zone. For the contrary case, it is necessary to make tens of kilometers to find it, if the day corresponds to that of a market of the sub-prefecture. The other alternative is to make recourse to the usurers to have the necessary means for the care.

The money put in loan by the usurers has several forms of refunding with interest rates which vary according to the mode of refunding. The interest rate is 50% when refunding is in cash and a bag of millet or groundnut, respectively for 8,000 and 10,000 F CFA borrowed. Whereas, even for the harvest millet, the selling prices of a bag of millet and groundnut are, respectively 12,500 and 15,000 F CFA. The educational level also contributes partly to the option of the orientation of rural people for the health care in the abstract one. The statistics confer on Chad 67.1% illiterates (Inseed, 2009). But these statistics vary from one area to another. Also, the majority of the people who can read and write is concentrated in the cities. The rural mediums in general contain illiterate people and the more poor. 83% of the second categories of the surveyed people are illiterate. This situation can hardly enable them to understand that the missed treatment or not kept tract can immunize the bacteria and contribute to complicate the disease. Or, they can no longer understand

Figure 2. Sight of a room of hospitalization. In the absence of bed of patient, a hospitalized woman is lengthened on two juxtaposed benches which are supposed to be used to sit in the waiting room. Source: Stereotypes Mbaïro (2013).

either that the badly preserved products or that of which the exceeded period of validity can harm the health in one way or another.

Beyond populations' poverty and illiteracy, beliefs oppose, they also serve as a barrier with the access to the health care. The latter is maintained by the tradition. The duality tradition-medicine is strong in the community where any phenomenon finds explanations in the supernatural one and through the ancestors. The illustrative cases are numerous. For example, a case of malaria with convulsion can be interpreted like the effect of sorcery. Thus, parents rather lead the patient at the tradi-pratician than in a health center to receive adequate care. In the village of Kaïmit, a wound on the leg of a man did not cure for 4 months. The explanations of the "clairvoyant healer" which could not bring solutions to the sufferings of this one sent him in the fate according to which its wound will never cure because he offended his ancestors. But in truth, at close view, the germs of the wounds are rather maintained by the recurring use of the same dirty band for the car-bandage without sterilization of any since the wound.

Actors and qualities of the health care of the rural mediums

The results provided by two general censuses of the population and habitat which Chad knew are gathered from the area, which does not make it possible to make the ratio of looking after per capita. But the sub-prefecture of Donon Manga counts 12 great agglomerations. On the other hand, the hospital complex within the competence of the sub-prefecture counts two general practitioners and six male nurses. This numerical insufficiency of looking after personnel, reception facilities (Figure 2) and the distance of the center, evoked more and jointly contributed to create private "health care cabinet" in each agglomeration. It was given us to note, during our observations of grounds that, in each of the 12 agglomerations which the sub-prefecture counts, there is at least a cabinet. Some are old care centers resuscitated by the communities and others, residences of the individuals without any training in the field of health, are set up and held by these.

Three types of distinct actors, from their training and their mode of service, dispute market of health care in the rural space in Chad in general and in the sub-prefecture of Donon Manga in particular. The first group is consisted of the actors who operate under the banner of the religion and generally have a framework built. The second is composed of the semi-well-read men who, for lack of school or professional success, find a means of subsistence in the trade where the request does not miss. On the other hand, the third is a hold-all and is distinguished from the others by a type of trade hastily of

Table 1. Geographical distance, distance-cost, distance-time between Donon Manga and other areas.

Period	Time-distance (h)		Coût-distance	
	Dry	Wet	Dry	Wet
Donon Manag-Laï	2	4	2,500	5,000
Donon Mang-Koumra	2	2	2,500	3,500
Dono Manga-Doba	2	3	3,000	5,000
Donon Manga Bébaloum	3	7	4,500	7,000
Donon-Moundou	4	8	5.000	8,000

Our investigations, 2013

Table 2. Comparative examples of the prices of the products on the markets.

Designation	Price CFA	
	Pharmacy	Market
	Value (FCFA)	
Ceftriaxon	2,500	500
SAT	4,000	300
Palujet	2,000	1,000
Quinine injec.	2,500	1,500
Auréomycine	1,500	600

the pharmaceutical products. They are indicated by the term of Doctor Choukou. The common character of the first group is the use of a part or a room which makes office, at the same time, of room of consultation and medical care. The setting in observation of the patients under the trees and the out-of-stock condition of the products are quite usual. For example, the care center of Ter-Mission which is of the colonists' heritage to supply themselves must make recourse to the leading authorities of the evangelic churches. The response to the request can spend several months. Also, it is found there as a male nurse and an agent first-aid worker. The public ones such as those of Guidari, Darbet and Dar Modehelnagar are not better than the others. They are not equipped and function only with one looking after.

The deficiency of the first group generated a proliferation and made credible another. If the actors of the first await the decision and the means of the higher authorities to supply pharmacy, the independent ones who constitute the second group do not haggle over the means to implement to furnish the Table 1 and 2 case or "stamp". Especially, the trade is profitable which makes them efficacious to the eyes of the peasants. But the quality of services does not reflect appearances. The fact that these actors' group is mainly literate does not justify their knowledge of the domane and health care. In Gaga Mbassa, after having missed several times the baccalaureat, an old Mister of forty withdrew himself at the village to open a health care cabinet where he consults and manages the treatments. Another care center is held in Ter-village by former Pastor. In Darbet, a former "déflaté" soldier exerts the same trade. With the absence of the training in health care, deontology and the practice of the trade which is practiced in the rural mediums, two interpretations with annoying consequences are possible: traumatisms and infirmities to the patients.

By the pecuniary spirit of profitability which animates the experts, the latter can sell to the illiterate peasants, in the search of relieves, of the badly adapted products or of which the period of validity exceeded. Or, they can during the care, miss the veins with the attempts by the perfusion to the physiological serum. The attack of the same vein due to attempts of injection can entail not only traumatism but the damage such as the infirmity of the patient. In the village Kabogo, a pastor's girl lost a part of her right buttock following a missed injection having made the abscess. She spent two months in the hospital complex of Dono Manga before finding health care. During the observations of ground, it was given to us to meet 3 people who suffer from the infirmity due to missed injections.

Certain actors of the zone practice until today the null and void system of health care at risks which consists in

Figure 3. Trade of products in a street. A 12 year old boy hardly holds a trade of products of care of human health.Source: Stereotypes Ndoutorlengar (2012).

Using the materials of work for the treatment of the people after having boiled them. This practice opens the door to the various transmissible infections. The damages caused by the non-professionals' practices are numerous. For example, without knowing the serologic state of a patient, the amateur who poses the perfusion of the serum may entail the death of this one by posing the glucose serum in the place of Ringer, if the patient is diabetic. In Kagama and Ter-Mission, located, respectively at 3 and 7 km of Donon Manga, two young people saw, each one, a part of their penis-tip carried by the blades at the time, in the attempts of circumcision by the amateurs.

The third group is that of the doctors choukou called while still strolling around town. It is composed of people of all horizons, all ages and levels. Their common characteristic is mobility and convincing art. In large bags, they carry pharmaceutical products and cross the public places with the research of the customers instead of the reverse. In the weekly markets, a product, even little known by the carrier, can be commented on and with conceit by this one to be accepted by people not knowing neither to read nor to write.

Supply and risks

The proliferation of the actors of health care in the rural mediums is due to easy access to products, poverty and lack and/or insufficiency of repressions. Before the nineties, on the extent of the territory of Chad, one could find products of health care and buy only in health centers and in pharmacies only on presentation of a medical ordinance. But nowadays, one can find the same products, at least of same name, in markets, streets (Figure 4) and in the shops like ordinary goods. In each market of each city of the country, a place concentrates shops (Figure 5) for the marketing of products of health care. They are of all qualities and any origin. They penetrate by the porous borders of Sudan, Cameroun and Nigeria close countries because Chad does not produce any of these remedies. They are spread through the country to reach today, even the most moved back corners. The increase in the quantity of health care products in the rural mediums has been supported by the reprisals undertaken by the public authorities for 3 years. These latter are only limited in Ndjamena, the capital. Thus, the privileged places of refuges and market are then provinces. Donon Manga is supplied in the large markets of Koumra in Mandoul, Doba in Logone Oriental, Moundou in Logone Occidental and Laï which surround it (Figure 3).

The doubtful origins, the bad conservation and the damage of some of these products are known to all. But the preference of their choice by the consumers is often guided by the weak purchasing power of the population

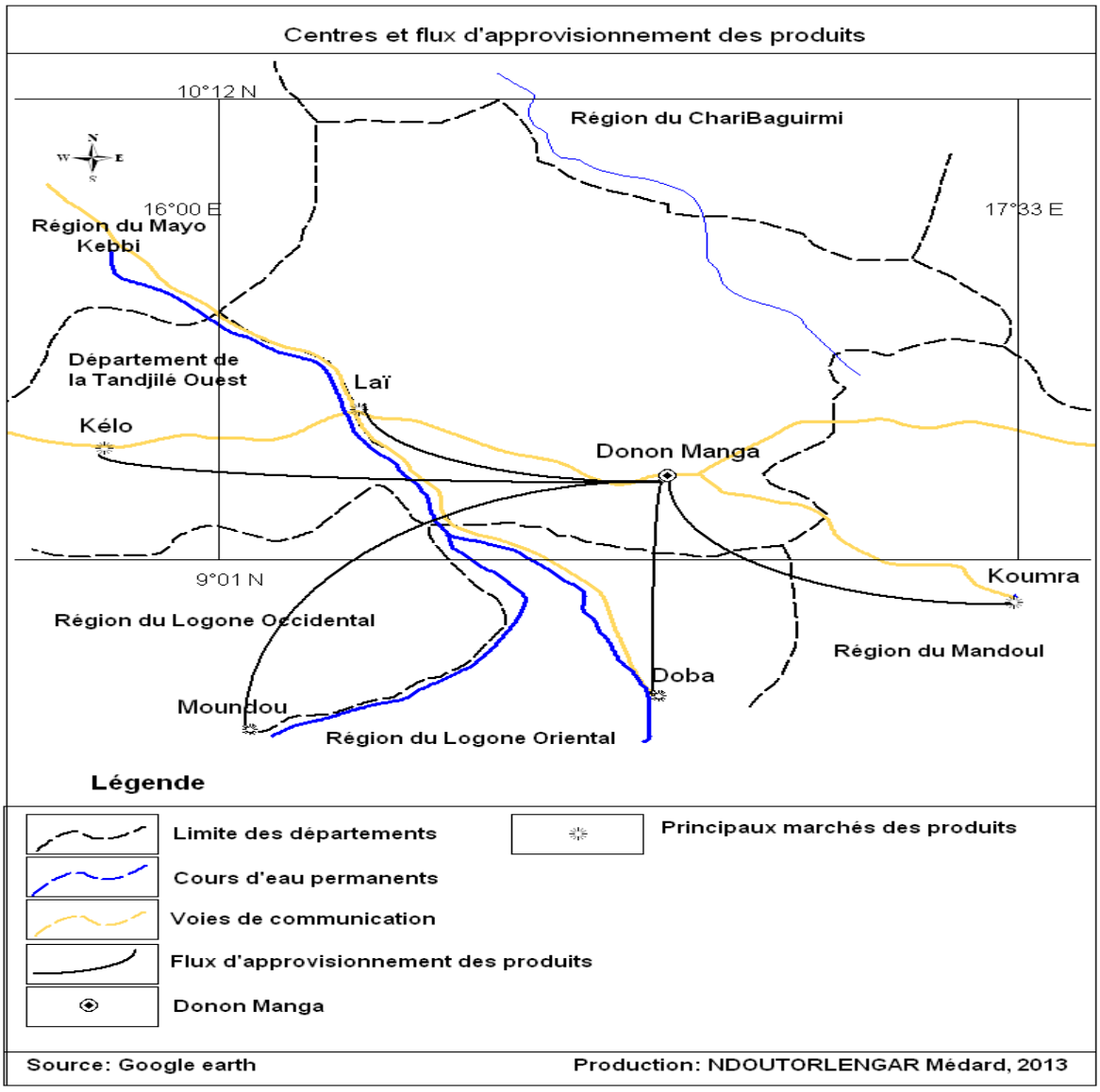

Figure 4. Provisioning and flow of the pharmaceutical products**.**

with equal finality that is to calm the pains or to cure a disease, prices of the products differ according to whether one buys those in the approved pharmacy or market.

The difference between prices of the products paid in the pharmacy and the same bought in the markets is such that it cannot leave indifferent. For example, for the same product ceftriaxon, the one who buys at the market earns four times less expensive than the other who pays in pharmacy. With this price, it arrives sometimes that the legal actors supply themselves in the markets for pharmacies of health centers in making consequent benefit. The expensiveness of the medical care products to pharmacies is legitimate. They are justified by the fact of the loads of hiring, taxation and of the labour to be supported, whereas at the market, the tradesmen are only satisfied to pay the right of place perceived daily by the communes. In this latter, the head of company ensures all the activities which are supposed to generate expenditure.

CONCLUSION AND RECOMMENDATION

In spite of the place of the health sector among the priority ones which profit from the particular investments

Figure 5. A shop of the pharmaceutical products. Ci-high, a trademan discussing the price of products in its shop.An example of the shops which one can find in each market on all the extent of the territory. Source: Stereotypes Ndoutorlengar (2012).

and thanks to the oil incomes, the question of access to human health care in Chad still remains delicate. If in the capital, efforts are agreed, this facade is often betrayed by great insufficiencies in the provinces and the disorders maintained in the rural mediums. In general, in the provinces, the hospital complexes are, not only distant to more than one hundred of kilometers round, but often badly equipped and are lacked, looking after personnel. The insufficiency of the structures and looking after personnel generated a new type of actors who benefit from the faults of the authorities. Poverty, in addition to limiting the access to health care services, entails a preference with the products at lower cost and of quality which does not respect the requirements of the life. To achieve the goals of the millenium to which Chad adhered and of which the Health sector gathers to it, for only items 4, 5 and 6, it is almost imperative to reconsider dimensions of the actions and to re-orientate them when even the cutoff date is less than two years.

Conflict of interest

On behalf of all authors, the corresponding author states that there is no conflict of interest.

REFERENCES

ONU (2002). Premier rapport Pays sur la mise en œuvre de la déclaration des objectifs du millénaire. 4-8.

Ministère de la Santé et des Affaires Sociales (2008). Plan national de développement sanitaire du Tchad 2009-2012. 2:7-46.

PAM (2005). Analyse et cartographie de la vulnérabilité structurelle à l'insécurité alimentaire en milieu rural au Tchad. CSFVA (J-S 2005):17-18

INSEED (2009). Tchad, profil de pauvreté. 2e enquêtes sur la consommation et le secteur informel au Tchad (ECOSIT 2). 4-15.

Ndoutorlengar M (2012). Le coton face à l'arachide : enjeux et perspectives des deux filières concurrentes dans le Mandoul au Tchad. EUE. 241-256.

academicJournals

Vol. 6(11), pp. 347-389, November 2014
DOI: 10.5897/JPHE2014.0629
ISSN 2006-9723
Article Number: 614874747911

http://www.academicjournals.org/JPHE

Journal of Public Health and Epidemiology

Full Length Research Paper

Denoising a model employing automated bandwidth selection procedures and pre-whitened Euclidean-based quadratic surrogates in PROC ARIMA for optimizing asymptotic expansions and simulations of onchocerciasis endemic transmission zones in Burkina Faso

Benjamin G. Jacob[1], Robert J. Novak[1], Laurent Toe[2], Moussas S. Sanfo[2], Rose Tingueria[4], Alain Pare[3], Mounkaila Noma[3], Daniel Griffith[4] and Thomas R. Unnasch[1]

[1]Department of Global Health, College of Public Health, University of South Florida, Tampa, FL, USA.
[2]Multi-Disease Surveillance Centre (MDSC), 1473 Avenue Naba Zombré - Ouagadougou, Burkina Faso.
[3]African Programs for Onchocerciasis Control (APOC), Epidemiology and Vector Elimination, 1473 Avenue Naba Zombré, Ouagadougou, Burkina Faso.
[4]United Nations Office for the Coordination of Humanitarian Affairs (OCHA) Ouagadougou, Burkina Faso.
[5]School of Economic, Political and Policy Sciences. The University of Texas, Dallas, 800 West Campbell Road, Richardson, TX 75080-3021, USA.

Received 15 February, 2014; Accepted 22 August, 2014

In this research we constructed multiple predictive ArcGIS Euclidean distance–based autoregressive infectious disease transmission oriented models for predicting geographic locations of endemic onchocerciasis (“river blindness”) transmission risk zones in Burkina Faso. We employed multiple spatiotemporal-sampled empirical ecological data sets of georeferenced covariates of riverine larval habitats of *Similium damnosum s.l.,* a black fly vector of onchocerciasis and their surrounding villages with their retrospective tabulated prevalence rates. The estimators were regressed employing the modified sum of squares technique. The model also revealed that 5 to 10 km was mesoendemic, 10 to 15 was hypoendemic and after 15 km there was no transmission. Semi-parametric spatial filtering matrices, orthogonal eigenvectors and interpolated endmember signatures can be used to render robust ARIMA risk model residual forecasts by reducing latent unobservable error coefficients in regressed spatiotemporal field-sampled immature *S. damnosum s.l.* density count data for optimizing risk mapping of seasonal onchocerciasis endemic transmission zones.

Key words: Autoregressive integrated moving average (ARIMA), QuickBird, *Similium damnosum s.l.*, onchocerciasis, Burkina Faso.

INTRODUCTION

In predictive autoregressive vector arthropod-related infectious disease transmission-oriented risk-based

statistics, ordinary least squares (OLS) would be amethod for estimating unknown seasonal parameter error estimators in a linear regression-based model (Griffith, 2005). The OLS is a method for estimating the unknown parameters in a linearized regression model (Hosmer and Lemeshew, 2000). This method would minimize the sum of squared vertical distances between the observed responses in the sampled dataset and the responses predicted by the linear approximation. The resulting estimator can then be expressed by a simple formula, especially in the case of a single regressor in a seasonal, vector, arthropod-related, endemic, transmission-oriented, explanatory model. The OLS estimator is consistent when the regressors are exogenous and there is no perfect multicollinearity, and optimal in the class of linear unbiased estimators when the errors are homoscedastic and serially uncorrelated (Cressie, 1993).

Optimally, thereafter, the class of linear, unbiased, seasonal, autoregressive, vector, arthropod-related, infectious disease, parameter estimators would be then homoscedastic and serially uncorrelated. A sequence or a vector of random variables is homoscedastic if all random variables in the sequence or vector have the same finite variance (Cressie, 1993). In a spatiotemporal, predictive, autoregressive, arthropod-related, risk-based, infectious disease distribution model, this would be known as homogeneity of variance (Mcdonald, 2008). Under these conditions, the method of OLS would provide minimum-variance, mean-unbiased, estimation when the endemic, transmission-oriented, regression-based, risk-based distribution model residual error coefficients have finite variances. Unfortunately, when employing an autoregressive prediction model for quantitating georeferenced, predictive, seasonal, vector, arthropod-related, spatially, error-prone, explanatory, predictor variables from past time-series, dependent, covariate, coefficient, indicator values for the forecasting equation must be initialized in order to fit the explanatory, observational predictors, employing OLS estimates for ascertaining robust inferences.

Fortunately, an eigenvector spatial filtering procedure can capture dependence based on the standard OLS estimator and is apart from the assumptions of independence and constant variance of the disturbances, a distribution freely owed to the Gauss Markov theorem. The Gauss Markov theorem states that in a linearized regression model in which the errors have expectation zero and are uncorrelated and have equal variances, the best linear, unbiased estimator of the sampled, covariate, coefficient indicator values would be provided by the OLS estimator *(*Aitken, 1935). This non-parametric spatial filtering approach can employ eigenvectors that are extracted from a transformed spatial link matrix for quantizing time-series, dependent, arthropod-related, autoregressive, infectious disease, transmission-oriented, risk-based, model residual autocorrelation error coefficients. The spatial, filtering estimator is fairly robust to endemic, transmission-oriented, model specification uncertainties compared with a spatial maximum likelihood estimator (McDonald, 2008). Commonly, assumptions of asymptotic properties of the maximum likelihood estimator and the quasi-maximum likelihood estimator have been employed for deducing parameter estimator significance in spatial autoregressive models (Cressie, 1993). For example, asymptotic expansions in a spatiotemporal, arthropod-related infectious disease, transmission-oriented risk-based stochastic interpolator would be represented as an increasing-domain asymptotic as it would be based on increasingly dense observational predictors in a fixed and bounded region.

In this research, we employed a space–time eigen decomposition spatial filter algorithm and multivariate autoregressive integrated moving average (ARIMA) for identifying onchocerciasis, endemic-oriented, transmission zones by quantitating a large, ecological, empirical dataset of georeferenced, riverine black fly larval habitat of *Similium damnosum s.l.* (that is, capture point) spatiotemporally-sampled in a study site in Burkina Faso.

Simuliidae or black flies in the *Simulium damnosum* Theobald complex are the only insect vectors of human onchoceriasis in West African countries (www.who.gov).ARIMA models are, in theory, the most general class of models for forecasting a time-series which can be stationarized by transformations such as differencing and logging. In fact, the easiest way to think of ARIMA models is as fine-tuned versions of random-walk and random-trend models: the fine-tuning consists of adding lags of the differenced series and/or lags of the forecast errors to the prediction equation, as needed to remove any last traces of autocorrelation from the forecast errors (Cressie 1993). In West Africa, members of *Simulium damnosum* complex are the only known vectors of human onchocerciasis (Crosskey 1960). Onchocerciasis a parasitic disease caused by infection by *Onchocerca volvulus*, a nematode (roundworm) which is the world's second-leading infectious cause of blindness. The parasite is transmitted to humans through the bite of a blackfly of the genus *Simulium* commonly found in fast flowing rural river ecosystems. *Similium* larval stages are commonly found in running water where Precambrian rocks break the water surface and the turbulence of the water results in a higher level of oxygenation (Crosskey 1960).

Our assumption was that spatial dependence in the *S.*

*Corresponding author. E-mail: bjacob1@.health.usf.ed.

damnosum s.l. riverine larval habitat in the data was from unobservable latent predictor variables that were correlated. Spatial dependence is the existence of statistical dependence in a collection of random variables or a collection time series of random variables, each of which is associated with a different geographical location (Goodchild, 1980). This dependence is naturally formulated within the framework of hierarchical, spatiotemporal, arthropod-related, infectious, disease, parameter estimator models and over the past decade, a variety of spatial models have been proposed for quantitating the latent level(s) of the hierarchy in these models. This is because dependence is of prime impor-tance in these applications where it is quite reasonable to postulate the existence of corresponding set of random variables at specific endemic transmission zones (for example, hyperendemic) that have not been included in a sample. Unfortunately, the specific issues posed by the sparseness of competent error estimators in predictive algorithms for arthropod-related infectious disease related data for quantitating local spatial dependence have not been thoroughly addressed in literature.

As such, initially, in this research, a georeferenced immature *S. damnosum s.l*. riverine habitat capture point was overlaid onto QuickBird visible and near-infra-red (NIR) (www.digitalglobe.com) data based on stratified geographical locations at 5, 10 and 15 km Euclidean-based distances from a capture point. Numerous studies have been undertaken using satellite-derived environmental data to predict the distribution, abundance and prevalence of diseases and their vectors, including malaria (Hay et al., 2000; Rogers et al., 2002), leishmaniasis (Elnaiem et al., 2003), filariasis (Lindsay and Thomas, 2000), trypanosomiasis (Rogers, 2000) and schistosomiasis (Brooker et al., 2001; Malone et al., 2001; Brooker et al., 2002a, 2002b; Moodley et al., 2003; Kabatereine et al., 2004). Univariate and Poisson regression models were then constructed for each delineated transmission zone. Thereafter, an autoregressive approach was employed to spatially extrapolate the existence of any residualized stochastic processes in the mean of the regression models.

Euclidean, distant-based, explanatory measurements were generated in ArcGIS spatial analyst from the georeferenced *S. damnosum s.l.,* riverine, larval habitat capture point which was then employed to delineate the endemic, transmission-oriented zones thresholds at the study site, employing stratified prevalence rates as independent variables in the regression-based estimation matrices. The asymptotic distribution of an empirical dataset of georeferenced, standardized, linear model parameter estimators were then derived to detect if the serially correlated latent processes were present in the ArcGIS Euclidean distant-based measurements. This technique qualitatively assessed the time series dependence in the spatiotemporal-sampled dataset of explanatory, predictor, covariate, coefficient estimates which were then log-transformed into Gaussian independent variables. These covariate coefficients were then exported into an autoregressive, uncertainty, probabilistic estimation model framework in SAS/GIS. Currently, within SAS/GIS the ARIMA procedure provides parameter estimation for constructing autoregressive integrated moving average (that is, Box-Jenkins) models, seasonal ARIMA models, transfer function models and intervention models (www.sas.edu).

Prior to mapping the onchocerciasis-related variables, exploratory spatial data analysis (ESDA) tools in ArcGIS were used to assess the statistical properties of the field-sampled data. Having explored the data, we created a variety of output map types (that is, prediction, error of prediction, probability and quantile) using a variant of a stochastically-based, kriged-based, explanatory algorithm (that is an, ordinary interpolator) and associated tools (for example, data transformation, declustering and detrending). Our research also considered the construction of specific parameter estimators of regression coefficients in a linear regression model, employing stochastically oriented a priori information. A priori information can be framed as stochastic restrictions (Cressie, 1993). In this research, the dominance conditions of the estimators were derived under the criterion of mean squared error matrix. Simple probabilistic and disjunctive formulas for quantitating the effect of the estimated predictive, residual, standard, autocovariance error variables were then generated. Thereafter, we adjusted the bias in eigenspace using spatiotemporal-sampled Euclidean, distance-based parameter estimators for deriving precise endemic transmission zones (that is, 5, 10 and 15 km) as depicited by the ArcGIS delineated maps created from the georeferenced, riverine *S. damnosum s.l.* riverine larval habitat capture point. We employed spatiotemporal-sampled data obtained from the African Programme for Onchocerciasis Control (APOC, 1974–2002) for remotely constructing our robust, endemic,*S. damnsoum s.l,.* riverine topographic, riverine –based landscape forecasting risk models. Large scale control of onchocerciasis commenced over three decades ago, initially through the Onchocerciasis Control Programme in West Africa (OCP, 1974–2002), and more recently by the African Programme for Onchocerciasis Control (APOC, 1995–2010). The goals of OCP were to eliminate onchocerciasis as a public health problem and to mitigate its negative impact on the social and economic development of affected regions (Toe, 1993). The strategic objective of APOC is to permanently protect the remaining 120 million people at risk of this debilitating and disfiguring disease in 19 countries in Africa through the establishment of community-directed treatment with ivermectin (CDTI) that is capable of being sustained by the communities after APOC financing has ended.

Additionally, in this research, robust, predictive endmember signatures were generated from a spectrally decomposed georeferenced, *S. damnosum s.l.,* riverine

Figure 1. Map of Burkina Faso.

larval habitat capture point using QuickBird mixel data, employing multiple un-mixing models and object-based classifiers (for example, Li –Strahler geometric –optical model, ENVI's Spectral Angular Mapper). Because of the design specifications of sensors, rarely, if ever does the spatial resolution match the size of an item on the ground; when one pixel includes the signatures of two or more endmembers, it is considered a mixed pixel or a 'mixel' (Jensen, 2005). In this research, the endmembers derived were stochastically interpolated for identifying unknown, unsampled riverine, larval habitats along the study site corridor. The analyses also included the spatial-spectral, endmember extraction algorithm (SSEE), which was employed using the SPA. Our assumption was that by interpolating unmixed, sub-meter, resolution, sub-mixel, image, riverine, larval, habitat, capture point endmember, emissivity spectra extracted from various unmixing algorithms in a least squares estimation algorithm, the residual would reveal unsampled *S damnosum s.l.,*riverine larval habitats and their within canopied features (for example, Precambrian rock and ripple water). Spectral unmixing algorithms have proliferated in a variety of ecological disciplines by exploiting remotely sensed data (Jensen, 2005).

Therefore, this research objectives were to: (1) Remotely display all spatiotemporal, seasonal-sampled, empirical empirical, ecological-based, *S. damnosum s.l.*- related spatial feature attributes with their surrounding riverine–based communities using QuickBird visible and near infra-red (NIR) data; (2) construct multiple predictive, autoregressive models employing time series-dependent, explanatory, covariate coefficients; (3) spectrally extract and decompose a QuickBird mixel to derive and classify endmember emissivity spectra for interpolating a target signature; (4) construct residual uncertainty covariance matrices based on regression-derived observational predictors and; (4) adjust any bias in the Euclidean distance–based parameter estimators at distances of 5, 10 and 15 km from a capture point to generate a robust, autoregressive, endemic, transmission-oriented, predictive risk map, delineating onchocerciasis-related endemic transmission zones at a georeferenced, epidemiological riverine study site in Burkina Faso.

METHODOLOGY

Study site

Burkina Faso is a landlocked country in West Africa. It is surrounded by six countries: Mali to the north, Niger to the east, Benin to the southeast, Togo and Ghana to the south, and Côte d'Ivoire to the southwest (Figure 1) . Its size is 274,200 km^2 (105,900 sq. m)

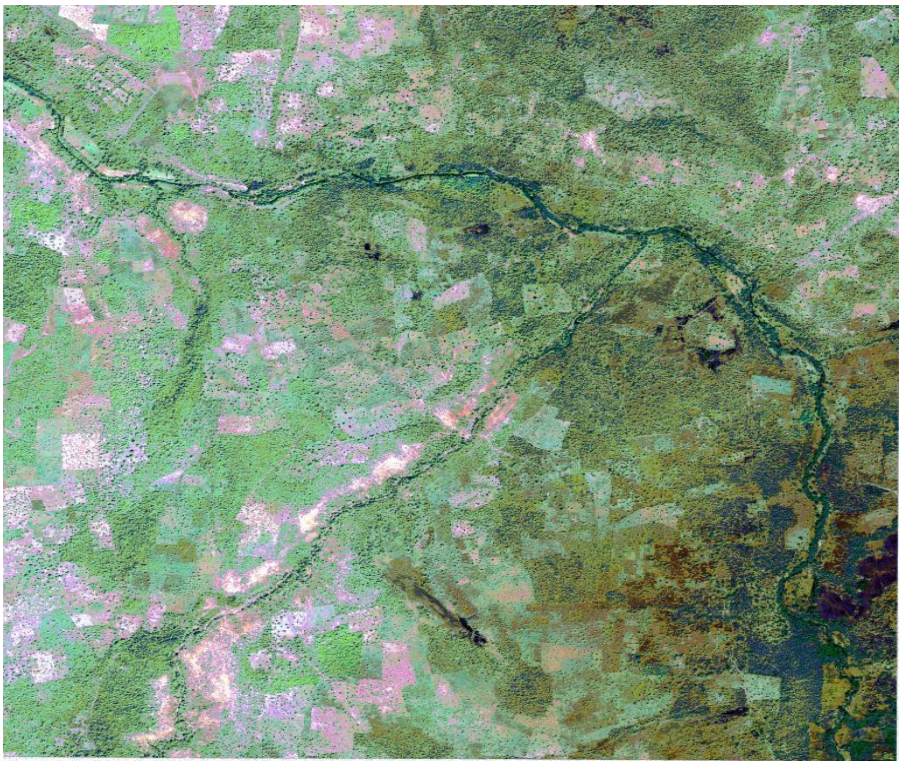

Figure 2. QuickBird visible and near infra-red data for the Chutes-Dienkoa study site.

with an estimated population of more than 15,757,000. Total land area is 274,200 km² of which water covers approximately 400 km². Burkina Faso has three distinct seasons: warm and dry (November to March), hot and dry (March to May), and hot and wet (June to October). Annual rainfall varies from about 250 mm to 1,000 mm in the riverine study site region. The terrain is mostly flat, with undulating plains and hills. Most of the study site region lies on a savanna plateau, with fields, brush and scattered tree. Burkina Faso lies mostly between latitudes 9° and 15°N (a small area is north of 15°), and longitudes 6° W and 3° E. It is made up of two major types of countryside. The larger part of the country is covered by a peneplain, which forms a gently undulating landscape with, in some areas, a few isolated hills, the last vestiges of a Precambrian Massif. The Southwest of the country, on the other hand, forms a sandstone massif, where the highest peak, Ténakourou, is found at an elevation of 749 m (2,457 ft). The massif is bordered by sheer cliffs up to 150 m (492 ft) high. The average altitude of Burkina Faso is 400 m (1,312 ft) and the difference between the highest and lowest terrain is no greater than 600 m (1,969 ft). Burkina Faso is therefore a relatively flat country. The country owes its former name of Upper Volta to three rivers which crosses it: the Black Volta the White Volta and the Red Volta. The Black Volta is one of the country's only two rivers which flow year-round, the other being the Komoé, which flows to the southwest. The basin of the Niger River also drains 27% of the country's surface. The Niger's tributaries – the Béli, the Gorouol, the Goudébo and the Dargol are seasonal streams and flow for only four to six months a year.

Remote sensing data

Raster image data from the DigitalGlobe QuickBird satellite service were acquired for the study site for the periods of 15th July, 2010, within the riverine study site area (Figure 2). In this research the QuickBird image data were delivered as pan-sharpened composite products in infra-red (IR) colors. QuickBird multispectral products provided four discrete non-overlapping spectral bands in the 0.45 to 0.72 µm range. The QuickBird sensors were able to identify dug wells that were 1 to 2 cm in depth. Results revealed that well-digging was practiced on 387 (1.4%) rainfed land cover classified areas, 15,638 (54.7%) with the majority located in dryer arid regions. The field-plot revealed an accuracy of 92% with an error of omission and commission of less than 10%. Only the clearest, cloud-free imagery was available of the contiguous sub-areas of the study site. The Order Polygon contained 5 vertices consisting of longitude/latitude (decimal degrees) geographic coordinates using a WGS-84 ellipsoid. The satellite data contained 64 km^2 of the land cover in the riverine epidemiological study site. The QuickBird imagery was classified using the Iterative Self-Organizing Data Analysis Technique (ISODATA) unsupervised routine in ERDAS *Imagine* v.8.7™ (ERDAS, Inc., Atlanta, Georgia). A base map of the riverine study site was then generated in ArcGIS using the QuickBird data and differentially corrected global positioning systems (DGPS) ground coordinates of the spatiotemporal-sampled *S. damnsoum s.l.* habitat epidemiological capture point and the surrounding georeferenced villages (Figure 3).

The DGPS were acquired from a CSI max receiver which has a positional accuracy of +/- 0.178. (http://www.omnistar.com/). Using a local DGPS broadcaster can compensate for ionospheric and ephemeris effects which can improve horizontal accuracy significantly and can bring altitude error down in a predictive vector insect habitat model (Jensen, 2005). Each georeferenced *S.damnosum s.l.* habitat was entered into the VCMS™ relational database software product (Clarke Mosquito Control Products, Roselle, IL). The VCMS™ database supports a mobile field data acquisition component module called Mobile VCMS™ that synchronizes field-sampled arthropod-related data from industry standard Microsoft Windows Mobile™ devices and can support

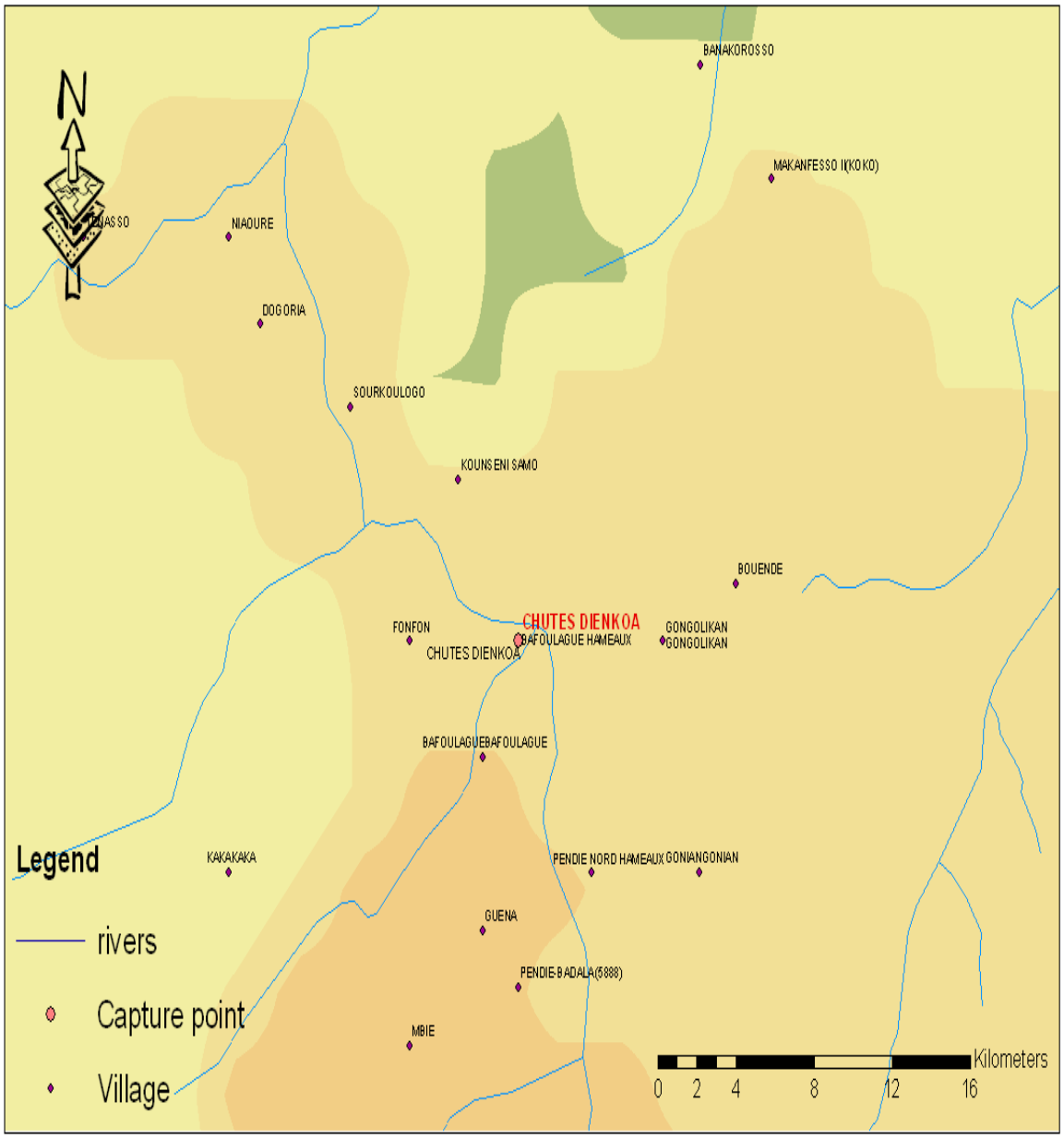

Figure 3. Base map of the sampled study site capture point and surrounding epidemiological sampled riverine villages.

add-on DGPS data collection (Jacob et al., 2008b, c). A digitized grid-based algorithm was then constructed in ArcGIS by applying a mathematical algorithm in order to fit the continuous and bounded sampled larval habitat surfaces from a field-sampled attribute. A grid is a raster data storage format native to ESRI (www.esri.com) (Figure 3).

Environmental parameters

Multiple observational georeferenced explanatory observational predictors were then examined extensively using longitude, latitude, and altitude data (Table 1). The criteria involved the centrographic measures of spatial mean and distance between the epidemiological prevalence stratified villages and the georeferenced capture point. The data was also comprised of individual spatiotemporal-sampled observations of *S. damnosums.l.* habitat capture point together with a battery of categorical attribute measures which were expanded to include multiple, endemic, transmission-oriented, risk-based, explanatory, predictor, covariate, coefficient estimates.

The habitat distances were then measured as Euclidean distances in the ArcGIS projection units of the raster which computed the digitized grid cell matrix. The Euclidean distance output raster contained the measured distances. The Euclidean distance functions provided information according to Euclidean or straight-line distance between georeferenced epidemiological villages and from the riverine capture point to the villages (that is, geometric

Table 1. Environmental predictor variables sampled at the epidemiological capture point.

Variable	Description	Units
GCP	Ground control points	Decimal-degrees
FlOW	flowing water	Presence or absence
HGHT	Height of water	-
TURB	Turbidity of water	Formazin Turbidity Unit
AQVEG	Aquatic vegetation	Percentage
HGVEG	Hanging vegetation	Percentage
DDVEG	Dead vegetation	Percentage
RCKS	Rocks	Percentage
MMB	Man-made barriers	Type (damns, bridges)
DISHAB	Distance between habitats	Meters

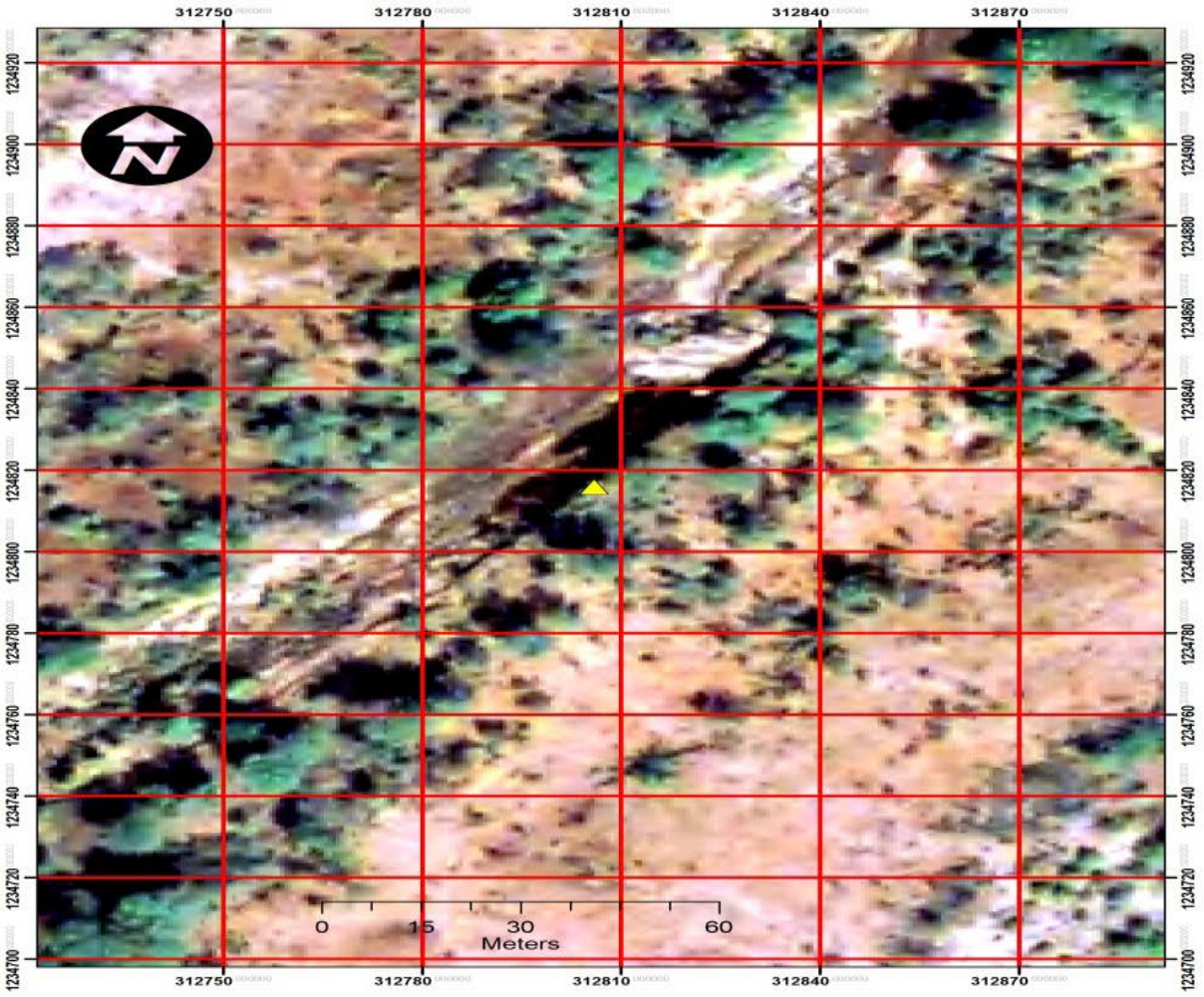

Figure 4. An ArcGIS digitized grid matrix overlaid onto the georeferenced *S. damnosum s.l.* riverine habitat capture point.

distances in the multidimensional space). In this research, the Euclidean distances were computed as: distance (x,y) = $\{ \sum_i (x_i - y_i)^2 \}^{½}$. Every cell in the Euclidean allocation output raster was the then assigned the value of the source to which it was closest. The nearest source was then determined by the Euclidean distance function in ArcGIS®. This function assigned space between the georeferenced *S. damnosums.l*. riverine habitat capture point and the villages with their stratified prevalence rates. The Euclidean direction output raster contained the Azimuth direction from each grid cell centroid to the nearest source. Then the Euclidean allocation function identified the nearest human habitation center closest to each grid cell. The distance between sampled and human habitation areas were then categorized into numerous classes (for example, 1: 0 to 5 km, 2: 5 to 10 km and 10 to 15 km) Figure 4.

Regression model

Poisson models were constructed for determining significance levels of the Euclidean distance-based explanatory covariates and the other endemic transmission-oriented LULC attributes in SAS GEN MOD. The Poisson process was provided by the limit of a binomial distribution of the spatiotemporal-sampled, covariate, coefficient estimates within each distance boundary set at 5 km intervals from the capture point up to a maximum distance of 15 km employing:

$$P_p(n \mid N) = \frac{N!}{n!\,(N-n)!}\, p^n\,(1-p)^{N-n}. \quad (1).$$

Prevalence rates were used as the response variable in the models. We viewed the distribution as a function of the expected number of e predictor variables sampled employing the sample size*N* for quantifying the fixed *p* in equation (1), which then was transformed into the linear equation:

$$P_{\nu/N}(n \mid N) = \frac{N!}{n!\,(N-n)!}\left(\frac{\nu}{N}\right)^n\left(1-\frac{\nu}{N}\right)^{N-n},$$

Based on the sample size *N*, the distribution approached $P_\nu(n)$ in this research was expressed as:

$$\lim_{N\to\infty} P_p(n \mid N) \lim_{N\to\infty} \frac{N(N-1)\cdots(N-n+1)}{n!}\,\frac{\nu^n}{N^n}\left(1-\frac{\nu}{N}\right)^N\left(1-\frac{\nu}{N}\right)^{-n} = \lim_{N\to\infty} \frac{N(N-1)\cdots(N-n+1)}{N^n}\,\frac{\nu^n}{n!}\left(1-\frac{\nu}{N}\right)^N\left(1-\frac{\nu}{N}\right)^{-n}$$

$$= 1\cdot\frac{\nu^n}{n!}\cdot e^{-\nu}\cdot 1 = \frac{\nu^n\, e^{-\nu}}{n!},$$

The GENMOD procedure then was used to fit multiple generalized linear models (GLMs) equations to the sampled riverine epidemiological data by maximum likelihood estimation of the parameter vector β. In this research the GENMOD procedure estimated the explanatory covariate coefficients of each Euclidean distance-based model at 5, 10 and 15 km numerically through an iterative fitting process. The dispersion parameter was then estimated by the residual deviance and by employing the product of Pearson's chi-square divided by the degree of freedom (d.f.) in the model. Covariances, standard errors, and *p*-values were then computed for the estimated explanatory, observational, predictor at each distant-dependent, geographical location based on the asymptotic normality derived from the maximum likelihood estimation. Note that the sample size *N* completely dropped out of the probability function, which in this research had the same functional form for all the spatiotemporal-sampled, distant-dependent parameter estimator values (that is, ν). As expected, the Poisson distribution was normalized so that the sum of probabilities equaled 1 (Haight, 1967). The ratio of probabilities was then:

$$\sum_{n=0}^{\infty} P_\nu(n) = e^{-\nu}\sum_{n=0}^{\infty}\frac{\nu^n}{n!} = e^{-\nu}\,e^{\nu} = 1. \quad \text{provided by:} \quad \frac{P_\nu(n=i+1)}{P(n=i)} = \frac{\frac{\nu^{i+1}\,e^{-\nu}}{(i+1)!}}{\frac{e^{-\nu}\,\nu^i}{i!}} = \frac{\nu}{i+1}.$$

The Poisson distribution revealed that the covariate coefficients reached a maximum when: $\frac{d\,P_\nu(n)}{d\,n} = \frac{e^{-\nu}\,n\,(\gamma - H_n + \ln\nu)}{n!} = 0,$

where γ was the Euler-Mascheroni constant and H_n was a harmonic number, leading to the transcendental equation: $\gamma - H_n + \ln\nu = 0$.

The model revealed that the Euler-Mascheroni constant arose in the integrals as:

$$\gamma = -\int_0^\infty e^{-x}\ln x\,dx = -\int_0^1 \ln\ln\left(\frac{1}{x}\right)dx = \int_0^\infty\left(\frac{1}{1-e^{-x}}-\frac{1}{x}\right)e^{-x}\,dx = \int_0^\infty\frac{1}{x}\left(\frac{1}{1+x}-e^{-x}\right)dx \quad (2).$$

Commonly, integrals that render γ in combination with temporal constants include:

$$\int_0^\infty e^{-x^2}\ln x\,dx = -\tfrac{1}{4}\sqrt{\pi}\,(\gamma+2\ln 2) \text{ and } \int_0^\infty e^{-x}(\ln x)^2\,dx = \gamma^2 + \tfrac{1}{6}\pi^2.$$ (Haight 1967).

Thereafter, the double integrals in the distant-based regression models included:

$$\gamma = \int_0^1\int_0^1 \frac{x-1}{(1-x\,y)\ln(x\,y)}\,dx\,dy$$

An interesting analog of equation (2) in the models was then provided by:

$$\ln\left(\frac{4}{\pi}\right)_{=}\sum_{n=1}^{\infty}(-1)^{n-1}\left[\frac{1}{n}-\ln\left(\frac{n+1}{n}\right)\right]\Big|_{=}\int_0^1\int_0^1\frac{x-1}{(1+x\,y)\ln(x\,y)}\,dx\,dy_{=}0.241564\ldots\gamma.$$

This solution was also provided by incorporating Mertens theorem:

$$e^{\gamma}=\lim_{n\to\infty}\frac{1}{\ln p_n}\prod_{i=1}^{n}\frac{1}{1-\frac{1}{p_i}},$$

[i.e.,]

where the product was aggregated over the sampled explanatory, predictor,covariate, coefficient values found in the ecological datasets. Mertens' 3rd theorem:

$$\lim_{n\to\infty}\ln n\prod_{p\le n}\left(1-\frac{1}{p}\right)=e^{-\gamma},$$

is related to the density of prime numbers, where γ is the Euler–Mascheroni constant. By taking the logarithm of both sides in the regression models, an explicit formula for γ was then dervived using:

$$\gamma=\lim_{x\to\infty}\left[\sum_{p\le x}\ln\left(\frac{1}{1-\frac{1}{p}}\right)-\ln\ln x\right].$$

This product was also given by series due to Euler, which followed from equation (2) by first replacing:

$\ln n$ by $\ln(n+1)$, in the equation $\gamma=\sum_{k=1}^{\infty}\left[\frac{1}{k}-\ln\left(1+\frac{1}{k}\right)\right]$ and then generating $\lim_{n\to\infty}[\ln(n+1)-\ln n]=\lim_{n\to\infty}\ln\left(1+\frac{1}{n}\right)=0,$.

We then substituted the telescoping sum: $\sum_{k=1}^{n}\ln\left(1+\frac{1}{k}\right)$ for $\ln(n+1)$ which rendered $\ln\left(1+\frac{1}{k}\right)=\ln(k+1)-\ln k$.

Thereafter, we obtained: $\lim_{n\to\infty}\left[\sum_{k=1}^{n}\frac{1}{k}-\sum_{k=1}^{n}\ln\left(1+\frac{1}{k}\right)\right]_{\gamma=}\lim_{n\to\infty}\sum_{k=1}^{n}\left[\frac{1}{k}-\ln\left(1+\frac{1}{k}\right)\right]$

Additionally, other series in the distant-based regression models included the equation (∩) where:

$$\gamma=\sum_{n=2}^{\infty}(-1)^n\frac{\zeta(n)}{n}=\ln\left(\frac{4}{\pi}\right)+\sum_{n=1}^{\infty}\frac{(-1)^{n-1}\,\zeta(n+1)}{2^n\,(n+1)}$$

and where $\zeta(z)$ was $\gamma=\sum_{n=1}^{\infty}(-1)^n\frac{\lfloor \lg n\rfloor}{n}$ and the Riemann zeta function. The Riemann zeta function ζ(s), is a function of a complex, explanatory, predictor variables that analytically continues the sum of the infinite series: $\sum_{n=1}^{\infty}\frac{1}{n^s},$

which converges when the real part of *s* is greater than 1 where lg is the logarithm to base 2 and $\lfloor x\rfloor$ is the floor function (see Haight 1967).

In this research $\binom{n}{k}$ was employed as a binomial coefficient, and then it was rearranged to achieve the conditionally convergent series in our Euclidean, distant-based, endemic, transmission-oriented, regression-based, epidemiological, predictive, risk model as the plus and minus terms were first grouped in pairs of the sampled covariate coefficients using the resulting series of the actual seasonal-sampled values. The double series was thereby equivalent to Catalan's integral:

$$\gamma = \int_0^1 \frac{1}{1+x} \sum_{n=1}^{\infty} x^{2^n-1}\, dx.$$

[i.e.,]

Catalan's integrals are a special case of general formulas due to:

$$J_0\left(\sqrt{z^2-y^2}\right) = \frac{1}{\pi}\int_0^{\pi} e^{y\cos\theta}\cos(z\sin\theta)\, d\theta,$$

where $J_0(z)$ is a Bessel function of the first kind. The Bessel function is a function $Z_n(x)$ defined in a robust regression model by employing the recurrence relations:

$$Z_{n+1} + Z_{n-1} = \frac{2n}{x} Z_n \quad \text{and} \quad Z_{n+1} - Z_{n-1} = -2\frac{dZ_n}{dx}.$$

solutions and quantify heteroskedastic parameters in a spatiotemporal regression models using the differential equation: $x^2\frac{d^2y}{dx^2} + x\frac{dy}{dx} + \left(x^2-n^2\right)y = 0.$ (Haight 1967), which more recently has been employed to define (Ross, 2007).

In this research the Bessel function $J_n(z)$ was defined by the contour integral:

$$J_n(z) = \frac{1}{2\pi i}\oint e^{(z/2)(t-1/t)}\, t^{-n-1}\, dt,$$

where the contour enclosed the origin and was traversed in a counterclockwise direction. This function generated:

$$J_0\left(2i\sqrt{z}\right) = \frac{1}{\pi}\int_0^{\pi} e^{(1+z)\cos\theta}\cos\left[(1-z)\sin\theta\right] d\theta.$$

where $z \equiv 1 - z'$ and $y \equiv 1 + z'$. Thereafter, to quantify the equivalence in the sampled empirical dataset of the regression-based parameter estimators, we expanded $1/(1+x)$ in a geometric series and multiplied the district-level sampled data by x^{2^n-1}, and integrated the term wise as in Sondow and Zudilin (2006). Other series for γ then included:

$$\gamma = \frac{3}{2} - \ln 2 - \sum_{m=2}^{\infty}(-1)^m \frac{m-1}{m}\left[\zeta(m) - 1\right] \quad \text{and} \quad \gamma = \frac{2^n}{e^{2^n}}\sum_{m=0}^{\infty}\frac{2^{mn}}{(m+1)!}\sum_{t=0}^{m}\frac{1}{t+1} - n\ln 2 + O\left(\frac{1}{2^n e^{2^n}}\right),$$

A rapidly converging limit for γ was then provided by: $\gamma = \lim_{n\to\infty}\left[\frac{2n-1}{2n} - \ln n + \sum_{k=2}^{n}\left(\frac{1}{k} - \frac{\zeta(1-k)}{n^k}\right)\right] =$ $\lim_{n\to\infty}\left[\frac{2n-1}{2n} - \ln n + \sum_{k=2}^{n}\frac{1}{k}\left(1 + \frac{B_k}{n^k}\right)\right]$, where B_k was a Bernoulli number.

Another limit formula was then provided by the equation:

$$\gamma = -\lim_{n\to\infty}\left[\frac{\Gamma\left(\frac{1}{n}\right)\Gamma(n+1)\, n^{1+1/n}}{\Gamma\left(2+n+\frac{1}{n}\right)} - \frac{n^2}{n+1}\right]$$

Limits to the model was then rendered by:

$$\gamma = \lim_{x\to\infty}\zeta(\zeta(z)) - 2^x + \left(\frac{4}{3}\right)^x + 1$$

where $\zeta(z)$ was the Riemann zeta function. Another model output was rendered from the endemic transmission-oriented regression-based equation which was generated by $d(n) = \sigma_0(n)$ for the linearly, quantitated, explanatory, covariate coefficient numerical values in the empirical dataset 1 to n in the sampled dataset which in this research was found to be asymptotic to:

$$\frac{\sum_{k=1}^{n} d(k)}{n} \sim \ln n + 2\gamma - 1$$

An elegant identity for γ in our regression models was then provided by:

$$\gamma = \frac{S_0\,(z) - K_0\,(z)}{I_0\,(z)} - \ln\left(\tfrac{1}{2}\,z\right),$$

Where $I_0\,(z)$ was a modified Bessel function of the first kind, $K_0\,(z)$ was a modified Bessel function of the second kind, and:

$$S_0\,(z) \equiv \sum_{k=0}^{\infty} \frac{\left(\frac{1}{2}\,z\right)^{2\,k} H_k}{(k!)^2},$$

where H_n was a harmonic number. This provided an efficient iterative algorithm for γ by computing:

$$B_k = \frac{B_{k-1}\,n^2}{k^2}, A_k = \frac{1}{k}\left(\frac{A_{k-1}\,n^2}{k} + B_k\right), U_k V_k = U_{k-1} + A_k \text{ and } V_k = V_{k-1} + B_k \text{with } A_0 = -\ln n B_0 = 1 U_0 = A_0 \text{ and } V_0 = 1.$$

Reformulating this identity rendered the limit in our endemic, transmission-oriented, regression-based,risk model as:

$$\lim_{n\to\infty}\left[\sum_{k=0}^{\infty} \frac{\left(\frac{n^k}{k!}\right)^2 H_k}{\sum_{k=0}^{\infty}\left(\frac{n^k}{k!}\right)^2} - \ln n\right] = \gamma$$

.

In this research, infinite products involving γ also arose from the Barnes G-function using the sampled, explanatory, covariate coefficients. In mathematics, the Barnes G-function *G*(*z*) is a function that is an extension of super factorials to the complex numbers which is related to the Gamma function. In this research, this function provided:

$$\prod_{n=1}^{\infty} e^{-1+1/(2\,n)}\left(1+\frac{1}{n}\right)^n = \frac{e^{1+\gamma/2}}{\sqrt{2\,\pi}} \text{ and } \prod_{n=1}^{\infty} e^{-2+2/n}\left(1+\frac{2}{n}\right)^n = \frac{e^{3+2\,\gamma}}{2\,\pi}.$$

The Barnes *G*-function was thereafter linearly defined in our time-series, dependent,endemic, transmission-oriented distribution, risk model which was then defined by using the product of:

$$G(z+1) = (2\pi)^{z/2}\exp(-(z(z+1)+\gamma z^2)/2) \times \prod_{n=1}^{\infty}\left[\left(1+\frac{z}{n}\right)^n \exp(-z+z^2/(2n))\right],$$

Where γ was the Euler–Mascheroni constant, exp(*x*) = e^x, and ∏ was the capital pi notation. The Euler-Mascheroni constant was thereafter rendered by the expressions $\gamma = -\Gamma'\,(1) = -\psi_0\,(1)$, where $\psi_0\,(x)$ was the digamma function:

$$\gamma = \lim_{s\to 1}\left[\zeta\,(s) - \frac{1}{s-1}\right] \text{ and the symmetric limit form of: } \gamma = \lim_{s\to 1^+}\sum_{n=1}^{\infty}\left(\frac{1}{n^s} - \frac{1}{s^n}\right) \text{and } \gamma = \lim_{x\to\infty}\left[x - \Gamma\left(\frac{1}{x}\right)\right]$$

The digamma function was then defined as the logarithmic derivative of the gamma function: $$\psi(x) = \frac{d}{dx}\ln\Gamma(x) = \frac{\Gamma'(x)}{\Gamma(x)}.$$

where it was the first of the polygamma functions in the endemic, transmission-oriented, regression-based, risk-related model. The digamma function, often denoted as $\psi_0(x)$, $\psi^0(x)$ is related to the harmonic numbers in a seasonal, infectious disease, arthropod-related, risk model in that $\psi(n) = H_{n-1} - \gamma$ where H_n is the n^{th} harmonic number, and γ is the Euler-Mascheroni constant (Jacob et al., 2012a). For half-integer values, the digamma function may be expressed as: $\psi\left(n+\frac{1}{2}\right) = -\gamma - 2\ln 2 + \sum_{k=1}^{n}\frac{2}{2k-1}$ (Hosmer and Lemeshow, 2000).

The digamma function in our model was denoted as $\psi_0(x)$ which was related to the harmonic numbers in $\psi(n) = H_{n-1} - \gamma$ when H_n was the n^{th} harmonic number, and γ was the Euler-Mascheroni constant. It had the integral representation:

$$\psi(x) = \int_0^\infty \left(\frac{e^{-t}}{t} - \frac{e^{-xt}}{1-e^{-t}} \right) dt$$

In this research this expression was written as: $$\psi(s+1) = -\gamma + \int_0^1 \frac{1-x^s}{1-x} dx$$ which followed from Euler's integral formula for the harmonic numbers derived from the linear endemic transmission regression-based risk-related model. In this research the Digamma of the linearized *S. damnosum s.l.* endemic-transmission-oriented risk-related model was computed in the complex plane, using:

$$\psi(z+1) = -\gamma + \sum_{n=1}^{\infty} \frac{z}{n(n+z)} \qquad z \neq -1, -2, -3, \ldots$$

and

$$\psi(z) = -\gamma + \sum_{n=0}^{\infty} \frac{z-1}{(n+1)(n+z)} = -\gamma + \sum_{n=0}^{\infty} \left(\frac{1}{n+1} - \frac{1}{n+z} \right) \qquad z \neq 0, -1, -2, -3, \ldots$$

These equations were utilized to evaluate infinite sums of rational functions, where $p(n)$ and $q(n)$ were polynomials of n. Performing partial fraction on u_n in the complex field, in the spatiotemporal, predictive, autoregressive, vector, arthropod-related, endemic, transmission-oriented, landscape, risk-based, distribution models employing all roots of $q(n)$ as simple roots then rendered:

$$u_n = \frac{p(n)}{q(n)} = \sum_{k=1}^{m} \frac{a_k}{n+b_k}.$$

We had to use $\lim_{n\to\infty} n u_n = 0,$ for the series to converge. Hence, the expression:

$$\sum_{k=1}^{m} a_k = 0, \text{ and } \sum_{n=0}^{\infty} u_n = \sum_{n=0}^{\infty} \sum_{k=1}^{m} \frac{a_k}{n+b_k} = \sum_{n=0}^{\infty} \sum_{k=1}^{m} a_k \left(\frac{1}{n+b_k} - \frac{1}{n+1} \right) = \sum_{k=1}^{m} \left(a_k \sum_{n=0}^{\infty} \left(\frac{1}{n+b_k} - \frac{1}{n+1} \right) \right) = -\sum_{k=1}^{m} a_k \left(\psi(b_k) + \gamma \right) = -\sum_{k=1}^{m} a_k \psi(b_k).$$

was rendered using the series expansion of higher rank polygamma function and a generalized formula:

[i.e., $$\sum_{n=0}^{\infty} u_n = \sum_{n=0}^{\infty} \sum_{k=1}^{m} \frac{a_k}{(n+b_k)^{r_k}} = \sum_{k=1}^{m} \frac{(-1)^{r_k}}{(r_k-1)!} a_k \psi^{(r_k-1)}(b_k)$$].

We noticed that in our endemic transmission-oriented model ψ was the only solution of the functional equation: $F(x+1) = F(x) + \frac{1}{x}$,that is monotone on $\mathbb{R}^+$ satisfied $F(1) = -\gamma$. The digamma then had a Gaussian sum of the form:

$$\frac{-1}{\pi k} \sum_{n=1}^{k} \sin\left(\frac{2\pi n m}{k} \right) \psi\left(\frac{n}{k} \right) = \zeta\left(0, \frac{m}{k} \right) = -B_1\left(\frac{m}{k} \right) = \frac{1}{2} - \frac{m}{k}.$$

Thereafter, the endemic, transmission-oriented, risk-based, distribution, model residuals revealed that $\zeta(s,q)$ was the Hurwitz zeta function and $B_n(x)$ which was a Bernoulli polynomial. The Bernoulli polynomials are an Appell sequence with $g(t) = \frac{e^t - 1}{t}$ (Roman 1984), giving the generating function $\frac{t\, e^{t\, x}}{e^t - 1} \equiv \sum_{n=0}^{\infty} B_n(x) \frac{t^n}{n!}$ (Abramowitz and Stegun 1972), first obtained by Euler (1738). The first few Bernoulli polynomials in this research were:

$B_0(x) = 1, B_1(x) = x - \frac{1}{2}, B_2(x) = x^2 - x + \frac{1}{6}, B_3(x) = x^3 - \frac{3}{2}x^2 + \frac{1}{2}x, B_4(x) = x^4 - 2x^3 + x^2 - \frac{1}{30}, B_5(x) = x^5 - \frac{5}{2}x^4 + \frac{5}{3}x^3 - \frac{1}{6}x,$
$B_6(x) = x^6 - 3x^5 + \frac{5}{2}x^4 - \frac{1}{2}x^2 + \frac{1}{42}.$

We also defined an older type of "Bernoulli polynomial" by writing:

$$t\,\frac{e^{z\,t}-1}{e^{t}-1}=\sum_{n=1}^{\infty}\frac{\phi_n\,(z)\,t^n}{n!}$$

This would then render the polynomials $\phi_n\,(x)=B_n\,(x)-B_n$, where B_n was a Bernoulli number, the first few of which are:

$$\phi_1\,(x)=x,\phi_2\,(x)=x^2-x,\phi_3\,(x)=x^3-\frac{3}{2}\,x^2+\frac{1}{2}\,x,\phi_4\,(x)=x^4-2\,x^3+x^2,\phi_5\,(x)=x^5-\frac{5}{2}\,x^4+\frac{5}{3}\,x^3-\frac{1}{6}\,x.$$

The Bernoulli polynomials also satisfied $B_n\,(1)=(-1)^n\,B_n\,(0)$ and $B_n\,(1-x)=(-1)^n\,B_n\,(x)$ for $n\neq 1, B_n\,(1)=B_n$, so $B_n\,(1)=B_n=0$ for odd $n>1$. The *S. damnosum s.l.* polynmoials also satisfied the relation $B_n\,(x+1)-B_n\,(x)=n\,x^{n-1}$ In this research, for deriving robust estimation values of x, $B_n\,(x)$ was expressed for the explanatory, predictor, covariate coefficients in the empirical dataset integers *n*in terms of Bernoulli and Euler numbers which led to:

$$B_n\,(1)=(-1)^n\,B_n, B_n\left(\tfrac{1}{2}\right)=\left(2^{1-n}-1\right)B_n, B_n\left(\tfrac{1}{4}\right)=-2^{-n}\left(1-2^{1-n}\right)B_n-4^{-n}\,n\,E_{n-1}, B_{2\,n}\left(\tfrac{1}{3}\right)=-\frac{1}{2}\left(1-3^{1-2\,n}\right)B_{2\,n}$$

$$, B_{2\,n}\left(\tfrac{1}{6}\right)=\frac{1}{2}\left(1-2^{1-2\,n}\right)\left(1-3^{1-2\,n}\right)B_{2\,n}.$$

Bernoulli (1713) defined the polynomials in terms of sums of the powers of consecutive integers:

$$\sum_{k=0}^{m-1}k^{n-1}=\frac{1}{n}\,[B_n\,(m)-B_n\,(0)].$$

Fortunately, our Bernoulli polynomials satisfied the recurrence relation:

$$\frac{d\,B_n}{d\,x}=n\,B_{n-1}\,(x)$$

in the*S. damnosum s.l.*model which obeyed the identity $B_n\,(x)=(B+x)^n$, where B^k was interpreted as the Bernoulli number [i.e.,$B_k=B_k\,(0)$] (Jacob et al., 2005b).When formulated as an equation to be solved, recurrence relations are known as recurrence equations, or sometimes difference equations (Everitt 2002). The difference between the n^{th} convergent and γ in the onchocericais, endemic, transmission-oriented, linearized,regression-based, risk model was then provided by:

$$\sum_{k=1}^{n}\frac{1}{k}-\ln n-\gamma=\int_{n}^{\infty}\frac{x-\lfloor x\rfloor}{x^2}\,d\,x,$$

where $\lfloor x\rfloor$ was the floor function which satisfied the inequality expression: $\frac{1}{2\,(n+1)}<\sum_{k=1}^{n}\frac{1}{k}-\ln n-\gamma<\frac{1}{2\,n}$.

The symbol γ was then $\gamma'\equiv e^{\gamma}\approx 1.781072$. This led to the radical representation of the seasonal-sampled, explanatory, predictor, covariate coefficients as:

$$e^{\gamma}=\left(\frac{2}{1}\right)^{1/2}\left(\frac{2^2}{1\cdot 3}\right)^{1/3}\left(\frac{2^3\cdot 4}{1\cdot 3^3}\right)^{1/4}\left(\frac{2^4\cdot 4^4}{1\cdot 3^6\cdot 5}\right)^{1/5}\cdots,$$

which was then related to the double series:

$$\gamma=\sum_{n=1}^{\infty}\frac{1}{n}\sum_{k=0}^{n-1}(-1)^{k+1}\binom{n-1}{k}\ln\,(k+1)$$

and $\binom{n}{k}$, a binomial coefficient.

Another proof of product in the regression models was then provided by the equation:

$$\frac{\pi}{2}=\left(\frac{2}{1}\right)^{1/2}\left(\frac{2^2}{1\cdot 3}\right)^{1/4}\left(\frac{2^3\cdot 4}{1\cdot 3^3}\right)^{1/8}\left(\frac{2^4\cdot 4^4}{1\cdot 3^6\cdot 5}\right)^{1/16}\cdots.$$

The solution was then made clearer by changing $n\to n+1$. In this research both these regression-based formulas were also analogous to the product for $e$which was then rendered by the computation:

$$e = \left(\frac{2}{1}\right)^{1/1}\left(\frac{2^2}{1\cdot 3}\right)^{1/2}\left(\frac{2^3\cdot 4}{1\cdot 3^3}\right)^{1/3}\left(\frac{2^4\cdot 4^4}{1\cdot 3^6\cdot 5}\right)^{1/4}\ldots$$

Unfortunately, extra-Poisson variation was detected in the estimated predictive, residual variance estimates in our model. As such, we constructed a robust negative binomial regression model in SAS with non-homogenous gamma distributed n means by incorporating $\alpha = \frac{1}{\theta}(\alpha > 0)$ in equation (2.1) .The distribution in the linear regression was then rewritten:

$$f(y_i|\mathbf{x}_i) = \frac{\Gamma(y_i+\alpha^{-1})}{y_i!\Gamma(\alpha^{-1})}\left(\frac{\alpha^{-1}}{\alpha^{-1}+\mu_i}\right)^{\alpha^{-1}}\left(\frac{\mu_i}{\alpha^{-1}+\mu_i}\right)^{y_i}, \quad y_i = 0,1,2,\ldots$$

The negative binomial distribution was thus derived as a gamma mixture of the Poissonian randomized variables. The conditional mean in the model was then $E(y_i|\mathbf{x}_i) = \mu_i = e^{\mathbf{x}_i'\boldsymbol{\beta}}$ and the variance was:

$$V(y_i|\mathbf{x}_i) = \mu_i[1+\frac{1}{\theta}\mu_i] = \mu_i[1+\alpha\mu_i] > E(y_i|\mathbf{x}_i).$$

To further estimate the district-level models, we specified DIST=NEGBIN (p=1) in the MODEL statement in PROC REG. The negative binomial model NEGBIN1 was set $p = 1$, which revealed the variance function [i.e., $V(y_i|\mathbf{x}_i) = \mu_i + \alpha\mu_i$] was linear in the mean of the models. The log-likelihood function for each NEGBIN1 regression model was then provided by the following equation:

$$\mathscr{L} = \sum_{i=1}^{N}\left\{\sum_{j=0}^{y_i-1}\ln\left(j+\alpha^{-1}\exp(\mathbf{x}_i'\boldsymbol{\beta})\right) - \ln(y_i!) - \left(y_i+\alpha^{-1}\exp(\mathbf{x}_i'\boldsymbol{\beta})\right)\ln(1+\alpha) + y_i\ln(\alpha)\right\}$$

where

The gradient for the risk model was then:

$$\frac{\partial\mathscr{L}}{\partial\boldsymbol{\beta}} = \sum_{i=1}^{N}\left\{\left(\sum_{j=0}^{y_i-1}\frac{\mu_i}{(j\alpha+\mu_i)}\right)\mathbf{x}_i - \alpha^{-1}\ln(1+\alpha)\mu_i\mathbf{x}_i\right\}$$ and

$$\frac{\partial\mathscr{L}}{\partial\alpha} = \sum_{i=1}^{N}\left\{-\left(\sum_{j=0}^{y_i-1}\frac{\alpha^{-1}\mu_i}{(j\alpha+\mu_i)}\right) - \alpha^{-2}\mu_i\ln(1+\alpha) - \frac{(y_i+\alpha^{-1}\mu_i)}{1+\alpha} + \frac{y_i}{\alpha}\right\}.$$

In this research, the negative binomial regression district-level model with variance function $V(y_i|\mathbf{x}_i) = \mu_i + \alpha\mu_i^2$, was referred to as the NEGBIN2 model. To estimate this model, we specified DIST=NEGBIN (p=2) in the MODEL statements. A test of the Poisson distribution was then performed by examining the hypothesis that $\alpha = \frac{1}{\theta_i} = 0$. A Wald test of this hypothesis was also provided which were the reported t statistics for the estimates in the negative binomial regression model. The log-likelihood function of the model (that is, NEGBIN2) was then generated by

$$\mathscr{L}\text{n} = \sum_{i=1}^{N}\left\{\sum_{j=0}^{y_i-1}\ln(j+\alpha^{-1}) - \ln(y_i!) - (y_i+\alpha^{-1})\ln(1+\alpha\exp(\mathbf{x}_i'\boldsymbol{\beta})) + y_i\ln(\alpha) + y_i\mathbf{x}_i'\boldsymbol{\beta}\right\}$$ where y was an integer when the gradient was:

$$\frac{\partial\mathscr{L}}{\partial\boldsymbol{\beta}} = \sum_{i=1}^{N}\frac{y_i-\mu_i}{1+\alpha\mu_i}\mathbf{x}_i.$$

The variance in the model was then assessed by: $\frac{\partial\mathscr{L}}{\partial\alpha} = \sum_{i=1}^{N}\left\{-\alpha^{-2}\sum_{j=0}^{y_i-1}\frac{1}{(j+\alpha^{-1})} + \alpha^{-2}\ln(1+\alpha\mu_i) + \frac{y_i-\mu_i}{\alpha(1+\alpha\mu_i)}\right\}$.

Object-oriented classification

Once an ecological dataset of the remotely-dependent, explanatory, predictor, covariate coefficients was constructed in ArcGIS, the data was exported to ENVI® which used various spectral–based algorithms to analyze the QuickBird visible and NIR data of the georeferenced *S. damnosums.l.*riverine larval habitat capture point.

The two main algorithms employed in our endmember decomposition was the spectral angle mapper (SAM) and spectral information divergence (SID) classification. SAM is a deterministic method that looks for an exact pixelmatch and weights the differences as same while SID is a probabilistic method that allows for variations in pixel measurements, where probability is measured from zero to a user-defined threshold.

In our research the basic workflow involved importing the data collected in the field from the riverine study site into a spectral library (http://www.exelisvis.com). Thereafter, SAM employed an *n*-dimensional angle to match the QuickBird pixels to the reference spectra. The algorithm determined the spectral similarity between the spectra by calculating the angle between the spectra and treating them as vectors in a space with dimensionality equal to the number of satellite bands. SAM compared the angle between the endmember spectrum vector and each QuickBird pixel spectrum vector in *n*-D space. Smaller angles represented in the dataset revealed closer matches to the reference spectrum. Pixels further away than the specified maximum angle threshold in radians were not classified. SID is a spectral classification method that uses a divergence measure to match pixels to reference spectra (http://www.exelisvis.com). The smaller the divergence, the more likely the pixels are similar. Pixels with a measurement greater than the specified maximum divergence threshold are not classified. In ENVI 4.6®, a spectrum plot, known as a *z*-profile, of the pixel under the cursor was run through all bands of the QuickBird image (Figure 5).

Additionally, in this research we used the Sequential Maximum Angle Convex Cone (SMACC) spectral tool in ENVI to determine the spectral endmembers and their abundances throughout the image. SMACC is designed to use a convex cone model (that is, residual minimization) to identify image endmember spectra (http://www.exelisvis.com). Extreme points were used to determine a convex cone, which defined the first *S. damnsoum s.l.* riverine larval habitat endmembers in the dataset. A constrained oblique projection QuickBird was then applied to the existing cone to derive the next larval habitat endmember. The cone was increased to include new endmembers. The process was repeated until a projection derived at endmember that already existed within the convex cone (to a specified tolerance) or until the specified number of endmembers were found.

The image endmembers of the georeferenced, *S.damnosum s.l.,*riverine, larval habitat and its associated spatial, date, feature, attributes were then extracted them from ENVI®'s spectral library. Several spectra corresponding to the different backgrounds in the sampled, canopy-oriented, capture, point structures (that is, Precambrian rock and rippled water pixel components) had to be included, since multiple scatterings between floating leaves in the habitat, for example, and a bright soil background increased the QuickBird NIR reflectance. Leaf cells have evolved to scatter (that is, reflect and transmit) solar radiation in the NIR spectral region (Schowengerdt, 1997). After calibration, the spectrally defined covariate coefficient estimates from the image were converted to match the library. Analogously, the QuickBird reference endmembers spectra in the library was transformed into the endmembers spectra of the image. Image classification was then performed, employing the FLAASH™ object-oriented approach which rendered a gmd file that converted the image's digital number (DN) to at-sensor radiance and computed at-sensor reflectance while normalizing the solar elevation angle. The equation was as follows:

$$\rho_B = \frac{\pi (L_B * G_{nBd} + aB_{nBid}) * D_n^2}{E_B * (C_n (\vartheta - \theta) * \pi / 1S)} \quad \text{where,}$$

ρ_{BandN} = Reflectance for Band N
L_{bandN} = DN for Band N
D = Normalized Earth-Sun Distance
E_{bandN} = Solar Irradiance for Band N

Spectral decomposition

A predictive 3-Dimensional (D) radiative transfer equation employing the sampled *S. damnosum s.l.* riverine larval habitat spatial,data, feature attributes was constructed. In order to characterize larval, habitat, hotspot phenomenon effectively and obtain stable solutions of canopy, multiple scattering, the radiation field was decomposed into three parts; unscattered radiance

[i.e., $\mathrm{I}^0(\tau,\Omega)$],

single scattering radiance

[i.e., $\mathrm{I}^1(\tau,\Omega)$],

and the multiple scattering radiance

[i.e., $\mathrm{I}^{\mathrm{M}}(\tau,\Omega)\,\mathrm{I}(\tau,\Omega) = \mathrm{I}^0(\tau,\Omega) + \mathrm{I}^1(\tau,\Omega) + \mathrm{I}^{\mathrm{M}}(\tau,\Omega)$].

A simple scheme was then represented by $\mathrm{I}^0(\tau,\Omega)$ which in this research was denoted by 1, which was neither scattered by the atmosphere nor canopy, but was reflected directly by the canopy surface. In this research, $\mathrm{I}^1(\tau,\Omega)$ was radiance either scattered once by the atmosphere, denoted by 2, or once by the canopy, denoted by the value 3. Also $\mathrm{I}^{\mathrm{M}}(\tau,\Omega)$ was the most complicated spectral component, which included all of other riverine larval, habitat, canopy components in the radiation field of the coupled medium. Unscattered sunlight radiances $\mathrm{I}^0(\tau,\Omega)$ were then characterized by the following radiative transfer equation and corresponding boundary conditions. When T < Ta the *S. damnosum s.l.,*riverine, larval habitat, radiative transfer model rendered:

$$\begin{cases} -\mu \dfrac{\partial \mathrm{I}^0(\tau,\Omega)}{\partial \tau} + \mathrm{I}^0(\tau,\Omega) = 0 \\ \mathrm{I}^0(0,\Omega) = \delta(\Omega - \Omega_0) i_0 \qquad \mu < 0 \\ \mathrm{I}^0(\tau_\alpha^{bot},\Omega) = \mathrm{I}^0(\tau_c^{top},\Omega) \qquad \mu > 0 \end{cases}$$

where τ_a^{bot} and τ_c^{top} were the optical depths at the bottom of the atmosphere and the top of the riverine, larval, habitat canopy, respectively. Here different notations were employed to indicate the physical meaning of the canopy boundary condition. The model

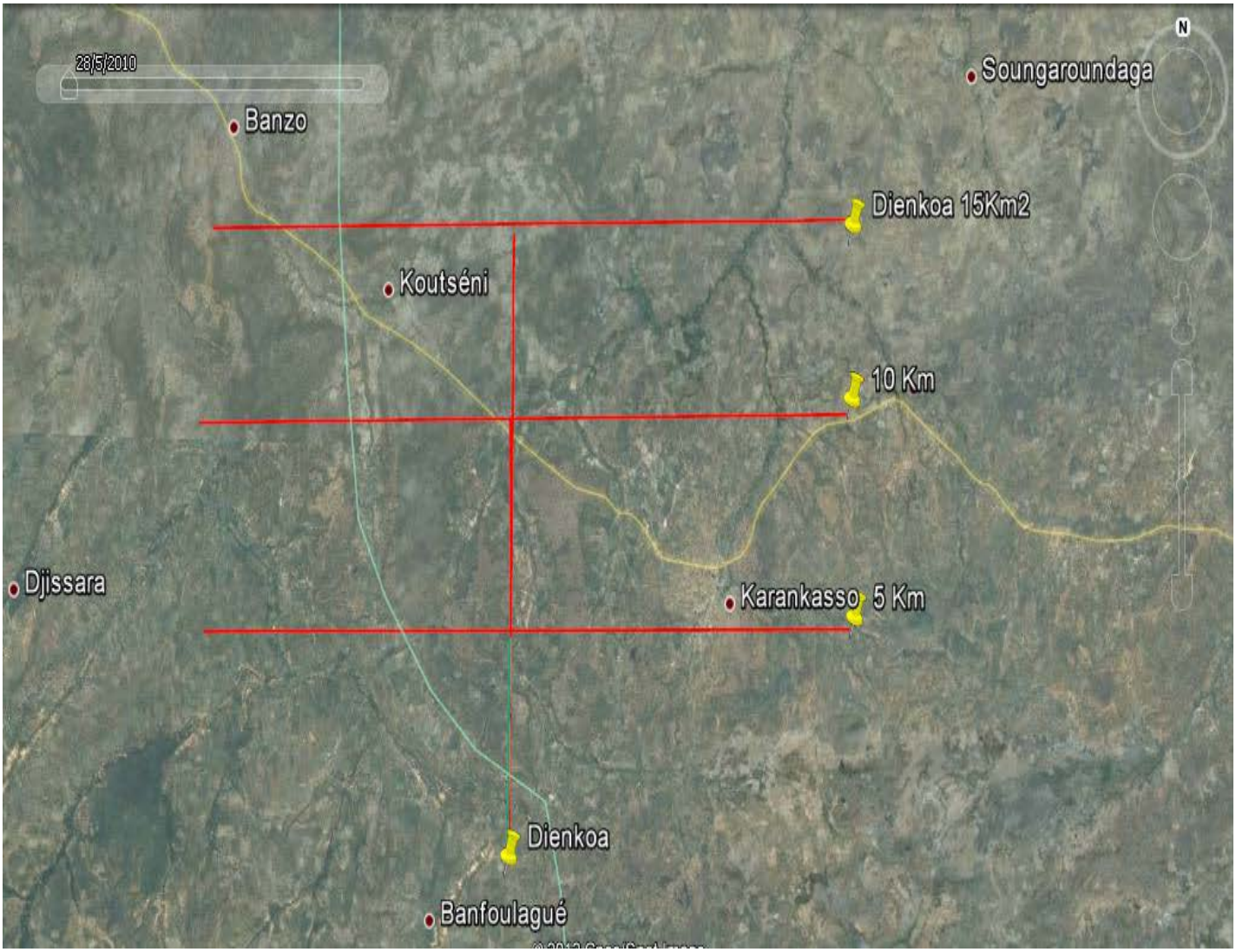

Figure 5. A Euclidean-distance matrix overlaid onto the georeferenced *S. damnosum s.l.* riverine habitat capture point.

provided the upper boundary condition, which meant only parallel sunlight illuminated the atmosphere at the top in the direction Ω_0. When $\tau > \tau_\alpha$, the residuals were:

$$\begin{cases} -\mu \dfrac{\partial \mathrm{I}^0(\tau,\Omega)}{\partial \tau} + h(\tau,\Omega)G(\Omega)\mathrm{I}^0(\tau,\Omega) = 0 \\ \mathrm{I}^0\left(\tau_c^{top},\Omega\right) = \mathrm{I}^0\left(\tau_\alpha^{bot},\Omega\right) \qquad \mu < 0 \\ \mathrm{I}^0(\tau_t,\Omega) = fs(\Omega_0,\Omega)|\mu_0|\mathrm{I}^0(\tau_t,\Omega_0) \qquad \mu > 0 \end{cases}$$

Jointly solving the equations with these boundary conditions, it was easy to obtain

$$
\mathrm{I}^0(\tau,\Omega) =
\begin{cases}
\mathrm{I}^0_{d1}(\tau,\Omega) = i_0 \exp\left(-\tau/|\mu|\right)\delta(\tau,\Omega_0) & \mu<0, \tau \le \tau_\alpha \\
\mathrm{I}^0_{d2}(\tau,\Omega) = \mathrm{I}^0_{d1}(\tau,\Omega) & \\
\cdot \exp\left[-C(\Omega)(\tau-\tau_\alpha)/|\mu|\right] & \mu<0 \tau_\alpha < \tau \le \tau_t \\
\mathrm{I}^0_{u2}(\tau,\Omega) = i_0 & \\
\cdot \exp\left[-\dfrac{\tau_\alpha + (\tau_t-\tau_\alpha)G(\Omega_0)}{|\mu_0|}\right] & \\
\cdot\ fs(\Omega_0,\Omega)|\mu_0|\exp\left[-\varepsilon(\tau,\Omega)\right] & \mu>0, \tau_\alpha < \tau \le \tau_t \\
\mathrm{I}^0_{u1}(\tau,\Omega) = \mathrm{I}^0_{u2}(\tau_\alpha,\Omega) & \\
\cdot \exp\left[-(\tau_\alpha-\tau)/\mu\right] & \mu>0, \tau \le \tau_\alpha
\end{cases}
$$

where $\mathrm{I}^0_{u2}(\tau,\Omega)$ represented the upwelling sunlight radiance within the georeferenced canopied *S. damnosum s.l.* riverine larval habitat capture point, and the function $\varepsilon(\tau,\Omega)$, due to modifying the extinction coefficient of the canopy. We then incorporated the extracted canopy radiance values including the Precambrian rock and ripple water spectral components using:

$$
\varepsilon(\tau,\Omega) = \frac{1}{\pi}\int_{\tau}^{\tau_t} h(t,\Omega)G(\Omega)dt
$$

$$
= G(\Omega)\frac{\tau_t-\tau}{\mu} - \left[\sqrt{\frac{G(\Omega_0)G(\Omega)}{\mu|\mu_0|}}\frac{k\mathrm{H}}{\Delta(\Omega_0,\Omega)}\right]t_0
$$

Where t0 was defined as $t_0 = \exp\left[-\dfrac{\Delta(\Omega_0,\Omega)\tau}{k\mathrm{H}}\right] - \exp\left[-\dfrac{\Delta(\Omega_0,\Omega)\tau_t}{k\mathrm{H}}\right]$

Since for single scattering radiances, unscattered sunlight becomes the scattering source (Kimes, 1991). In this research, boundary conditions were determined based on the fact that no incident single scattering radiances where from above the top of atmosphere or below the bottom of the canopy. When T < Ta the model rendered:

$$
\begin{cases}
-\mu\dfrac{\partial \mathrm{I}^l(\tau,\Omega)}{\partial\tau} + \mathrm{I}^l(\tau,\Omega) = & \\
\dfrac{\omega i_0}{4\pi}p(\Omega_0 \to \Omega)\exp\left(-\dfrac{\tau}{\mu_0}\right) & \\
r^1(0,\Omega) = 0 & \mu<0 \\
\mathrm{I}^1\left(\tau_\alpha^{bot},\Omega\right) & \mu>0
\end{cases}
$$

Thereafter, when T > T the georeferenced *S.damnosum s.l.* riverine larval hábitat capture point spectral decomposition rendered:

$$\begin{cases} -\mu\dfrac{\partial\tau^1(\tau,\Omega)}{\partial\tau}+h(\tau,\Omega)G(\Omega)\mathrm{I}^1(\tau,\Omega) \\ \dfrac{i_0'}{\pi}\Gamma(\Omega_0,\to\Omega)\exp\left[-(\tau-\tau_\alpha)\dfrac{G(\Omega_0)}{|\mu_0|}\right] \\ \mathrm{I}^1(\tau_c^{top},\Omega)=\mathrm{I}^1(\tau_\alpha^{bot},\Omega) \qquad \mu<0 \\ \mathrm{I}^1(\tau_t,\Omega)=0 \qquad \mu>0 \end{cases}$$

Where i_0' was the incident solar net flux arriving at the top of the riverine larval habitat canopy when $i_0'=i_0\exp\left(-\tau_\alpha/|\mu_0|\right)$

In the downward direction $\mu<0$, the solution was easily derived. When T < Ta, the spectral decomposition model was solved using:

$$\mathrm{I}^{l}(\tau,\Omega)=$$

$$\begin{cases} \dfrac{\omega Fop(\Omega_0\to\Omega)|\mu_0|}{4(|\mu_0|\leftarrow|\mu|)}\left[\exp\left(-\dfrac{\tau}{|\mu_0|}\right)-\exp\left(-\dfrac{r}{|\mu|}\right)\right] & \Omega\neq\Omega_0 \\ \dfrac{\omega F_0\tau}{4|\mu_0|}P(\Omega_0\to\Omega)\exp\left(-\dfrac{\tau}{\mu_0}\right) & \Omega=\Omega_0 \end{cases}$$

When $\tau_\alpha<\tau<\tau_t$ the model was solved using the equation:

$$\mathrm{I}^1(\tau,\Omega)=$$

$$\begin{cases} \dfrac{i_0'|\mu_0|\Gamma(\Omega_0\to\Omega)}{\pi\left[G(\Omega)|\mu_0|-G(\Omega_0)|\mu|\right]}t_1+\Delta\mathrm{I}^1(\tau,\Omega) & \Omega\neq\Omega_0 \\ \dfrac{(\tau-\tau_\alpha)i_0'\Gamma(\Omega_0\to\Omega)}{\pi|\mu_0|}\exp\left[-G(\Omega_0)\dfrac{\tau-\tau_\alpha}{|\mu_0|}\right] \\ \qquad +\Delta\mathrm{I}^1(\tau,\Omega) \end{cases}$$

Where $t_1$iwas defined by the equations:

$$t_1=\exp\left[-G(\Omega_0)\frac{\tau-\tau_\alpha}{|\mu_0|}\right]-\exp\left[-G(\Omega)\frac{\tau-\tau_\alpha}{|\mu|}\right]$$ and $\Delta\mathrm{I}^1(\tau,\Omega)=\mathrm{I}^1(\tau_\alpha,\Omega)\exp\left[-G(\Omega)(\tau-\tau_\alpha)/|\mu|\right.$

which was the single scattering riverine larval habitat capture point canopy radiance emerging from the atmosphere without further scattering in the canopy. In the upward direction (p > 0), the solutions were a little more complicated because of the hotspot effect:

$$I^1(\tau,\Omega)=\begin{cases}\dfrac{1}{\mu}\int_r^{\tau_t}F(\tau',\Omega)\\ \cdot\exp\left[-\dfrac{1}{\mu}\int_\tau^{\tau'}h(\varepsilon,\Omega)G(\Omega)d\varepsilon\right]d\tau' & \tau_\alpha\le\tau\le\tau_t\\ \dfrac{\omega F_0 p(\Omega_0\to\Omega)|\mu_0|}{4(\mu+|\mu_0|)}t_2\\ +I^1(\tau_\alpha,\Omega)\exp\left(\dfrac{\tau-\tau_\alpha}{\mu}\right) & \tau<\tau_\alpha\end{cases}$$

Where t_2 was defined using: $t_2=\exp\left[-\dfrac{\tau}{|\mu_0|}\right]-\exp\left[\dfrac{\tau}{\mu}-\left(\dfrac{1}{\mu_0}+\dfrac{1}{\mu}\right)\tau_\alpha\right]$ and the second integration as Ta < T < Tt which in this research was explicitly obtained by means of an alternative intergrand range. This range was solved using:

$$F(\tau',\Omega)=\frac{i_0'}{\pi}\Gamma(\Omega_0\to\Omega)\exp\left[-G(\Omega_0)(\tau-\tau_\alpha)/|\mu_0|\right]$$

.

The radiance $I^1(\tau,\Omega)$ at Ta < T < Tt needed to be numerically evaluated without further assumptions. An explicit approximation to $I^1(\tau,\Omega)$ was then derived and used for inversion.

In the spectral *S.damnosum s.l.*rivrerine larval habitat capture point endmember model the Gausse-Legendre quadrature was also employed to calculate the integration. An *n*-point Gaussian quadrature rule is a quadrature rule constructed to yield an exact result for polynomials of degree 2*n* − 1 or less by a suitable choice of the points x_i and weights w_i for i = 1,...,*n*. The domain of integration for such a rule is conventionally taken as [−1, 1], so the rule is stated as

$$\int_{-1}^{1} f(x)\,dx \approx \sum_{i=1}^{n} w_i f(x_i).$$

We we used the Li-Strahler geometric-optical model based on the assumption that the BRDF would retrieve *S. damnosum s.l.* habitat capture point shaded riverine canopy structural variables. The BRDF was defined by:

$$f_r(\omega_i,\omega_o)=\frac{dL_r(\omega_o)}{dE_i(\omega_i)}=\frac{dL_r(\omega_o)}{L_i(\omega_i)\cos\theta_i\,d\omega_i}$$

Where *L* was the radiance, *E* was the irradiance, and θ_i was the angle made between ω_i and the riverine habitat and its associated Precambrian rock and ripple water surface reflectance emissivities. Because the BRDF is a four-dimensional function that defines how light is reflected at an opaque surface (Jensen, 2005), the function in our model took an incoming light direction, ω_i, and outgoing direction, ω_o, which were both defined with respect to the georeferenced *S. damnosum* riverine larval habitat and its neighboring Precambrian rock and ripple water surface *n*, and returned the ratio of reflected radiance exiting along ω_o to the irradiance incident from direction ω_i. Note, each direction ω was itself parameterized by azimuth angle φ and zenith angle θ, therefore, in this research, the BRDF was 4-dimensional. The BRDF had units sr^{-1}, with steradians (sr) being a unit of solid angle.

The inverted Li-Strahler geometric-optical model was then used to retrieve specific spectral habitat explanatory predictor covariate coefficient estimates. The reflectance associated with a georeferenced habitat was treated as an area-weighted sum of four fixed radiance components: sunlit canopy, sunlit background, shaded canopy, and shaded background. In most arthropod-related, infectious disease, larval, habitat–related, geometric-optical, simulation models these four components could be simplified to three: sunlit canopy–C, sunlit background–G and shadow–T (Jacob et al., 2011c). In this research, the endmember spectral components were derived using G, C, T components' classes which were initially estimated by the QuickBird image using ENVI®. For inverting the model, parts of the three spectral components were then represented by (kg) which was calculated using:

$$K_g=e^{-\pi\cdot M\cdot[\mathrm{s}\quad(\theta_i)+\mathrm{es}\quad(\theta_v)+O(\theta_i,\theta_v,\varphi)]} \tag{3}$$

$$O(\theta_i,\theta_v,\varphi)=1/\pi(\mathrm{s}\quad\theta_i+\mathrm{s}\quad\theta_v)(t-\mathrm{s\ c\ t\ ci\ \ t}) \tag{3}$$

$$\mathrm{c}\quad\mathrm{to}=\frac{h|\mathrm{t\ \ a}\theta_i-\mathrm{nt\ \ a}\theta_v\ \mathrm{cn}\ \ \varphi|}{r(\mathrm{s}\quad\theta_i+\mathrm{s}\quad\theta_v)\ \mathrm{c}} \tag{4}$$

$$M=\frac{-1\ (K_g)}{(\mathrm{s}\quad\theta_i+\mathrm{s\ c}\theta_v)(\pi-t+\mathrm{c}\quad t\ \mathrm{so}\ \ t)} \tag{5}$$

$$C\ \ G=1-e^{-\pi\cdot M} \tag{6}$$

Where, *I q u q* were the zenith angles of illumination and viewing, *O* was the average of the overlap function between illumination and viewing shadows of the capture point and their associated Precambrian rock and ripple water spectral components as

projected onto the background. In this research, *j* was the difference in azimuth angle between illumination and viewing.

In our analyses, the BRDF of the larval habitat capture point mixel was modeled as the limit of its directional reflectance factor using:

$$R(i,v):\ R(i,v)=\frac{\iint_A R(s)\langle i,s\rangle\langle v,s\rangle I_i(s)I_v(s)ds}{A\cos\theta_i\theta_v} \quad (7)$$

Where ds was a small Lambertian surface element over area A of the QuickBirdmixel; $R(s)$ was the reflectance of ds ; i , v , and s represented the directions of illumination and viewing based on the Precambrian rock surface and ripple water reflectance components, respectively. In the model $\langle .,. \rangle$ was the cosine of the phase angle between two directions; θ was the zenith angle of a direction; $I_i(s)$ and $I_v(s)$ were indicator functions, equal to one when ds was illuminated (I_i) or viewed (I_v) or zero otherwise. If a surface exhibits Lambertian reflectance, light falling on it is scattered such that the apparent brightness of the surface to an observer is the same regardless of the observer's angle of view, thus, the surface luminance is isotropic (Schowengerdt, 1997).

Lambert's cosine law states that the radiant intensity or luminous intensity observed from an ideal diffusely reflecting surface or ideal diffuse radiator is directly proportional to the cosine of the angle θ between the observer's line of sight and the surface normal (Pedrotti and Pedrotti, 1993). In this research the luminous intensity of the geo-refernced *S. damnosum s.l.* riverine larval habitat model endmember point varied by direction. We then defined with peak luminous intensity in the normal direction using the cosine law. As the Lambertian assumption held, we then calculated the total luminous flux, F_{tot}, from the peak luminous intensity by integrating the cosine law:

$$F_{tot}=\int_0^{\pi/2}\int_0^{2\pi}\cos(\theta)I_{max}\,\sin(\theta)\,\mathrm{d}\,\phi\,\mathrm{d}\,\theta\ =2\pi\cdot I_{max}\int_0^{\pi/2}\cos(\theta)\sin(\theta)\,\mathrm{d}\,\theta\ =2\pi\cdot I_{max}\int_0^{\pi/2}\frac{\sin(2\theta)}{2}\,\mathrm{d}\,\theta$$

and so $F_{tot}=\pi\ \mathrm{sr}\cdot I_{max}$ where $\sin(\theta)$ was the determinant of the Jacobian matrix for the unit sphere, and I_{max} is was the luminous flux per steradian. In vector calculus, the Jacobian matrix is the matrix of all first-order partial derivatives of a vector- or scalar-valued function with respect to another vector (Cressie, 1993). Similarly, the peak intensity was $1/(\pi\ \mathrm{sr})$ of the total radiated luminous flux. For quantitation of the Lambertian surfaces, the same factor of π sr related the larval habitat luminance to luminous emittance, radiant intensity to radiant flux, and radiance to radiant emittance. Solvingour double integral equation revealed s that ds was integrated over the decomposed QuickBird mixel (that is, the footprint of the sensor' sinstantaneous field of view (iFOV)) .

In this research, there were two kinds of prominent habitat surfaces in the sub-mixel spectra; A -background surface (that is, Precambrian rock) and surface ripple water-which were represented by Lambertian reflectance G and C , respectively. We then re-wrote equation (7) as:

$$R(i,v)=K_gG+\frac{C}{A}\iint_{A_c}\frac{\langle i,s\rangle}{\cos\theta_i}\frac{\langle v,s\rangle}{\cos\theta_v}ds\ ,$$

where $K_g=A_g/A$ which was the proportion of background spectral data illuminated and viewed by the georefernced, QuickBird, imaged, *S. damnosum s.l.,* riverine, larval, habitat, capture points attributes. In this equation the union of A_g and A_c were the intersection of the dataset of the larval, riverine, habitat, capture, point, surface elements which were illuminated and viewed, only when v and i coincided. The directional reflectance of the habitat scene depended also on the Precambrian rock and ripple water reflectance values related to G and C .

In our analyses we focused on the two terms of $R(i,v)=K_gG+\frac{C}{A}\iint_{A_c}\frac{\langle i,s\rangle}{\cos\theta_i}\frac{\langle v,s\rangle}{\cos\theta_v}ds$. The first term described how the sunlit background proportion proceeded to a maximum point as viewing and illumination positions in the hemisphere coincided. The second term in the model described how the sunlit *S. damnosum s.l.*riverine larval habitat capture point surface composed of the Lambertian facets, became maximally exposed to view at the hotspot, while those facets on tops became dominant at large viewing zenith angles. The hot spot correlation effect refers to the observed brightening which can occur when viewing a scene from the same direction as the solar illumination (Burrough and McDonnell, 1998) which for robust, predictive, spatiotemporal, arthropod-related, infectious disease modeling is commonly noted in the visible and NIR spectral regions (Jacob et al., 2011a). We then analyzed how the first term K_gG varied with illumination and viewing geometry. As in Strahler and Jupp (1990), we assumed that the spatial object of interest (that is, *S. damnosum s.l.* habitat) and its associated georeferenced, explanatory, spectral, predictor, covariate coefficient had the shape of a spheroid, with vertical half-axis equal to b , horizontal radius equal to R , and a height to the center of the spheroid h . To accommodate the spheroidal shape in the derivations of the shadowed,riverine, larval,habitat areas, we used the transformation $\theta'=\tan^{-1}\left(\frac{b}{R}\tan\theta\right)$. We solved this equation by replacing θ with the angle that would generate the same shadow area for a sphere. For simplicity, we assumed that the centers of the spheroids were randomly distributed in depth from h_1 to h_2 over A . We then assumed that G and C were constants and also they were as average signatures over A_g and A_c for properly modelling K_g and $K_c=A_c/A$. Next, the equation $R(i,v)=K_gG+\frac{C}{A}\iint_{A_c}\frac{\langle i,s\rangle}{\cos\theta_i}\frac{\langle v,s\rangle}{\cos\theta_v}ds$ was employed

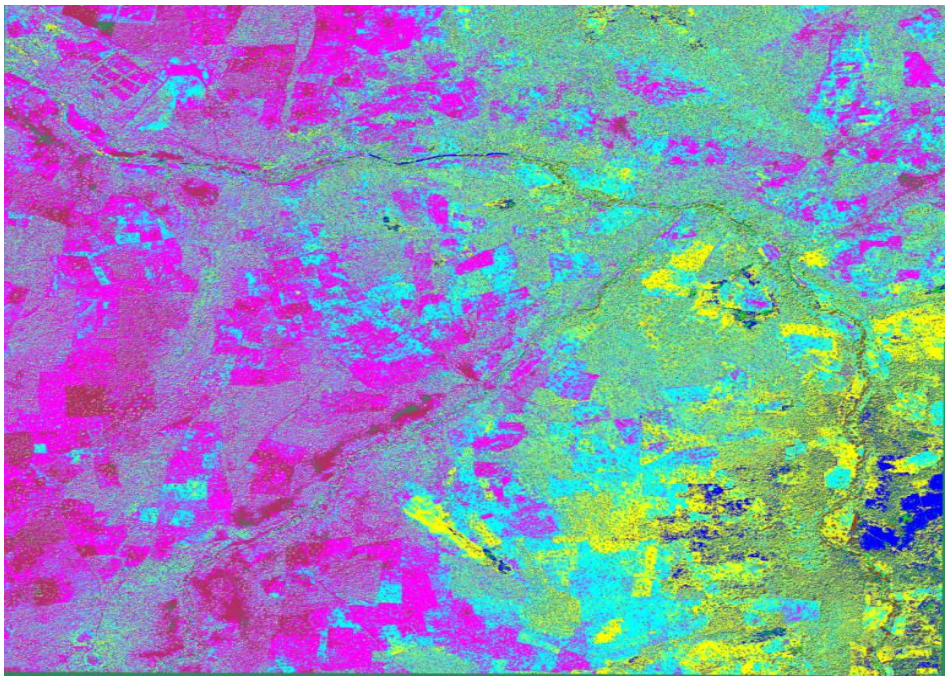

Figure 6. Object-based ENVI classification of the Dienkoa-Chutes riverine breeding study site.

.

whereby K_g was expressed in a Boolean model and $K_g = e^{-\lambda\pi R^2\left[\sec\theta_i' + \sec\theta_v' - \overline{O}(\theta_i,\theta_v,\phi)\right]}$ where $\overline{O}(\theta_i,\theta_v,\phi,)$ represented the average of the overlap function $O(\theta_i,\theta_v,\phi,h)$ between illumination and viewing shadows of the spatiotemporal, field-sampled, *S. damnosum s.l.,* riverine, larval, habitat, capture point and its associated within-canopy structures (for example, Precambrian rock and spectral ripple water components). Furthermore, ϕ was the difference in azimuth angle between viewing and illumination positions of the QuickBird classified objects associated to the geo-refernced capture point habitat. To simplify the equation, we approximated the overlap function by the overlap area and center positions of the ellipses. This approximation is justified when solar zenith and viewing zenith angles are not too large (Strahler and Jupp, 1990). In the case of long ellipsoidal shadows, however, this approximation could have overestimated the width of the riverine, habitat capture point hotspot in the Azimuthal direction and underestimated the width of the hotspot in the Azimuthal direction. To improve the accuracy and to preserve the proper hotspot width information, we developed another approximation as follows. We used the equations $\phi = 0$ *or* $\phi = \pi$ First, we considered the overlap function in the principal plane. We used W $\phi = 0$ or π as the elliptical illumination and then viewed shadows that were aligned in the same direction. The overlap area was approximated by an ellipse with one axis equal to the overlap length and the other equal to the georeferenced, *S. damnosum s.l.,*riverine, larval, habitat, width, encompassing the Precambrian rock and ripple, water, mixel, spectral components which yielded

$$O(\theta_i,\theta_v,\phi) = \frac{1}{2}\left[\sec\theta_i' + \sec\theta_v' - \frac{h}{b}\left|\tan\theta_i' - \tan\theta_v'\cos\phi\right|\right]$$

. By so doing, we were able to determine the waveband spectral signature for the riverine larval habitat based on a scattergram (Figure 6).

Interpolation analyses

Multiple, spatial, explanatory, linearized predictors were then generated from the *S. damnosum s.l* .riverine, larval, habitat, capture point, spatiotemporal-endmembers and its associated Precambrian rock and rippled water spectrally decomposed components using an ordinary kriged-based interpolator. The algorithms for our interpolation have already been described in

Jennsen (2005). Briefly, in this research, the dependent variable was the residualized, spectral, emissivity, estimates, rendered from the decomposition of the QuickBird mixel which was transformed to fulfill the diagnostic normality test prior for performing the kriging. Ordinary kriging was selected to interpolate the value $Z(x_0)$, an *S. damnosum s.l.* riverine larval habitat capture point canopy and its associated Precambrian rock and spectral ripple water components,$Z(x)$, at an unobserved, habitat, location x_0 from the field and remote-sampled, explanatory, predictor, covariate, coefficient estimates and $z_i = Z(x_i)$, i = 1..., *n* at nearby habitat locations, x_1, xn. In this research, ordinary kriging was computed as a linear unbiased estimator, $\check{Z}(x_o)$ of $Z(x_0)$ based on a stochastic model of the dependence quantified by the variogram $\gamma(x,y)$ and by the expectation $\mu(x) = E[Z(x)]$ and the covariance functionc (x,y) of the random field. The kriging estimator was given by a linear combination of the algorithm:

$$\hat{Z}(x_o) = \sum_{i=1}^{n} w_i(x_o)Z(x_i)$$

employing the spectral, riverine, larval, habitat, endmember dataset of $z_i = Z(x_i)$ with weights $w_i(x_o)$, i = 1,...,*n* chosen, such that the variance in the spectral autoregressive model was calculated using:

$$\sigma_k^2(x_0) := V\left(\hat{Z}(x_0) - Z(x_0)\right) = \sum_{i=1}^{n}\sum_{j=1}^{n} w_i(x_0)w_j(x_0)c(x_i,x_j) + V\left(Z(x) - 2\sum_{i=1}^{n} w_i(x_0)c(x_i,x_0)\right)$$

which was further minimized using:

$$E[\hat{Z}(x) - Z(x)] = \sum_{i=1}^{n} w_i(x_0)\mu(x_i) - \mu(x_0) = 0$$

.

Spatial analyses

An autoregressive (*p*) model was then constructed in SAS/GIS,

$$X_t = c + \sum_{i=1}^{p} \varphi_i X_{t-i} + \varepsilon_t.$$

thereafter using where $\varphi_1, \ldots, \varphi_p$ were the georeferenced study site geosampled parameter estimators, C was a constant, and the random variable and ε_t was white noise. An AR is essentially an all-pole infinite impulse response filter with some additional interpretation placed on it (Griffith, 2003). In this research, some constraints were necessary on the values of the parameter estimators of the model in order that the residuals remained stationary. For example, processes in the autoregressive models generated at each 5 km interval from the capture point with $|\varphi_1| \geq 1$ were not stationary. The notation MA (*q*) was then also constructed to the moving average model of order *q*:

$$X_t = \mu + \varepsilon_t + \sum_{i=1}^{q} \theta_i \varepsilon_{t-i}$$

Where the $\theta_1, .., \theta_q$ were the riverine estimators, μ was the expectation of X_t (often assumed to equal 0), and the ε_t, ε_{t-1},...were white noise error terms. In this research the notation ARMA (*p*, *q*) referred to the model with *p* autoregressive terms and *q* moving-average terms. This model contained the AR (*p*) and MA (*q*) models which was expressed as:

$$X_t = c + \varepsilon_t + \sum_{i=1}^{p} \varphi_i X_{t-i} + \sum_{i=1}^{q} \theta_i \varepsilon_{t-i}.$$

In this research, the error terms ε_t were assumed to be independent identically distributed (i.i.d.), randomized, variables, sampled from a normal distribution with zero mean: $\varepsilon_t \sim N(0,\sigma^2)$. The spatially-dependent, transmission-oriented, endemic, models were then specified in terms of the lag operator *L*. In these terms then the AR (*p*) models was provided by:

$$\varepsilon_t = \left(1 - \sum_{i=1}^{p} \varphi_i L^i\right) X_t = \varphi X_t$$

where φ represented the polynomial $\varphi = 1 - \sum_{i=1}^{p} \varphi_i L^i$.

The MA(*q*) model was then given by the equation $X_t = \left(1 + \sum_{i=1}^{q} \theta_i L^i\right) \varepsilon_t = \theta \varepsilon_t$, where θ represented the polynomials. Finally, the combined ARMA (*p*, *q*) endemic models were provided by:

$$\left(1 - \sum_{i=1}^{p} \varphi_i L^i\right) X_t = \left(1 + \sum_{i=1}^{q} \theta_i L^i\right) \varepsilon_t,$$

or more concisely, $\varphi X_t = \theta \varepsilon_t$.

Thereafter, a misspecification perspective for the estimation, endemic, transmission-oriented, risk based, distribution model was constructed in SAS/GIS using $y = X\beta + \varepsilon^*$ (that is, regression equation) for decomposing ε^*, into a white-noise component, ε, (that is, autocorrelation-oriented disturbances) and a set of unspecified and/or misspecified sub- models that had the structure $y = XB + \underbrace{E\gamma + \varepsilon}_{=\varepsilon^*}$. White noise in a spatiotemporal-sampled, arthropod-related, infectious disease, larval, habitat, epidemiological, risk model is a univariate or multivariate discrete-time stochastic process whose terms are i.i.d. with a zero mean (Jensen, 2003).

RESULTS

Initially, we constructed a Poisson regression models using the spatiotemporal-sampled, district-level, covariate, coefficient, measurement values to determine covariate coefficients of significance with each ArcGIS classified Euclidean-distance dependent zone. Our model was generalized by introducing an unobserved heterogeneity term for each spatiotemporal, field-sampled, *S. damnosum s.l.* related, riverine, larval, habitat observation i. The weights were assumed to differ randomly in a manner that was not fully accounted for by the other time series-dependent covariate coefficients. In this research this process was formulated as $E(y_i|\mathbf{x}_i, \tau_i) = \mu_i \tau_i = e^{\mathbf{x}_i'\boldsymbol{\beta} + \varepsilon_i}$ where the unobserved heterogeneity term $\tau_i = e^{\varepsilon_i}$ was independent of the vector of regressors $\mathbf{x}_i$ for each ArcGIS delineated onchocerciasis, endemic, transmission zone. Then the distribution of y_i was conditional on $\mathbf{x}_i$ and had a Poisson specification with conditional mean where the conditional variance was:

$\mu_i \tau_i$: $f(y_i|\mathbf{x}_i, \tau_i) = \dfrac{\exp(-\mu_i \tau_i)(\mu_i \tau_i)^{y_i}}{y_i!}$.

We then let $g(\tau_i)$ be the probability density function of τ_i. Then, the distribution $f(y_i|\mathbf{x}_i)$ was no longer conditional on τ_i. Instead it was obtained by integrating $f(y_i|\mathbf{x}_i, \tau_i)$

with respect to τ_i: $f(y_i|\mathbf{x}_i) = \int_0^\infty f(y_i|\mathbf{x}_i, \tau_i) g(\tau_i) d\tau_i$. We then found that an analytical solution to this integral existed in the Poisson-relatedendemic model when τ_i was assumed to follow a gamma distribution. The models also revealed that y_i, was the vector of the sampled covariate coefficients while $\mathbf{x}_i$, was independently Poisson distributed with:

$$P(Y_i = y_i|\mathbf{x}_i) = \frac{e^{-\mu_i}\mu_i^{y_i}}{y_i!}, \quad y_i = 0, 1, 2, \ldots$$

and the mean parameter, that is, the mean number of sampling events per spatiotemporal period was given by $\mu_i = \exp(\mathbf{x}_i'\boldsymbol{\beta})$ where $\boldsymbol{\beta}$ was a $(k+1) \times 1$ parameter vector. The intercept in the model was then β_0 and the coefficients for the k regressors were $\beta_1, \ldots, \beta_k$. Taking the exponential of $\mathbf{x}_i'\boldsymbol{\beta}$ ensured that the mean parameter μ_i was non-negative. Thereafter, the conditional mean was provided by $E(y_i|\mathbf{x}_i) = \mu_i = \exp(\mathbf{x}_i'\boldsymbol{\beta})$. The parameter estimators were then evaluated using $\ln[E(y_i|\mathbf{x}_i)] = \ln(\mu_i) = \mathbf{x}_i'\boldsymbol{\beta}$. Note, in this research, that the conditional variance of the count random variable was equal to the conditional mean (that is, equidispersion) ($V(y_i|\mathbf{x}_i) = E(y_i|\mathbf{x}_i) = \mu_i$). In a log-linear model the logarithm of the conditional mean is linear (Hosmer et al., 2002). The marginal effect of any district-level, explanatory regressor in the models was then provided by:

$$\frac{\partial E(y_i|\mathbf{x}_i)}{\partial x_{ji}} = \exp(\mathbf{x}_i'\boldsymbol{\beta})\boldsymbol{\beta}_j = E(y_i|\mathbf{x}_i)\beta_j$$

In the model we noticed that a one-unit change in the jth regressor led to a proportional change in the conditional mean $E(y_i|\mathbf{x}_i)$ of β_j

Further, we found that given the Poisson process in our endemic, transmission-oriented, risk-based model, the limit of the binomial distribution in the sampled parameter estimators was:

$$P_p(n|N) = \frac{N!}{n!\,(N-n)!}\, p^n (1-p)^{N-n}.$$

Viewing the distribution as a function of the expected number of successes [$\nu \equiv N p$] instead of the sample size N for fixed p, transformed the equation to:

$$P_{\nu/N}(n|N) = \frac{N!}{n!\,(N-n)!}\left(\frac{\nu}{N}\right)^n \left(1 - \frac{\nu}{N}\right)^{N-n}$$

As the sample size N become larger, the distribution then approached P when:

$$\lim_{N\to\infty} P_p(n|N), \lim_{N\to\infty} \frac{N(N-1)\cdots(N-n+1)}{n!}\frac{\nu^n}{N^n}\left(1-\frac{\nu}{N}\right)^N\left(1-\frac{\nu}{N}\right)^{-n}, \lim_{N\to\infty} \frac{N(N-1)\cdots(N-n+1)}{N^n}\frac{\nu^n}{n!}\left(1-\frac{\nu}{N}\right)^N\left(1-\frac{\nu}{N}\right)^{-n},$$

$$1 \cdot \frac{\nu^n}{n!} \cdot e^{-\nu} \text{ and } \frac{\nu^n e^{-\nu}}{n!},$$

Note that the sample size N had completely dropped out of the probability function, which had the same functional form for all values of ν. Next, the moment-generating function of the Poisson distribution was provided by:

M = $e^{-\nu} e^{\nu e^t} = e^{\nu(e^t-1)}$, M=$\nu e^t e^{\nu(e^t-1)}$ and M=$\left(\nu e^t\right)^2 e^{\nu(e^t-1)} + \nu e^t e^{\nu(e^t-1)}$, when R=$\nu\left(e^t - 1\right)$, R'=$\nu e^t$ so R=$R'(0) = \nu$.

The raw moments were also computed directly by summation, which yielded an unexpected connection with the exponential polynomial $\phi_n(x)$ and the stirling numbers of the second kind

$$\phi_n(x) = \sum_{k=0}^{\infty} \frac{e^{-x} x^k}{k!} k^n = \sum_{k=1}^{n} x^k S(n, k)$$

which in this research was represented as Dobiński's formula for the Bell polynomial and Bell numbers. This generalized formula revealed $B_n(x) = e^{-x}\sum_{k=0}^{\infty}\frac{k^n}{k!}x^k$, where $B_n(x)$ was a Bell polynomial .Setting $x = 1$gives the special case of the nth Bell number, $B_n = \frac{1}{e}\sum_{k=0}^{\infty}\frac{k^n}{k!}$. The formula was derived by dividing the generating function formula for a Stirling number of the second kind$S(n,k)$ and by quantitating by $m!$, yielding $\frac{m^n}{m!} = \sum_{k=1}^{n}\frac{S(n,k)}{(m-k)!}$. Then:

$\sum_{m=1}^{\infty}\frac{m^n}{m!}\lambda^m = \left(\sum_{k=1}^{n}S(n,k)\lambda^k\right)\left(\sum_{j=0}^{\infty}\frac{\lambda^j}{j!}\right)$, and $\sum_{k=1}^{n}S(n,k)\lambda^k = e^{-\lambda}\sum_{m=1}^{\infty}\frac{m^n}{m!}\lambda^m$. (Roman, 1984).

Then in the endemic Euclidean distance–based models: $\nu(1+\nu)$, $\nu\left(1+3\nu+\nu^2\right)$ and $\nu\left(1+7\nu+6\nu^2+\nu^3\right)$.

We then tested the model for over-dispersion with a likelihood ratio test based on the linear distributions. This test quantitated the equality of the mean and the variance imposed by the Poisson distribution against the alternative that the variance exceeded the mean. For the negative binomial distribution, the variance = mean + k mean^2 k > = 0 and the negative binomial distribution reduces to Poisson when k = 0 (Haight, 1967). The probability mass function of the negative binomial distributions with a gamma distributed mean was then expressed as:

$$f(k) \equiv \Pr(X = k) = \binom{k+r-1}{k}(1-p)^r p^k \quad \text{for } k = 0, 1, 2, \ldots$$

In this equation, the quantity in parentheses was the binomial coefficient, and was equal to:

$$\binom{k+r-1}{k} = \frac{(k+r-1)!}{k!\,(r-1)!} = \frac{(k+r-1)(k+r-2)\cdots(r)}{k!}.$$

In this research, this quantity was also alternatively written as:

$$\frac{(k+r-1)\cdots(r)}{k!} = (-1)^k\frac{(-r)(-r-1)(-r-2)\cdots(-r-k+1)}{k!} = (-1)^k\binom{-r}{k}$$

for explaining “negative binomialness’ in the onchocerciasis, endemic, transmission-oriented, risk model. Results from both a Poisson and a negative binomial (that is, a Poisson random variable with a gamma distrusted mean) revealed that the explanatory, predictor, covariate coefficients were highly significant, but furnished virtually no predictive power. In other words, the sizes of the population denominators were not sufficient to result in statistically significant relationships, while the detected relationships were inconsequential. For χ^2 fitting, the likelihood wa sprovided by:

$L = \prod\left(\frac{1}{2\pi\sigma_i^2}\right)^{1/2}\exp\left(-\sum\frac{(y_i - f(\mathbf{x}))}{2\sigma_i^2}\right)$ (that is, $\ln L = \ln\left(\prod\left(\frac{1}{2\pi\sigma_i}\right)^{1/2}\right) - \frac{1}{2}\sum\frac{(y_i - f(\mathbf{x})}{\sigma_i^2} = C - \chi^2/2$)

where C wasa constant independent of the model and dependent only on the use of particular data points (that is, it does not change if the data do not change). In this research we employed a correlation analysis method to check the cross correlation between the input and output signals as an estimation of the impulse response, as shown by the following equation:

$$y(k) = \sum_{n=0}^{\infty}u(k-n)h(n) + e(k)$$

The input signal must be zero-mean white noise with a spectral density that is equally distributed across the whole frequency range (Cressie 1993). The SI estimate impulse response VI can prewhiten input signals that are not white noise (Hosmer et al., 2000). Thus, assuming the input $u(k)$ of the system was stochastic process and statistically independent of the disturbance $e(k)$, we assumed the following equation was true:

$$R_{uy}(\tau) = \sum_{k=0}^{\infty} R_{uu}(k-\tau)h(k)$$

When R_{uy} represented the cross-correlation function between the stimulus signal $u(k)$ and the response signal $y(k)$, as defined by:

$$R_{uy}(\tau) = \frac{1}{N} \sum_{k=min(\tau,0)}^{N-max(\tau,0)-1} y(k+\tau)u(k)$$

When R_{uu} represented the autocorrelation of the stimulus signal $u(k)$, as defined by the following equation:

$$R_{uu}(\tau) = \frac{1}{N} \sum_{k=0}^{N-\tau-1} u(k+\tau)u(k)$$

We employed N as the number of sampled, onchocerciasis-related, endemic, transmission-oriented, risk-based, georeferenced data points. If the stimulus signal is a zero-mean white noise signal, the autocorrelation function reduces to the following equation. $R_{uu}(\tau) = \sigma_u^2 \delta(\tau)$ where σ_u is the standard deviation of the stimulus white noise and $\delta(\tau)$ is the Dirac function (Cressie, 2993). Thereafter, we substituted $R_{uu}(\tau)$ into the cross-correlation function between the stimulus signal $u(k)$ and the response signal $y(k)$ which yielded the following equation:

$$R_{uy}(\tau) = \sigma_u^2 \sum_{k=0}^{\infty} \delta(k-\tau)h(k) = \sigma_u^2 h(\tau)$$

We rearranged the terms of this equation to obtain the following equation defining the impulse response:

$$h(k) = \frac{R_{uy}(k)}{\sigma_u^2}$$

$h(k)$.

The correlation analysis method then estimated the impulse response to be robust but only when the input signal $u(k)$ was a zero-mean white noise signal. However, the input signal is not white noise in most real-world applications (Cressie, 1993). Therefore, we preconditioned the input $u(k)$ and output $y(k)$ signals before we applied them to our e correlation analysis method. We then generated a set of $k+1$ transmission-oriented risk based data points $(x_0, y_0), \ldots, (x_k, y_k)$ where no two x_j were the same employing an interpolation polynomial in the Newton form. By so doing, a linear combination of Newton basis polynomials:

$$N(x) := \sum_{j=0}^{k} a_j n_j(x)$$

[That is,] with the Newton basis polynomials was defined as $n_j(x) := \prod_{i=0}^{j-1}(x - x_i)$ for $j > 0$ and $n_0(x) \equiv 1$. The coefficients were then defined as $a_j := [y_0, \ldots, y_j]$ where $[y_0, \ldots, y_j]$ which in this research was represented using the notation for divided differences. As such, the endemic, transmission-oriented, Newton polynomial was then written as

$$N(x) = [y_0] + [y_0, y_1](x - x_0) + \cdots + [y_0, \ldots, y_k](x - x_0)(x - x_1)\cdots(x - x_{k-1}).$$

The Newton polynomial was then expressed in a simplified form when $x_0, x_1, \ldots, x_k$ which in this research was

arranged consecutively with equal spacing. Introducing the notation $h = x_{i+1} - x_i$ for each $i = 0, 1, \ldots, k-1$ and $x = x_0 + sh$, then rendered the difference $x - x_i$ which was then re-written as $(s-i)h$. So the onchocerciasis, endemic, transmission-oriented, Newton polynomial became:

$$N(x) = [y_0] + [y_0, y_1]sh + \cdots + [y_0, \ldots, y_k]s(s-1)\cdots(s-k+1)h^k$$ which in this research was:

$$= \sum_{i=0}^{k} s(s-1)\cdots(s-i+1)h^i[y_0, \ldots, y_i] = \sum_{i=0}^{k} \binom{s}{i} i!h^i[y_0, \ldots, y_i]N(x) = \sum_{i=0}^{k} \binom{s}{i} i!h^i[y_0, \ldots, y_i]$$

(that is, Newton forward divided difference formula). The polynomial interpolation was then used to construct the polynomial of degree $\leq n$ that passes through the *n*+1 sampled points $(x_k, y_k) = (x_k, f(x_k))$, for $k = 0, 1, \cdots, n$. If multiple "centers" $x_0, x_1, \ldots, x_n$ are used, then the result is the so called Newton polynomial (Hosmer et al., 2000). We then assumed that $f \in C^{n+1}[a, b]$ and $x_k \in [a, b]$ for $k = 0, 1, \cdots, n$ were distinct spatiotemporal-sampled values. Then $f(x) = P_n(x) + R_n(x)$ where $P_n(x)$ was a polynomial which in this research was used to approximate $f(x)$ and also:

$$P_n(x) = a_0 + a_1(x - x_0) + a_2(x - x_0)(x - x_1) + a_3(x - x_0)(x - x_1)(x - x_2) + a_n(x - x_0)(x - x_1)(x - x_2) \ldots (x - x_{n-1}) .$$

Thereafter, we wrote $f(x) \approx P_n(x)$. Our model revealed that the Newton polynomial went through the $n+1$ onchocerciasis, transmission–oriented, risk-based, sampled epidemiological points $\{(x_k, y_k)\}_{k=0}^{n}$, (that is, $P_n(x_k) = f(x_k)$ for $k = 0, 1, \ldots, n$). The remainder term $R_n(x)$ had the form:

$$R_n(x) = \frac{f^{(n+1)}(c)}{(n+1)!}(x - x_0)(x - x_1)(x - x_2) \ldots (x - x_{n-1})(x - x_n)$$, for any model parameter estimator value when $c = c(x)$ such that lay in the interval $[a, b]$. The covariate coefficients a_i were then constructed using divided differences.

In this research, the divided differences for a function $f[x]$ in our onchocerciasis, endemic, transmission-oriented, risk-based, landscape, distribution, epidemiological model were defined as:

$$f[x_{i-1}, x_i] = \frac{f[x_i] - f[x_{i-1}]}{x_i - x_{i-1}}, \quad f[x_{i-2}, x_{i-1}, x_i] = \frac{f[x_{i-1}, x_i] - f[x_{i-2}, x_{i-1}]}{x_i - x_{i-2}},$$

$$f[x_{i-3}, x_{i-2}, x_{i-1}, x_i] = \frac{f[x_{i-2}, x_{i-1}, x_i] - f[x_{i-3}, x_{i-2}, x_{i-1}]}{x_i - x_{i-3}}$$

and also

$$f[x_{i-j}, x_{i-j+1}, \ldots, x_i] = \frac{f[x_{i-j+1}, \ldots, x_i] - f[x_{i-j}, \ldots, x_{i-1}]}{x_i - x_{i-j}}$$

The divided difference formulae were then used to construct the endemic, transmission-oriented, risk-related, epidemiological model divided difference table as:

$x_i\ f[x_i]\ f[x_{i-1}, x_i]\ f[x_{i-2}, x_{i-1}, x_i]\ f[x_{i-3}, x_{i-2}, x_{i-1}, x_i]\ f[x_{i-4}, x_{i-3}, x_{i-2}, x_{i-1}, x_i]; x_0\ f[x_0], x_1\ f[x_1], x_2\ f[x_2]\ f[x_0, x_1], x_3\ f[x_3]\ f[x_1, x_2], x_4\ f[x_4]\ f[x_2, x_3]\ f[x_0, x_1, x_2], f[x_3, x_4]\ f[x_1, x_2, x_3]\ f[x_2, x_3, x_4]\ f[x_0, x_1, x_2, x_3]\ f[x_1, x_2, x_3, x_4]\ f[x_0, x_1, x_2, x_3, x_4], x_i\ f[x_i]\ f[x_{i-1}, x_i]\ f[x_{i-2}, x_{i-1}, x_i]\ f[x_{i-3}, x_{i-2}, x_{i-1}, x_i]\ f[x_{i-4}, x_{i-3}, x_{i-2}, x_{i-1}, x_i]$

The coefficient of our endemic, transmission-oriented, risk-based, landscape, distribution model was then directly related to the Newton polynomial when $P_n(x)$ was $a_i = f[x_0, x_1, \ldots, x_i]$. The coefficient also was the top element in the column of the *i*-th divided differences. The Newton polynomial of degree ≤ n then passed through n+1, risk-based, sampled points (that is, $(x_k, y_k) = (x_k, f(x_k))$, for $k = 0, 1, \cdots, n$) which was then quantitated as:

$$P_n(X) = a_0 + a_1 (X - X_0) + a_2 (X - X_0)(X - X_1) + a_3 (X - X_0)(X - X_1)(X - X_2)$$

$$+ a_n (x - x_0)(x - x_1)(x - x_2) \ldots (x - x_{n-1}) \quad .$$

The form the Newton polynomials of degree for the function $f[x] = \mathrm{Cos}[x]$ over the interval $[x_0, x_n]$ was then used along with equally spaced nodes selected from the following list:

$$\{\{x_k, y_k\}_{k=0}^{5}\} = \left\{\{0, 1\}, \left\{\frac{1}{5}, \mathrm{Cos}\left[\frac{1}{5}\right]\right\}, \left\{\frac{2}{5}, \mathrm{Cos}\left[\frac{2}{5}\right]\right\}, \left\{\frac{3}{5}, \mathrm{Cos}\left[\frac{3}{5}\right]\right\}, \left\{\frac{4}{5}, \mathrm{Cos}\left[\frac{4}{5}\right]\right\}, \{1, \mathrm{Cos}[1]\}\right\}$$ and so on. Thereafter, we let:

$$\pi_n(x) \equiv \prod_{k=0}^{n} (x - x_k), \qquad f(x) = f_0 + \sum_{k=1}^{n} \pi_{k-1}(x)\,[x_0, x_1, \ldots, x_k] + R_n,$$

and as such: where $[x_1, \ldots]$ was a divided difference, and the remainder was: $R_n(x) = \pi_n(x)\,[x_0, \ldots, x_n, x] = \pi_n(x)\,\dfrac{f^{(n+1)}(\xi)}{(n+1)!}$ for $x_0 < \xi < x_n$ (Figure 7).

The error terms corresponding to these onchocerciasis, endemic, transmission-oriented, explanatory, risk-based landscape model had the following useful bounds on their magnitude:

(i). $|R_1(x)| \le \dfrac{M_2}{8} h^2$ which was valid for $x \in [x_0, x_1]$,

(ii). $|R_2(x)| \le \dfrac{M_3}{9\sqrt{3}} h^3$ which was valid for $x \in [x_0, x_2]$,

(iii). $|R_3(x)| \le \dfrac{M_4}{24} h^4$ which was valid for $x \in [x_0, x_3]$,

(iv). $|R_4(x)| \le \dfrac{\sqrt{4750 + 290\sqrt{145}}}{3000} M_5 h^5$ which was valid for $x \in [x_0, x_4]$,

(v). $|R_5(x)| \le \dfrac{10 + 7\sqrt{7}}{1215} M_6 h^6$ which was valid for $x \in [x_0, x_5]$

The seasonal-sampled onchocerciasis related-endemic, transmission-oriented, polynomials of Newton basis e_k were then defined by:

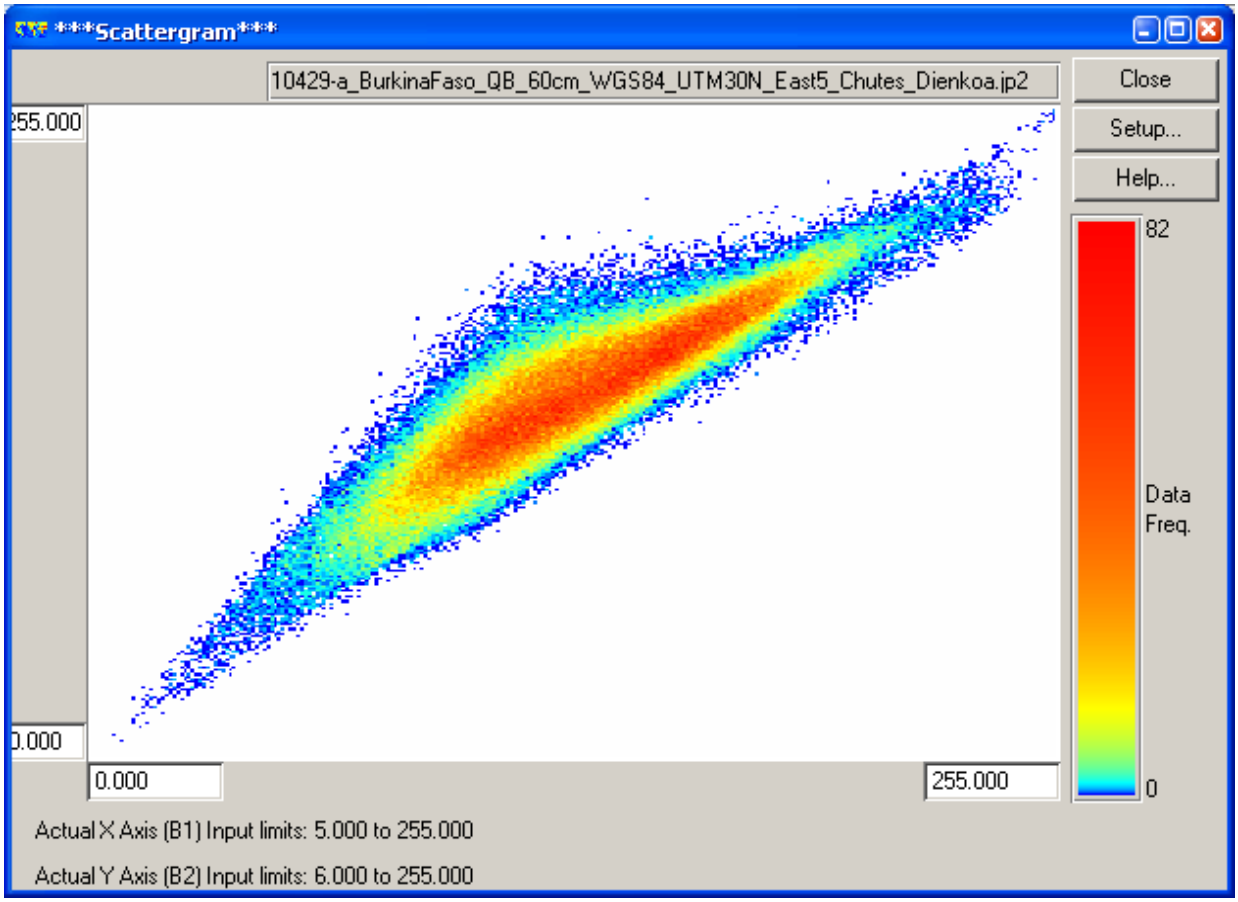

Figure 7. An endmemberspectral signature of the georeferenced *S. damnosum s.l.* riverine habitat capture point.

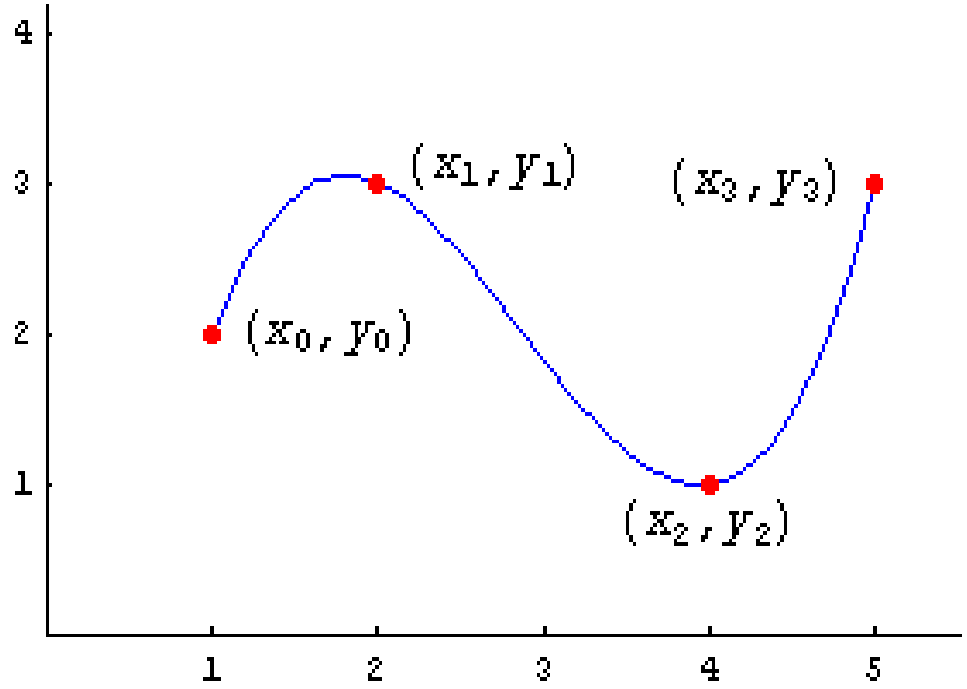

Figure 8. A cubic curve below illustrating the risk-based Newton polynomial of degree *n*=3.

$$e_k(x) = \prod_{i=0}^{k-1}(x - x_i) = (x - x_0)(x - x_1)\cdots(x - x_{k-1}), \quad k = 1, \ldots, n.$$

employing the following convention: $e_0 = 1$. Moreover

$$\begin{array}{lllllllll} e_1 & = & (x - x_0) & e_2 & = & (x - x_0)(x - x_1) & e_3 & = & (x - x_0)(x - x_1)(x - x_2) \\ e_n & = & (x - x_0)(x - x_1)\cdots(x - x_{n-1}) & & & & & & \end{array}$$

.

The set of robust transmission-oriented, risk-based, epidemiological polynomials [that is, $(e_k)_{0\le k\le n}$] were the basis of P_N , which in this research represented the space of polynomial of degree and was at most equal to *n*. Indeed, they constituted an echelon-degree set of $(n+1)$ polynomial. Newton interpolation of degree n in this research was thereafter related to the subdivision

$\{(x_0, y_0), (x_1, y_1), \ldots, (x_n, y_n)\}$ = $P_n(x) = \sum_{k=0}^{n} \alpha_k e_k(x) = a_0 + a_1(x - x_0) + a_2(x - x_0)(x - x_1)$ where

$P_n(x_i) = f(x_i), \quad \forall i = 0, \ldots, n.$

We then determined the explanatory, predictor, covariate coefficients $(\alpha_k)_{0\le k\le n}$ using divided differences. Newton's interpolation polynomial of degree n , $P_n(x)$, were then evaluated at x_0 rendering:

$$P_n(x_0) = \sum_{k=0}^{n} \alpha_k e_k(x_0) = \alpha_0 = f(x_0) = f[x_0]$$

We then re-wrote $f[x_i] = f(x_i), \quad \forall i = 0, \ldots, n\ f[x_0]$ as a zero-order divided difference. The onchocerciasis –related, Newton's interpolation, polynomial of degree n , $P_n(x)$ was then evaluated at x_1 rendering:

$$P_n(x_1) = \sum_{k=0}^{n} \alpha_k e_k(x_1) = a_0 + a_1(x - x_0) + a_2(x - x_0)(x - x_1) \ldots + \alpha_n(x - x_0)(x - x_1)\cdots(x - x_{n-1})$$

Hence: $\alpha_1 = \dfrac{f[x_1] - f[x_0]}{x_1 - x_0} = f[x_0, x_1]$.

In our model $f[x_0, x_1]$ was the first -order divided difference. The interpolation polynomial of degree *nPn*(*x*)was then evaluated at x_2 rendering:

$$\begin{array}{l} P_n(x_2) = \sum \alpha_k e_k(x_2) = \alpha_0 + \alpha_1(x_2 - x_0) + \alpha_2(x_2 - x_0)(x_2 - x_1) = \alpha_0 + \alpha_1(x_2 - x_0) + \alpha_2(x_2 - x_0)(x_2 - x_1) \\ = f[x_0] + f[x_0, x_1](x_2 - x_0) + \alpha_2(x_2 - x_0)(x_2 - x_1) = f[x_2] \end{array}$$

Then: $\alpha_2(x_2 - x_0)(x_2 - x_1) = f[x_2] - f[x_0] - f[x_0, x_1](x_2 - x_0)$

$$\alpha_2 = \frac{f[x_2] - f[x_0]}{(x_2 - x_0)(x_2 - x_1)} - \frac{f[x_0, x_1]}{x_2 - x_1}$$

$$\alpha_2 = \frac{f[x_2] - f[x_0]}{(x_2 - x_0)(x_2 - x_1)} - \frac{f[x_0, x_1]}{x_2 - x_1} \quad \alpha_2 = \frac{f[x_0, x_2] - f[x_0, x_1]}{x_2 - x_1}$$ and

The final following form of the polynomialized,onchocerciasis-related, regression-based,parameter estimators was then:

$$\begin{aligned}
\alpha_2(x_2 - x_0)(x_2 - x_1) &\equiv f[x_2] - f[x_0] \\
\alpha_2(x_2 - x_0)(x_2 - x_1) &\equiv f[x_2] - f[x_0] \\
\alpha_2(x_2 - x_0)(x_2 - x_1) &\equiv f[x_2] - f[x_1] \\
\alpha_2(x_2 - x_0)(x_2 - x_1) &\equiv f[x_2] - f[x_1] \\
\alpha_2(x_2 - x_0)(x_2 - x_1) &\equiv f[x_2] - f[x_1] \\
\alpha_2(x_2 - x_0) &\equiv \frac{f[x_2] - f[x_1]}{x_2 - x_1} \\
\alpha_2(x_2 - x_0) &\equiv f[x_1, x_2] - f[
\end{aligned}$$

$$\alpha_2 = \frac{f[x_1, x_2] - f[x_0, x_1]}{x_2 - x_0} = f[x_0, x_1, x_2]$$

Hence, in this research, was the second-order divided difference. By recurrence, we then obtained:

$$\alpha_k = \frac{f[x_1, \ldots, x_k] - f[x_0, \ldots, x_{k-1}]}{x_k - x_0} = f[x_0, \ldots, x_k]$$ which was then the k[th]-order divided difference. The Newton's interpolation polynomial of degree was then obtained via the successive divided differences:

$$P_n(x) = f[x_0] + \sum_{k=1}^{n} f[x_0, \ldots, x_k] e_k(x)$$

.

Thereafter, for quantizing interpolation error in our model, we assumed that:

$f \in \mathcal{C}^n([a, b])$ and $x \in [a, b]$.

We then let *I* be the closed set defined by:

$I = [\min(x, x_0), \max(x, x_n)]$ (that is, the smallest closed set containing x and the x_i's). We employed:

$\exists \xi \in I / f[x_0, \ldots, x_n] = \frac{f^n(\xi)}{n!}$ then we let: $d(x) = f(x) - p(x).$

The quantized, interpolation, error factor and its complement were then:

$\eta_q = \eta + \nu$ and $\overline{\eta}_q = \overline{\eta} - \nu$ where, $\eta, \overline{\eta}$ were unsigned; {that is, $|\nu| \leq 2^{-(n_\eta+1)}$].

The interpolated coefficient then rendered $\hat{h}_{qq}(t) = (\overline{\eta} - \nu)[h(t_0) + \epsilon_0] + (\eta + \nu)[h(t_1) + \epsilon_1]$ and $= \hat{h}(t) + \overline{\eta}\epsilon_0 + \eta\epsilon_1 + \nu[h(t_1) - h(t_0)]$ when the second-order errors $V\varepsilon_0$ and $V\varepsilon_1$ were dropped. Since $|h(t_1) - h(t_0)| \leq M_1$, we obtained the error bound for the onchocerciasis-related endemic transmission-oriented model using: $|e_{qq}(t)| \leq 2^{-n_c} + 2^{-(n_\eta+1)} M_1 + \frac{1}{8} M_2.$

By successively applying Rolle's theorem (*n*times) in the spatiotemporal, infectious disease model, $d^{(n)}(x)$ equaled zero at any given sampled point $\xi \in I$: $d^{(n)}(\xi) = 0.$ Thus, we had: $f^{(n)}(\xi) = P_n^{(n)}(\xi)$. Since the seasonal-sampled, onchocerciasis, explanatory, covariate coefficients of x^n in P_n in this research was $f[x_0, \ldots, x_n]$, $f^{(n)}(\xi) = P_n^{(n)}(\xi) = n! \cdot f[x_0, \ldots, x_n]$ hence $f[x_0, \ldots, x_n] = \frac{f^{(n)}(\xi)}{n!}$.

In calculus, Rolle's theorem essentially states that a differentiable function attains equal values at two distinct points which must have a point somewhere between them where the first derivative (that is, the slope of the tangent line to the graph of the function) is zero (Ross, 2007). We then assumed that: $f \in \mathcal{C}^{n+1}([a, b])$ and $x \in [a, b]$ in the transmission-oriented, risk-based, epidemiological, risk model .We then let *I* be the closed set defined by: $I = [\min(x, x_0), \max(x, x_n)]$ (that is, the smallest closed empirical data set containing *x*) and then solved for: We then let $\hat{x} \in [a, b]$ and then assumed that $\hat{x} \neq x_i$ for performing a Lagrange polynomial interpolation for mapping $\mathbf{x_i}$ = $\forall x \in [a, b], \quad \exists \xi \in I / f(x) - P_n(x) = \frac{f^{n+1}(\xi)}{(n+1)!} \prod_{i=0}^{n} (x - x_i)$ the endemic, transmission-oriented regions within the riverine study site. In numerical analysis, Lagrange polynomials are used for polynomial interpolation. For a given set of distinct points x_j and numbers y_j, the Lagrange polynomial is the polynomial of the least degree that at each point x_j assumes the corresponding value y_j (that is, the functions coincide at each point) (Cressie, 1993). We then considered the unique polynomial *Pn+1* of degree (n+1) which interpolated *f* at the transmission-oriented, risk-based, regression points [that is, $(x_0, y_0), (x_1, y_1), \ldots, (x_n, y_n), (\hat{x}, f(\hat{x}))$] and P_{n+1} which verified:

$$\begin{cases} P_{n+1}(x_i) = f(x_i), & \forall i = 0, \ldots, n \\ P_{n+1}(\hat{x}) = f(\hat{x}). \end{cases}$$

The polynomial P_{n+1} was then written as: $P_{n+1}(x) = P_n(x) + (x - x_0) \ldots (x - x_n) f[x_0, \ldots, x_n, \hat{x}]$

$$f[x_0,\ldots,x_n,\hat{x}]=\frac{f^{(n+1)}(\xi)}{(n+1)!}$$

According to our model , therefore, by setting the expressions:

$$x=\hat{x},\ P_{n+1}(\hat{x})=f(\hat{x}),\ f(\hat{x})=P_n(\hat{x})+(\hat{x}-x_0)\ldots(\hat{x}-x_n)\frac{f^{(n+1)}(\xi)}{(n+1)!}.$$

In our analyses we found three 3 data points $\{(0,1),(2,5),(4,17)\}$, which determined the Newton interpolation polynomial of degree 3 which passed through the following points:

$$x_0=0\quad f[x_0]=1,\begin{bmatrix} x_0=0 & f[x_0]=1 & \\ x_1=2 & f[x_1]=5 & f[x_0,x_1]=\frac{5-1}{2-0}=2 \end{bmatrix}$$

which represented the:

$$x_2=4\quad f[x_2]=17\quad f[x_1,x_2]=\frac{17-5}{4-2}=6\quad f[x_0,x_1,x_2]=\frac{6-2}{4-0}=1$$

0 (that is, capture point) from 0 to 5 km hyperendemic range, 5 to 10 km. Thereafter, a mesoendemic range was measured from 5 to 10 km, 10 to 15 km was hypoendemic and after 15 km no transmission.

To validate the Newton polynomial that passed through the transmission-oriented endemic points we tested $i=0,1,\cdots,n$ which in this research was performed where:

$d_{i,0}=y_i$ for $i=0,1,\ldots,n$ and $d_{i,j}=\frac{d_{i,j-1}-d_{i-1,j-1}}{x_i-x_{i-j}}$ for $i=1,2,\ldots,n$ and $j=1,2,\ldots,i$

Newton polynomials were then created "recursively." employing:

$$P_n(x)=P_{n-1}(x)+d_{n,n}(x-x_0)(x-x_1)(x-x_2)\ldots(x-x_{n-1}).$$

The divided difference $f[x_0,x_1,x_2,\ldots,x_n]$, was then denoted $[x_0,x_1,x_2,\ldots,x_n]$), whereby the transmission-oriented risk-based points, x_0, x_1, ..., x_n of a function $f(x)$ was defined by $f[x_0]\equiv f(x_0)$ and $f[x_0,x_1,\ldots,x_n]=\frac{f[x_0,\ldots,x_{n-1}]-f[x_1,\ldots,x_n]}{x_0-x_n}$ for $n\geq 1$. The first few differences were quantitated using:

$f[x_0,x_1]=\frac{f_0-f_1}{x_0-x_1}$, $f[x_0,x_1,x_2]=\frac{f[x_0,x_1]-f[x_1,x_2]}{x_0-x_2}$ and then:

$$f[x_0,x_1,\ldots,x_n]\frac{f[x_0,\ldots,x_{n-1}]-f[x_1,\ldots,x_n]}{x_0-x_n}.$$

Thereafter, we defined:

$\pi_n(x)\equiv(x-x_0)(x-x_1)\cdots(x-x_n)$ and then solved $\pi_n'(x_k)=(x_k-x_0)\cdots(x_k-x_{k-1})(x_k-x_{k+1})\cdots(x_k-x_n)$ which rendered the identity: $f[x_0,x_1,\ldots,x_n]=\sum_{k=0}^{n}\frac{f_k}{\pi_n'(x_k)}$.

All the time series-dependent, riverine, spatial, data, feature, attribute points based on the QuickBird mixel encompassing the Precambrian rock and rippled water components were then examined in *n*-dimensional space. A meaningful endmember spectrum for the vertex was calculated from the radiative transfer model residuals employing the vector Euclidean norm to the subspace as defined by the selected, georeferenced, *S. damnosum s.l.,*riverine, larval, habitat, capture point Precambrian rock and rippled water spectral endmembers. To find these candidate mixel spectra, we constructed a QuickBird endmember dataset using *P possible*, consisting of *r* sub- mixel spectral emissivities that were closest to the vertex. Then we generated an spectral endmember subset using $P_{candidate} = \left\{\vec{p}_{(x_1y_1)}, \vec{p}_{(x_1y_1)}, \ldots, \vec{p}_{(x_cy_c)}\right\} (c \le r, P_{candidate} \in P_{possible})$ which was selected from the *r* pixels ($P_{possible}$) which was subject to conditions based on: $x_i - x_j \le t\_pixel$ and $y_i - y_j \le t\_pixel (i \ne j)$. We used the equation $s\_angle(\bar{p}_{(x_iy_i)}, \bar{p}_{(x_jy_j)}) \le t\_\theta\ (i \ne j)$ as the spectral angle between the epidemiological capture point, Precambrian rock and ripple water sub-mixel radiance and calculated $s\_angle(\vec{p}_{(x_iy_i)}, \vec{p}_{(x_jy_j)}) = cos^{-1}\left(\frac{\vec{p}_{(x_iy_i)} \cdot \vec{p}_{(x_jy_j)}}{\|\vec{p}_{(x_iy_i)}\| \|\vec{p}_{(x_jy_j)}\|}\right)$ where *t_θ* was the threshold value for the spectral angle beyond which the endmember spectra were not considered similar. The value of *t_θ* was set at 2.5 degrees. The unmixing algorithm identified $\bar{e}_1, \bar{e}_2, \ldots, \bar{e}_m$ the brightest, sub-mixel, data, feature attribute (i.e., ripple water pixel components) and the darkest, sub-mixel, data attribute (that is, Precambrian rock). The algorithm then iteratively found the remaining endmembers using orthogonal projections until the number of endmembers defined was obtained.

A number of Precambrian rock, ripple water components and the sampled*S. damnosum s.l.*riverine, larval, habitat, capture point, and the endmembers (*m*) were used to find the spectral angle threshold *t_θ* and the spatial threshold (that is, *t_θ* QuickBird mixel) in the SPA algorithm. The first step was to extract the first endmembers. The vector norms of the QuickBird sub-mixel data determined the largest norm value. Sub-mixel heterogeneity at the simplex vertices were then calculated which revealed the radiance data in the image cube. The capture point first endmember was estimated. We then used an orthogonal projection for extraction of all the other related endmember, sub-mixel, *S. damnosum s.l.,*riverine, larval, habitat, capture point Precambrian rock and ripple water spectral components. All the QuickBird, sub-mixel, spectral data was then fractionally calculated based on the visible and NIR spectrum. We used an endmember matrix $U = [\bar{e}_1, \bar{e}_2, \bar{e}_3]$ which projected the QuickBird sub-mixel data into subspace .We noticed that S_{proj} was orthogonal to the space spanned by *U* as $\bar{p}_{(i,j)\_proj} = O\bar{p}_{(i,j)}$, where $\bar{p}_{(i,j)\_proj}$ and $\bar{p}_{(i,j)}$ were the projected and original mixel vector at the georeferenced capture point location (i, j), respectively.

In this research, O was the projection operator, $O = I - UU^{+}$where *I* was the identity matrix and U^{+} was the pseudo inverse of *U,* which was denoted by $U^{+} = (U^T U)^{-1} U^T$? We then validated the endmember matrix (that is, $U = [\bar{e}_1, \bar{e}_2, \bar{e}_3]$). We calculated the change of the simplex volume with each subspace projection. The volume of the simplex was then derived. The volume increase was determined by the spectral contrasts between the endmembers. Here, C_{l-1} and C_l denoted the simplexes defined by the original endmember set, $\{\bar{e}_1, \bar{e}_2, \ldots, \bar{e}_{l-1}, \bar{e}_l\}$ and the ratio of the volumes of C_{l-1} and C_l was calculated as $v\_ratio_l = \frac{V(C_l)}{V(C_{l-1})}$. $(3 < l \le m)$. Each *S. damnosum s.l.* riverine habitat endmember proportion was then calculated.

In our analyses, the BRDF of the decomposed *S. damnosum s.l.* habitat mixel using the geometric-optical model was modeled as the limit of its directional reflectance factor using:

$$R(i,v) \quad R(i,v) = \frac{\int\int_A R(s)\langle i,s\rangle\langle v,s\rangle I_i(s) I_v(s) ds}{A \cos\theta_i \theta_v} \tag{8}$$

Where *ds* was a small Lambertian surface element over area A of the QuickBirdmixel; $R(s)$ was the reflectance of ds; i, v, and s represented the directions of illumination and viewing based on the Precambrian rock surface and rippled water,spectral,reflectance components, respectively. In our model $\langle \cdot, \cdot \rangle$was the cosine of the phase angle between two directions; O was the zenith angle of a direction; $I_i(s)$ and $I_v(s)$ were indicator functions, equal to one when ds was illuminated (I_i) or viewed (I_v) or zero otherwise. If a surface exhibits Lambertian reflectance, light falling on it is scattered such that the apparent brightness of the surface to an observer is the same regardless of the observer's angle of view, thus, the surface luminance is isotropic (Schowengerdt, 1997). Solving the double integral equation revealed that ds was integrated over

the decomposed QuickBird mixel [that is, the footprint of the sensor's instantaneous field of vision (iFOV)]. We noticed that there were two kinds of prominent riverine larval habitat surfaces in the sub-mixel, endmember, spectra; A-background, surface (that is, Precambrian rock) and spectral ,surface-oriented, ripple, water, data, feature attributes were represented by Lambertian reflectance G and C, respectively. We then re-wrote equation (8) as:

$$R(i,v) = K_g G + \frac{C}{A}\iint_{A_c} \frac{\langle i,s\rangle}{\cos\theta_i}\frac{\langle v,s\rangle}{\cos\theta_v} ds \,, \quad \text{where}$$

$K_g = A_g / A$ was the proportion of background spectral data illuminated and viewed rendered by the QuickBird imaged capture point attributes. In this equation the union of *Ag* and A_c were the intersection of the dataset of the capture point surface elements which were illuminated and viewed, only when v and i coincided. The directional reflectance of the habitat scene depended also on the Precambrian rock and ripple water reflectance related to *G* and *C*.

In the mixel decomposition we focused on the two terms of:

$$R(i,v) = K_g G + \frac{C}{A}\iint_{A_c} \frac{\langle i,s\rangle}{\cos\theta_i}\frac{\langle v,s\rangle}{\cos\theta_v} ds$$

The first term described how the sunlit background proportion proceeded to a maximum point as viewing and illumination positions in the hemisphere coincided. The second term described how the sunlit *S. damnosum s.l.*riverine larval habitat surface, composed of the Lambert Ian facets became maximally exposed to view at the hotspot, while those facets on tops became dominant at large viewing zenith angles. The hot spot correlation effect refers to the observed brightening which can occur when viewing a scene from the same direction as the solar illumination (Burrough and McDonnell, 1998) which for predictive, vector, insect habitat, predictive, risk modeling is commonly noted in the visible and NIR spectral regions (Jacob et al., 2011a).

We then analyzed how the first term K_gG varied with illumination and viewing geometry. As in Strahler and Jupp (1990), we assumed that the spatial object of interest (that is, *S. damnosum s.l.* habitat) and its associated explanatory sub-mixel spectral, predictor, covariate, coefficient estimates had the shape of a spheroid, with vertical half-axis equal to *b*, horizontal radius equal to *R* and a height to the center of the spheroid *h*. To accommodate the spheroidal shape in the derivations of the shadowed habitat areas, we used the transformation:

$$\theta' = \tan^{-1}\left(\frac{b}{R}\tan\theta\right)$$

We solved this equation by replacing θ with the angle that would generate the same shadow area for a sphere. For simplicity, we assumed that the centers of the spheroids were randomly distributed in depth from h_1 to h_2 over A. We then assumed that *G* and *C* were constant average signatures over Ag and Ac for properly endmember modelling Kg and Kc = A_c/A.

Next, the equation:

$$R(i,v) = K_g G + \frac{C}{A}\iint_{A_c} \frac{\langle i,s\rangle}{\cos\theta_i}\frac{\langle v,s\rangle}{\cos\theta_v} ds$$

was employed where K_g was expressed in a Boolean model and $K_g = e^{-\lambda\pi R^2\left[\sec\theta_i' + \sec\theta_v' - \bar{O}(\theta_i,\theta_v,\phi)\right]}$ where $\bar{O}(\theta_i,\theta_v,\phi,)$ was the average of the overlap function $O(\theta_i,\theta_v,\phi,h)$ between illumination and viewing shadows of the georeferenced capture point and its associated Precambrian rock and ripple water features. The Boolean model for a random subset of the plane or higher dimensions, analogously is a common tractable models in stochastic geometry (Cressie, 1993). Jacob et al. (2011c) used a Poisson point process of rate λ in the plane of a spectrally, decomposed, georeferenced, aquatic, larval, habitat,of *An. arabiensis,* and then made each sampled point be the center of a random set. The resulting union of the overlapping sets was a realization of the Boolean model [$\mathcal{B}$]. More precisely, the spectral parameter estimators were λ. Then a probability distribution on compact sets was created for each sampled point ξ employing a Poisson point process which used a set C_ξ from the distribution, and then defined $\mathcal{B}$ as the union $\cup_\xi(\xi + C_\xi)$ of the translated sets. To illustrate tractability with one simple formula, the mean density of $\mathcal{B}$ was then defined by a QuickBird sub-mixel endmember classification which revealed that $1 - \exp(-\lambda \mathrm{E}\,\Gamma)$ where Γ denoted the sampled *S. damnosum s.l.* riverine habitat surface area of C_ξ.

In this research, ϕ was the difference in Azimuth angle between viewing and illumination positions of the QuickBird imaged objects associated to the *S. damnosum s.l.*, riverine, larval, habitat capture point. To simplify the equation, we approximated the overlap function by the overlap area and center positions of the ellipses. This approximation is justified when solar zenith and viewing zenith angles are not too large (Strahler and Jupp, 1990). In the case of long ellipsoidal shadows, however, this approximation could have overestimated the width of the capture point hotspot in the Azimuthal direction and underestimated the width of the hotspot in

the Azimuthal direction. To improve the accuracy and preserve the proper hotspot width information, we developed another approximation as follows. We used the equations $\phi = 0_{or}\ \phi = \pi$. First, we considered the overlap function in the principal plane. We used W $\phi = 0_{\text{and}}\ \pi$ as the elliptical illumination estimates to determine if all the viewing shadows were aligned in the same direction. The overlap area was then approximated by an ellipse with one axis equal to the overlap length and the other equal to the capture point width encompassing the Precambrian rock and ripple water mixel spectrally decomposed radiance components which yielded:

$$O(\theta_i, \theta_v, \phi) = \frac{1}{2}\left[\sec\theta_i' + \sec\theta_v' - \frac{h}{b}\left|\tan\theta_i' - \tan\theta_v' \cos\phi\right|\right]$$

In the geometric-optical model, the shape of the hotspot function was based on the viewing and illumination positions in the model, and these diverged due to the shape and height of the spheroids. The "hotspot" was defined as a site with a combination of Precambrian rock and turbid water, sub-mixel, endmember data associated with *S. damnosum* s.*l.* larval breeding habitat. The equation *S* = (AgG + ACC + AZZ + AtT) IA, where S represented the reflectance of the QuickBird mixel; G, C, Z, and T were the reflectances of sunlit ground and shadowed ground and canopy, respectively; Ag through A were the corresponding areas of the four components; and A was the mixel size, and was helpful to understand how the physical shape of the *S. damnosum s.l.* riverine habitat, Precambrian rock and riffle water components governed the shape of the overlap functions. The exact overlap function on the principal cone was also obtained using the hybrid of the geometric optical model for capturing bi-directional reflectance values over the riverine larval habitat attributes.

In the model, the viewing zenith was the viewing direction, which had a different Azimuth than the illumination position. Rather than computing the overlap of ellipses rendered from the *S. damnosum s.l.* habitat, the Precambrian rock and its riffle water spectral components at arbitrary inclinations and distances directly, we fit a linear function to the diminution of the overlaps generated from the model residuals using Azimuth angles. We approximated the Azimuthal cut off of the hotspot and linearly interpolated the model residuals. The residual output from the equation was then used to determine that; (1) the Azimuthal width of hotspot effect was basically determined by a ratio; (2) the outward width of hotspot on the principal plane was determined by ratio, and; (3) the inward width was determined by both. The composition of this signature was 34% red, 11% blue and 55% green. This signature corresponded to habitats consisting of fast flowing water over a base of Precambrian rock.

We then employed an ordinary kriged-based algorithm in ArcGIS Geostatistical Analyst for predicting other unknown, unsampled *S. damnosum s.l.* habitats at the study site using the reference signature generated from the canopy endmember extraction algorithms. For determining optimal explanatory predictor covariate coefficients, a variogram was constructed which expressed the variation in the spectral estimatators. In this research the variogram [that is, 2γ(*x*, *y*)] was a function describing the degree of dependence between the predictedgeoreferenced *S. damnosum s.l.* riverinelarval habitats [i.e., *Z*(*x*)]. This was defined as the expected squared increment of the forecasted values between the forecasted georeferenced habitat locations. Our model was nonnegative since it was the expectation of a square. The covariance function was related to variogram by 2γ(*x*,*y*) = *C*(*x*,*x*) + *C*(*y*,*y*) − 2*C*(*x*,*y*). In this research, the γ(*x*,*y*) = *E*(| *Z*(*x*) − *Z*(*y*) | ^{2}) was equivalent to γ(*y*,*x*) which was a symmetric function, consequently, $\gamma_s(h) = \gamma_s(-h)$ was an even function. In this research, the function was also a semivariogram as it was a conditionally negative definite function, (i.e., for all weights $w_1, \ldots, w_N$subject to $\sum_{i=1}^{N} w_i = 0$) and the *S. damnosums.l.* habitat geolocations ($x_1, \ldots, x_N$); thus,

$$\sum_{i=1}^{N}\sum_{j=1}^{N} w_i \gamma(x_i, x_j) w_j \leq 0$$

.

Semivariogram plot of the logit scale model residuals confirmed a short range spatial pattern up to a distance of approximately 20 km from the predicted *S. damnosum s.l.,*riverine, larval, habitat site. To carry out this process, residuals for all observed points were calculated on the logit (ln(*p*/1 - *p*)) scale of the model. A kriged map of deviance residuals was then calculated which was added to the predicted values on the logit scale. Spatial dependence, displayed by these plots was analyzed using the semivariogram. The addition of kriged residuals allowed the maps to deviate from the model and move closer to the original sampled, canopy-related, predictor, covariate, coefficient, indicator, measurement values. These smoothed values improved the final maps of the forecasted *S. damnosum s.l.* habitats and its associated canopy cover, Precambrian rock and rippled water components sampled. An exponential model was then fitted to the semivariogram, using a range of 72.6 m, a nugget of 0.21 (variance), a lag size of 11.5 m with 12 lags and a partial sill of 0.24 (variance) (Figure 8). Thereafter, a predictive *S. damnosum* s.l. habitat canopy-based map was generated for a neighbouring riverine study site (Figure 9). The forecasted *S. damnosum s.l.* habitats were then field-verified which revealed a 100% correlation with the predicted estimates. We then used

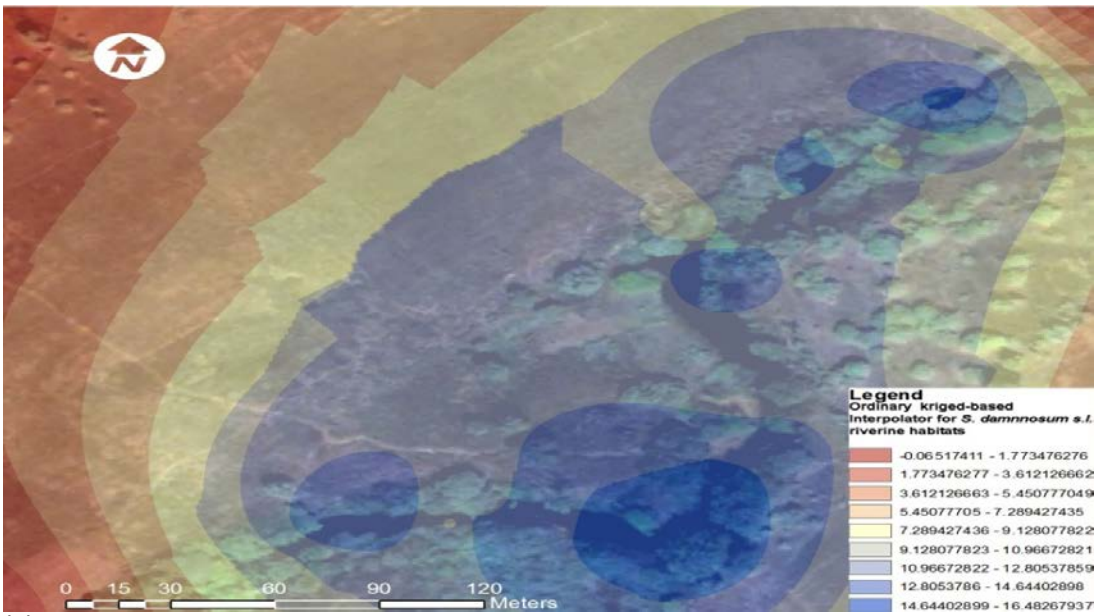

(A)

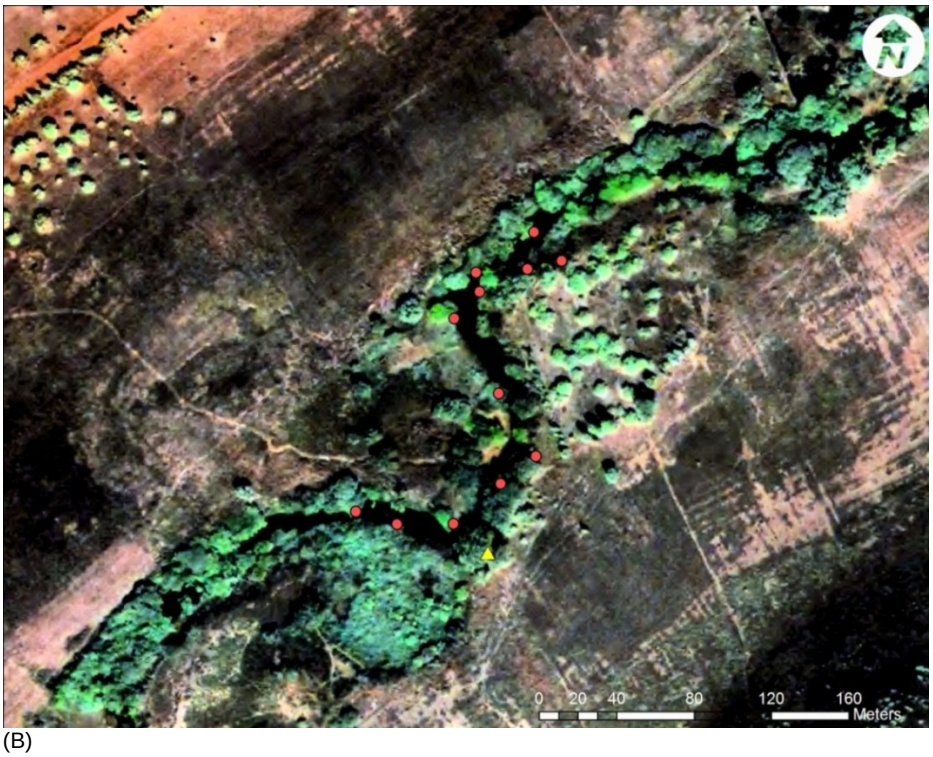

(B)

Figure 9. (A) Kriged*S. damnosum s.l.* habitat pixel spectral reflectance estimates with predicted using a QuickBird endmember reference signature, (B) Predicted *S. damnosum s. l.* habitats in a neighbouring riverine ecosystem at the *S. damnosum s. l.* riverine epidemiological study site.

the ARIMA procedure outlined by Box and Jenkins for quantifying the nonlinear least squares iterations. Given our time-series dependent data where t was an integer index and X_t was the sampled immature *S. damnosum s.l.* data, then an ARMA (*p*,*q*) model was constructed based on $\left(1-\sum_{i=1}^{p}\alpha_i L^i\right)X_t=\left(1+\sum_{i=1}^{q}\theta_i L^i\right)\varepsilon_t$ (9) where L was the lag operator, the α_i were the parameters of the autoregressive part of the model, the θ_i was the parameters of the moving average part and the ε_t were

error terms. The error terms [that is, ε_t] were generally assumed to be i.d.d variables sampled from a normal distribution with zero mean. Assuming now that the polynomial $\left(1-\sum_{i=1}^{p}\alpha_i L^i\right)$ has a unitary root of multiplicity *d*., we rewrote equation 9 as $\left(1-\sum_{i=1}^{p}\alpha_i L^i\right)=\left(1-\sum_{i=1}^{p-d}\phi_i L^i\right)(1-L)^d$. The ARIMA (*p*,*d*,*q*) process expressed this polynomial factorization property, which was then rendered by: $\left(1-\sum_{i=1}^{p}\phi_i L^i\right)(1-L)^d X_t=\left(1+\sum_{i=1}^{q}\theta_i L^i\right)\varepsilon_t$. Our model output resembled a particular case of an ARMA (*p*+*d*,*q*) process having the auto-regressive polynomial with some roots in the unity.

In terms of estimation methods, METHOD = ML option in PROC ARIMA which produced MLEs. The MLEs were computed by letting the univariate ARMA models be $\phi(B)(W_t-\mu_t)=\theta(B)a_t$ where a_t was an independent sequence of normally distributed innovations with mean 0 and variance σ^2. Here μ_t was the mean parameter μ plus the transfer function inputs. The log-likelihood function was then written as follows: $-\frac{1}{2\sigma^2}\mathbf{x}'\mathbf{\Omega}^{-1}\mathbf{x}-\frac{1}{2}\ln(|\mathbf{\Omega}|)-\frac{n}{2}\ln(\sigma^2)$. In this equation, *n* was the number of georeferenced *S. damnosum s. l.* spatiotemporal-sampled, riverine, spectral, larval, habitat observations, $\sigma^2\mathbf{\Omega}$ was the variance of x as a function of the ϕ and θ parameters, and $|\mathbf{\Omega}|$ denoted the determinant. The vector x was the time series $W_t$minus the structural part of the modelμ_t, written as a column vector, as follows:

$$\mathbf{x}=\begin{bmatrix}W_1\\W_2\\\vdots\\W_n\end{bmatrix}-\begin{bmatrix}\mu_1\\\mu_2\\\vdots\\\mu_n\end{bmatrix}$$

The MLE of σ^2 in the endemic, transmission-oriented, Euclidean, distance-based, transmission-oriented models was then computed as:

$$s^2=\frac{1}{n}\mathbf{x}'\mathbf{\Omega}^{-1}\mathbf{x}$$

Note that the default estimator of the variance was divided by $n-r$, where *r* was the number of estimators in the model, instead of by *n*. Specifying the NODF option caused a divisor of *n* to be used. The log-likelihood with respect to σ^2 was then optimized using additive constants which then rendered $-\frac{n}{2}\ln(\mathbf{x}'\mathbf{\Omega}^{-1}\mathbf{x})-\frac{1}{2}\ln(|\mathbf{\Omega}|)$ in the model residuals. We let H be the lower triangular matrix with positive elements on the diagonal such that $\mathbf{H}\mathbf{H}'=\mathbf{\Omega}$. We also let e be the vector $\mathbf{H}^{-1}\mathbf{x}$ in the model. The concentrated log-likelihood with respect to $\sigma^2$was then written as $-\frac{n}{2}\ln(\mathbf{e}'\mathbf{e})-\ln(|\mathbf{H}|)$ and $-\frac{n}{2}\ln(|\mathbf{H}|^{1/n}\mathbf{e}'\mathbf{e}|\mathbf{H}|^{1/n})$. The MLEs were then produced by using the LMA to minimize the following sum of squares: $|\mathbf{H}|^{1/n}\mathbf{e}'\mathbf{e}|\mathbf{H}|^{1/n}$ in the models. The subsequent analysis of the residuals was done by using e as the vector of residuals.

Thereafter the METHOD=CLS option produced robust conditional least squares (CLS) estimates. The series x_t was represented in terms of the seasonal-sampled *S. damnosum s.l.* riverine larval habitat observations, as follows:

$$x_t=a_t+\sum_{i=1}^{\infty}\pi_i x_{t-i}$$

The π weights were computed from the ratio of the ϕ and θ polynomials, as follows:

$$\frac{\phi(B)}{\theta(B)}=1-\sum_{i=1}^{\infty}\pi_i B^i$$

The CLS method produced estimates minimizing:

$$\sum_{t=1}^{n}\hat{a}_t^2=\sum_{t=1}^{n}\left(x_t-\sum_{i=1}^{\infty}\hat{\pi}_i x_{t-i}\right)^2$$

Whereby $\hat{\pi}_i$ was computed from the estimates of ϕ and θ at each iteration. For attaining robust METHOD=ULS and METHOD=ML, initial estimates were computed using the METHOD=CLS algorithm. The arthropod-related, infectious disease, transmission–oriented, risk-model, residual estimates were then obtained by applying least squares MLE to the noise series. Thus, for transfer function models, the MLE option did not generate the full multivariate ARMA MLEs employing only the univariate likelihood function which in this research was applied to the noise series.

Because PROC ARIMA in SAS/GIS employed all of the available data for the input series to generate the noise series, other start-up options for the transferred series was implemented by prefixing the seasonal-sampled, *S. damnsoum s.l.,* riverine, larval, habitat observations as non-interpolated covariate coefficients. For example, we fit a transfer function model to the sampled, onchocerciasis, transmission-oriented, variable Y with the single input X. Thereafter, we employed a start-up using 0 for the seasonal sampled values by prefixing the coefficients to the actual data using an observation with a missing value for Y and a value of 0 for X. PROC ARIMA was then computed which generated the information criteria, (AIC). The AIC can be used to compare competing

models fit to the same series (Cressie, 1993). The AIC rendered $AIC = 2k - 2\ln(L) = 2k - 2(C - \chi^2/2) = 2k - 2C + \chi^2$ for each Euclidean, distance-based ArcGIS, endemic, delineated, transmission-oriented zone. Thereafter, the model order depicted the pattern associated with an ARMA series.

In this research, the chi-square statistics employed in the test for lack of fit were computed using the Ljung-Box formula:

$$\chi^2_m = n(n+2)\sum_{k=1}^{m}\frac{r_k^2}{(n-k)} \text{ where } r_k = \frac{\sum_{t=1}^{n-k} a_t a_{t+k}}{\sum_{t=1}^{n} a_t^2}$$ and a_t were the residual series.

The Ljung–Box test is a type of statistical test of whether any of a group of autocorrelations of a series are different from zero (Griffith, 2003). Therefore, in this research instead of just testing randomness at each distinct lag, we also determined the "overall" randomness based on a number of lags (that is, a portmanteau test). A portmanteau test is a type of statistical hypothesis test in which the null hypothesis is well specified, but the alternative hypothesis is more loosely specified whereby tests constructed in this context can have the property of being at least moderately powerful against a wide range of departures from the null hypothesis (Cressie, 1993).

The extended, sample, autocorrelation, function method tentatively identified the orders of non-stationary ARMA process based on iterated least squares estimates of the autoregressive parameter estimators at each ArcGIS classified transmission zone at the study site. Given a stationary or non-stationary time series $\{z_t : 1 \le t \le n\}$ with mean corrected form $\tilde{z}_t = z_t - \mu_z$ with a true autoregressive order of $p+d$, a true moving-average order of q was estimated using the unknown orders $p+d$ and q by analyzing the autocorrelation functions associated with filtered series of the form:

$$w_t^{(m,j)} = \hat{\Phi}_{(m,j)}(B)\tilde{z}_t = \tilde{z}_t - \sum_{i=1}^{m}\hat{\phi}_i^{(m,j)}\tilde{z}_{t-i}$$

In this series B represented the backshift operator, where $m = p_{min},\ldots,p_{max}$ were the autoregressive test orders, where $j = q_{min}+1,\ldots,q_{max}+1$ represented the moving-average test orders, and where $\hat{\phi}_i^{(m,j)}$ were the optimized autoregressive parameter estimates under the assumption that the series was an ARMA (m,j) process. For purely predictive, autoregressive models $(j=0)$, OLS is used to consistently estimate $\hat{\phi}_i^{(m,0)}$ (Cressie, 1993).

In this research, consistent estimates from the ARMA models were obtained also by the iterated least squares recursion formula, which was initiated by the pure autoregressive estimates:

$$\hat{\phi}_i^{(m,j)} = \hat{\phi}_i^{(m+1,j-1)} - \hat{\phi}_{i-1}^{(m,j-1)}\frac{\hat{\phi}_{m+1}^{(m+1,j-1)}}{\hat{\phi}_m^{(m,j-1)}}$$

The jth lag of the sample autocorrelation function of the filtered series $w_t^{(m,j)}$ then extended the sample autocorrelation function, which in this research was denoted as $r_{j(m)} = r_j(w^{(m,j)})$ for each onchocerciasis, endemic transmission-oriented, risk-based, transmission zone. The standard errors of $r_{j(m)}$ were then computed in the usual way by using Bartlett's approximation of the variance based on the sample autocorrelation function:

$$var(r_{j(m)}) \approx (1 + \sum_{t=1}^{j-1} r_j^2(w^{(m,j)}))$$

The Barletts approximation calculates standard error with an approximation that was appropriate when the series represents a moving average process of order *k-1* (Hosmer et al., 2000). With this method, standard errors grew with increasing lags in the endemic, spatially, autoregressive model residuals. If the true model is an ARMA ($p+d,q$) process, the filtered series $w_t^{(m,j)}$ follows an MA (q) model for $j \ge q$ so that $r_{j(p+d)} \approx 0 \quad j > q$ and $r_{j(p+d)} \neq 0 \quad j = q$ (Tsay and Tiao, 1984). In this research, we showed that the extended sample autocorrelation from endemic, transmission-oriented, risk–based, epidemiological model satisfied $r_{j(m)} \approx 0 \quad j-q > m-p-d \le 0$ and $r_{j(m)} \neq c(m-p-d, j-q) \quad 0 \le j-q \le m-p-d$ when $c(m-p-d, j-q)$ was a non-zero constant or a continuous random variable bounded by –1 and 1.

An extended sample autocorrelation function (ESACF) table was then constructed by $r_{j(m)}$ for $m = p_{min},\ldots,p_{max}$ and $j = q_{min}+1,\ldots,q_{max}+1$ to identify the ARMA orders. The orders were tentatively identified by finding a right (that is, maximal) triangular pattern with vertices located at $(p+d,q)$ and $(p+d,q_{max})$ in which all elements were insignificant based on asymptotic normality of the autocorrelation function. The vertex $(p+d,q)$ thereafter identified the order associated with an ARMA (1,2) series.

The smallest canonical (SCAN) correlation method was then tentatively used to identify the orders of a stationary or non-stationary ARMA process in the endemic transmission-oriented model. We used simulation to study the efficacy of the modification for applying test statistics to analyze daily logSCAN for robust ARIMA

model selection in SAS/GIS. LogSCAN data can be applied to either non-transformed or differenced series (Tsay and Tiao, 1985). We then used the time series $\{z_t : 1 \le t \le n\}$ with mean corrected form $\tilde{z}_t = z_t - \mu_z$ with a true autoregressive order of $p+d$ employing a true moving-average order of q. We used the SCAN method to analyze eigenvalues of the correlation matrix of the ARMA process. Thus, for autoregressive test order $m = p_{min}, \ldots, p_{max}$ and for moving-average test order we had $j = q_{min}, \ldots, q_{max}$. We then let $Y_{m,t} = (\tilde{z}_t, \tilde{z}_{t-1}, \ldots, \tilde{z}_{t-m})'$. Then we computed the $(m+1) \times (m+1)$ matrix

$$\hat{\beta}(m, j+1) = \left(\sum_t Y_{m,t-j-1} Y'_{m,t-j-1}\right)^{-1} \left(\sum_t Y_{m,t-j-1} Y'_{m,t}\right) \left(\sum_t Y_{m,t} Y'_{m,t}\right)^{-1} \left(\sum_t Y_{m,t} Y'_{m,t-j-1}\right) = \hat{\beta}^*(m, j+1) \hat{A}^*(m, j) \hat{\beta}^*(m, j+1) \hat{\beta}(m, j+1)$$

Where t ranged from $j+m+2$ to n. We found the smallest eigenvalue was $\hat{\lambda}^*(m, j)$, of $\hat{A}^*(m, j)$ and its corresponding normalized eigenvector, $\Phi_{m,j} = (1, -\phi_1^{(m,j)}, -\phi_2^{(m,j)}, \ldots, -\phi_m^{(m,j)})$ in the model. The squared canonical correlation estimate was $\hat{\lambda}^*(m, j)$. Using the $\Phi_{m,j}$ as AR(m) coefficients, we obtained the residuals for $t = j+m+1$ to n, by using the formula:

$$w_t^{(m,j)} = \tilde{z}_t - \phi_1^{(m,j)} \tilde{z}_{t-1} - \phi_2^{(m,j)} \tilde{z}_{t-2} - \ldots - \phi_m^{(m,j)} \tilde{z}_{t-m}$$

From the sample autocorrelations of the residuals, $r_k(w)$, we approximated the standard error of the squared canonical correlation estimates using $var(\hat{\lambda}^*(m, j)^{1/2}) \approx d(m, j)/(n-m-j)$ which rendered $d(m, j) = (1 + 2\sum_{i=1}^{j-1} r_k(w^{(m,j)}))$. The test statistic we employed was an identification criterion which was $c(m, j) = -(n-m-j)\ln(1 - \hat{\lambda}^*(m, j)/d(m, j))$. This expression was asymptotically χ_1^2 if $m = p+d$ and $j \ge q$ or if $m \ge p+d$ and $j = q$ in the transmission-oriented, epidemiological, risk model. We noticed that in the residual for $m > p$ and $j < q$, there was more than one theoretical zero canonical correlation between $Y_{m,t}$ and $Y_{m,t-j-1}$. Since the $\hat{\lambda}^*(m, j)$ were the smallest canonical correlations for each (m, j), the percentiles of $c(m, j)$ were less than those of a χ_1^2; A SCAN table was then constructed using $c(m, j)$ to determine which of the $\hat{\lambda}^*(m, j)$ were significantly different from zero. The ARMA orders were then tentatively identified for the model by finding a pattern in which the $\hat{\lambda}^*(m, j)$ were insignificant for all test orders $m \ge p+d$ and $j \ge q$ which was then depicted in SAS/GIS l (Figure 9).

DISCUSSION

In this research we robustly quantitated the seasonal-sampled georeferenced endemic risk-based explanatory predictor covariate coefficients and their uncertainty indicators (for example, latent autocorrelated error coefficients) within an spatially dependent geographically weighted matrix in PROC ARIMA. By so doing, we attained fine-tuned unbiased versions of random-walk and random-trend model specifications. In our pre-whitening approach the autocovariate parameter error estimators were estimated and removed from the data and the model, and the GLM was re-fitted. We employed the pre-whitening method of Cochrane and Orcutt (1949) which in this research was performed in SAS/GIS assuming that the errors generated from the estimated predictive residual variance followed a first-order autoregressive process. Pre-whitening is a preconditioning technique for the correlation analysis method (Cressie, 1993).

In this research our pre-whitening involved applying a filter to the input signal *u*(*k*) and the output signal *y*(*k*) to obtain a pre-whitened input signal *u'*(*k*) and a pre-whitened output signal *y'*(*k*). After calculation of a GLM, the amount of serial correlation was successfully estimated using pairs of successive residual estimated values (for example, ET, $ET+_1$). In our model the filter was well designed such that *u'*(*k*) represented the white noise. By so doing, we also were able to successfully perform a correlation analysis on *u'*(*k*) and *y'*(*k*) to estimate the impulse response. The impulse response we estimated for the onchocerciasis, endemic, transmission-oriented risk model with *u'*(*k*) and *y'*(*k*) was equivalent to the impulse response estimate when the following equation remained true:

$$y'(k) = \sum_{n=0}^{\infty} u'(k-n) h(n) + e(k)$$

Therefore, in our predictive, autoregressive, spatiotemporal, arthropod-related risk model, *u*'(*k*) was white noise. We then selected "ARIMA" as the model type to evaluate the order of non-seasonal differencing, and to set all the AR and MA terms to zero. We noticed that the seasonal change-related, parameter estimators in our model had stationary noise, suggesting that the mean (that is, constant) forecasting estimator had to be applied to accurately quantitate seasonal differences in the onchocerciasis–related, spatiotemporal-sampled,

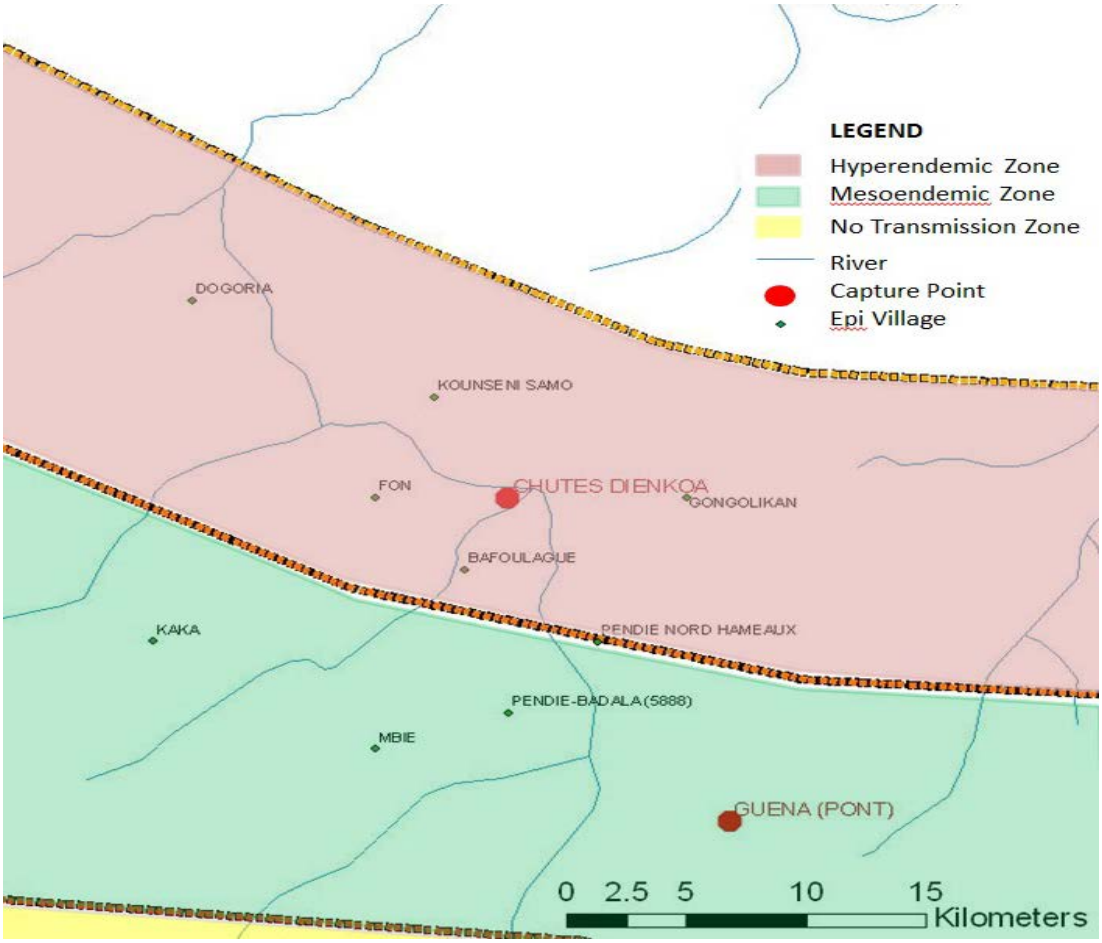

Figure 10. ARIMA predicted *S. damnosum s.l.*-related data feature attributes in riverine epidemiological study site.

epidemiological data. The ARIMA specifications then quantified geographically varying lags in the endemic risk-based distribution model employing the Euclidean-based distance measurements. The output revealed that the spatial data attribute features were positively spatially auto-correlated with each 5 km stratified geolocation.

Interestingly, the "mean" and the "constant" in risk-based distribution ARIMA model-fitting results were different numbers whenever the model included AR terms. Thus, in the future when fitting the ARIMA model to Y in which *p* is the number of autoregressive terms in an endemic, transmission-oriented, risk-based, onchocerciasis-related, distribution model, y can be used to denote the difference (that is, stationarized) version of Y- [for example, y(t) = Y(t)-Y(t-1)]. By so doing, only one non-seasonal difference would be required. Thereafter, the AR (p) forecasting equation for *y* in the model would be:

$$\hat{y}(t) = \mu + \phi_1 y(t-1) + \phi_2 y(t-2) + \ldots + \phi_p y(t-p)$$

Statistically speaking this equation would then be an ordinary multiple regression model where "mu" is the constant term, "phi-1" is the coefficient of the first lag of y, and so on. Thereafter, an infectious disease researcher or local program manager may be able to convert this slope-intercept form employing a predictive regression equation whose equivalent form represents in terms of deviations from the mean. Thus, by letting m denote the mean of the stationarized series y, a *p*-order autoregressive equation may be written in terms of deviations from the mean in their endemic transmission-oriented risk-based endmember, distribution model using the equation:

$$\hat{y}(t) - m = \phi_1 (y(t-1) - m) + \phi_2 (y(t-2) - m) + \ldots + \phi_p (y(t-p) - m)$$

Collecting all the constant terms in this equation would then allow identifying values rendered that are equivalent to the "mu" within a robust, onchocerciasis, endemic, transmission-oriented, predictive, regression-based, risk-based equation if:

$$\mu = m(1 - \phi_1 - \phi_2 - \ldots - \phi_p)$$

In this research we actually estimated "m" along with the other endemic, transmission-oriented, risk-based, distribution model *p* estimators and reported this as the mean in the model-fitting results, along with its standard error and *t*-statistic. Thereafter, a constant (that is, "mu") was calculated according to the preceding formula [that is, constant = mean *(1 **-** sum of AR coefficients]. If an ARIMA model does not contain any AR terms, the MEAN and the CONSTANT are identical (Cressie, 1993).

Thereafter, in our model the estimated predictive residual variance had one order of non-seasonal differencing only which was the mean trend factor (for example, average period-to-period change). Our final predictive, robust, spatiotemporal, autoregressive, arthropod-related, risk-based, epidemiological, distribution model had one order of seasonal differencing only and the mean was the annual trend factor (for example, average year-to-year change).

To accurately spatially forecast the appropriate dataset of spatiotemporal, onchocerciasis, endemic, transmission-oriented, risk-based ARIMA distribution model residuals, thereafter we employed lengthy, time-series, dependent, *S. damnosum s.l.,* georeferenced, feature attributes to identify and predict, endemic, transmission zones at the riverine study site. We identified the order(s) of differencing needed to stationarize the sampled data series. We then removed the gross features of seasonality from the sampled data. Differencing is an excellent way of transforming a non-stationary series to a stationary one (Cressie, 1993). In this research this differencing was facilitated in conjunction with a variance-stabilizing transformation which we constructed by deflating the seasonal-sampled, time series-dependent, observational, explanatory, predictorsin ArcGIS geospatial analyst.

In applied statistics, a variance-stabilizing transformation is a data transformation that is specifically chosen either to simplify considerations in graphical exploratory data analysis or to allow the application of simple regression-based or analysis of variance techniques (Everitt, 2002). The aim behind the choice of our variance-stabilizing transformation was to find a simple function *f* to apply to the sampled, endemic, onchocerciasis, transmission-oriented, covariate coefficient (that is, *x*) in the empirical, ecological, spatiotemporal-sampled, dataset to create new sampled values $y = f(x)$ such that the variability of the sampled values *y* was not related to their mean value. We knew the explanatory, covariate, coefficient values x in our risk-based model data realizations from the different calculated Poisson distributions we generated had different mean values (that is, μ). Further, we noticed that the variance in our model varied with the mean. Commonly, the Poisson distribution has a variance that is identical to the mean (Haight, 1967). Fortunately a simple variance-stabilizing transformation where $y = \sqrt{x}$ linearly rectified the sampling variance associated with the spatiotemporal-sampled, observational, predictor, explanatory estimates. The estimates were nearly constant. Our methods were similar to that of the Anscombe transform which proposed a form of the square root transform $z = 2\sqrt{x + 3/8}$ aimed at stabilizing the variance of the Poisson distribution to a value of approximately 1 with the transformed distribution being approximately normal especially for larger model mean values (for example, $m>20$) (Anscombe, 1948).

In our riverine-based, predictive, autoregressive, epidemiological, risk models we assumed a mean value of zero for forecasting the hyperendemic risk regions at the riverine epidemiological study site. Our auto-regressive, ARIMA, transmission-oriented, risk-based, time-series matrix contained monthly sampled feature attributes (for example, field-sampled larval habitat observational predictors), whose seasonal period was 12. The first difference of the seasonal difference at period *t* was then (Y(t) - Y(t-12)) - (Y(t-1) - Y(t-13). Applying the zero-mean forecasting model to this series yielded the equation: (Y(t) - Y(t-12)) - (Y(t-1) - Y(t-13)) = 0. Rearranging terms to put Y(t) by itself on the left, the equation then was Y(t) = Y(t-1) + Y(t-12) - Y(t-13) (10). For example, our spatiotemporal, onchocerciasis, endemic, transmission-oriented, risk-based data set we used September, 1987 to predict a seasonal, hyperendemic, *S. damnosum s.l.,* riverine–related, geolocational, transmission-oriented, explanatory predictor value of Y in October, 1987 by simply computing Y(Oct'1987) = Y(Sep'1987) + (Y(Oct'1986) - Y(Sep'1986) (11). In other words, October's hyperendemic transmission forecasts were equal to September's value plus the September-to-October regressed explanatory, observed, predictor, covariate, coefficient, indicator values from the previous sampled year in our model. Equivalently, equation 11 was rewritten as: Y(Oct'1987 = Y(Oct'1986) + (Y(Sep'1987) - Y(Sep'1986), therefore, the October's forecasts was equal to last October's sampled value plus the year-to-year change observed from the previous month. The preceding two equations then were mathematically identical; in actuality they were just rearranged terms on the right-hand-side.

Thereafter, a correlagram plotted the autocorrelation values in SAS/GIS for the time series at different lags (that is, "autocorrelation function"). The seasonal trend differences observed in a particular sampling period was the same or just a random step away from the trend that was observed from the previous sampling period in our model. Our ArcGIS-related forecasting risk model however revealed erroneous seasonal random trend model specifications. Even the most spatially accurate random walk or randomized, trend, seasonal, endemic,

Euclidean, distance-based, epidemiological model may contain undetected error residuals (for example, correlated disturbances) (Cressie, 1993). As such, we constructed a simple exponential smoothing model with a weighted moving average of past values to determine a predictive, regression-based, time series equation which was described as:

$$\hat{Y}(t) = Y(t-1) - \theta\, e(t-1)$$

where e (t-1) denoted the error at period t-1. The coefficient of the lagged forecast error was then written with a negative sign for reasons of mathematical symmetry while "Theta" in the predictive equation corresponded to the quantity "1-minus-alpha" in the exponential smoothing formulas. Note, our model resembled the predictive regressive-based equation for the ARIMA (1,1,0) model, except that instead of a multiple of the lagged difference the model included a multiple based on the lagged forecast error. Some non-stationary, time-series, dependent, non-seasonal, data feature attributes exhibit noisy fluctuations around a slowly-varying mean (Cressie, 1993). In other words, taking the most recent onchocerciasis–related, observation as the forecast of the next observation was better than using an average of the sampled observational predictors in order to filter out the noise for estimating a localized mean. Then theLjung–Box analyses tested whether any of a group of autocorrelations rendered from our time-series dependent data were different from zero. In this research the "portmanteau" test of Ljung-Box assessed the null hypothesis that a series of residuals exhibited no autocorrelation for a fixed number of lags *L*, against the alternative that some autocorrelation coefficient ρ (*k*), *k* = 1, ..., *L* was nonzero.

The test statistic was:

$$Q = T(T+2)\sum_{k=1}^{L}\left(\frac{\rho(k)^2}{(T-k)}\right),$$

where *T* was the sample size, *L* was the number of autocorrelation lags, and ρ (*k*) was the sample autocorrelation at lag *k*. Under the null, the asymptotic distribution of *Q* was the chi-square with *L* degrees of freedom. Instead of testing randomness at each distinct lag, our model effectively tested the overall randomness within a QuickBird-classified, Euclidean, distant-based, zone at the riverine study site based on a number of lags (that is, a portmanteau test). Values that equaled to 1 indicated rejection of the null of no autocorrelation in favor of the alternative. The qualitative observations from the eigen decomposition algorithm were then confirmed by the seasonal, random-walk, trend, model, dataset of residuals which revealed that seasonal hyeprendemic, stratified, epidemiological, prevalence rates and the ArcGIS derived Euclidean distance-based, algorithmic measurements were based on the 0 to 5 km transmission zone.

Thereafter, by letting y denote the differenced (that is, stationarized) version of Y in the autoregressive regression-based equation y(t) = Y(t)-Y(t-1), non-seasonal, differential variables were employed for targeting aggregations of prolific habitat locations (that is, hypernendemic area) based on spatiotemporal, field-sampled, count data. The AR(p) forecasting regression based, equation for y was $\hat{y}(t) = \mu + \phi_1 y(t-1) + \phi_2 y(t-2) + \ldots + \phi_p y(t-p)$. This was just an ordinary multiple, regression, risk model in which "mu" was the constant term, "phi-1" which was the coefficient of the first lag of y, and so on. Now, internally, the software (SAS/GIS) converted this slope-intercept form of the spatiotemporal, autoregressive, onchocerciasis, endemic, transmission-oriented, risk–based, predictive, regression equation to an equivalent form in terms of the model's deviations from the mean. Thereafter, by letting m denote the mean of the stationarized series y in the endemic, transmission-oriented, regression-based, model residuals, the *p*-order autoregressive, predictive, time series equation was re-written in terms of the deviations from the mean as:

$$\hat{y}(t) - m = \phi_1 (y(t-1) - m) + \phi_2 (y(t-2) - m) + \ldots + \phi_p (y(t-p) - m)$$

By collecting all the constant terms in this equation, the residuals were then determined to be equivalent to the "mu" form of the equation: [$\mu = m(1 - \phi_1 - \phi_2 - \ldots - \phi_p)$]

Conclusion

ArcGIS determined all distance-based measurements from the georeferenced *S. damnosum s.l*. riverine capture point using an Euclidean allocation algorithm. The algorithm rendered the direction from each cell to the closest georeferenced stratified village source. Poisson regression models prioritized the covariates at each demarcated ArcGIS-derived transmission zone. A spectral unmixing analyses then identified the spectral *S. damnosum s.l.,* habitat, canopy, endmember, sub-mixel components that encompassed illumination geometrical values reflected from the Precambrian rock and ripple water at the vertices of the simplex. The final endmember model output identified the correct fractional presence of each canopy-oriented, endmember, spectral, component, emitted from the georeferenced *S. damnosum s.l.,* habitat capture point and its associated Precambrian rock and rippled water. Thereafter, a kriged smoothed map displayed the spatial patterns of all productive *S. damnosum s.l.* habitats based on the endmember reference signature. By so doing, we were able to define the distance at which 95% of the sill was reached for the

asymptotic variogram model.

Multiple terms were caused by coefficient quantization, interpolation and linear-approximation error, respectively. The estimates where then analyzed with an eigenvector spatial filtering algorithm using a positive-definite covariance matrix in SAS/GIS® which removed the spatial covariate dependence by partitioning the original sampled endemic, transmission-oriented data feature attributes and into two synthetic variates: (1) a filter variate capturing latent spatial dependency and (2) a non-spatial variate that was free of spatial dependence. The space-time autocorrelation estimation actually involved two specifications: one casting a percentage at a sampled, prevalence, stratified, village, geographical location as a function of the preceding *in situ*, entomological-related, prevalence value as well as the preceding neighboring sampled villages values, a lagged specification; and the other casting a percentage at location as a function of the preceding *in situ* value as well as the contemporaneous neighboring values. The geographic distribution of the sampled explanatory co-variate coefficients based on the immature *S. damnosum s. l* counts exhibited positive spatial autocorrelation in all models tested: like larval counts aggregated in geographic space. After modeling the misspecification term explicitly, the remaining residuals become white noise. This allowed us to calibrate the autoregressive, endemic, transmission-oriented, landscape, risk-based models with the standard OLS estimation procedure which then revealed that the hyperendemic region was from 0 (georeferenced capture point) to 5 km from the capture point. This research demonstrated that the eigenvector spatial filtering approach can be embedded into a semi-parametric statistical framework for spatially targeting endemic onchocerciasis transmission zones.

ACKNOWLEDGEMENT

This work was produced by the US National Institute of Health/Fogarty International Center under Unnasch T.U. SR01TW008508.

Conflict of interest

The author declared he has no conflict of interest.

REFERENCES

Abramowitz M, Stegunl A (1972). *H*andbook of mathematical functions with formulas, graphs, *a*nd mathematical tables. 10th printing, with corrections. ed. United States National Bureau of Standards Applied mathematics series, Washington: U.S. Govt. Print. Off. xiv, 1046 p.

Burrough PA, McDonnell R (1998). Principles of geographical information systems. Spatial information systemsOxford ; New York: Oxford University Press.

Cochrane D, Orcutt GH (1949). Application of least squares regression to relationships containing auto-correlated error terms. J. Am. Stat. Assoc. 44:32-61.

Cressie NAC (1993). Statistics for spatial data. Wiley Series in probability and mathematical statistics Applied probability and statistics. New York: Wiley.

Goodchild MF (1980). *St*atistics in Geography - a Practical Approach - Ebdon, D. Geograp. l Anal.12:411-412.

Griffith DA (1996). *S*patial autocorrelation and eigenfunctions of the geographic weights matrix accompanying georeferenced data. Can. Geogr. 4:351-367.

Griffith DA (2000). Eigenfunction properties and approximations of selected incidence matrices employed in spatial analyses. Linear Algebra Appl. 321:95-112.

Griffith DA (2003). Spatial autocorrelation on spatial filtering Springer.

Griffith DA (2005). A comparison of six analytical disease mapping techniques as applied to West Nile Virus in the coterminous United States. Int. J. Health Geogr. 4:18-26..

Haight FA (1967). Handbook of the Poisson Distribution New York: John Wiley & Sons.

Jensen JR (2005). Introductory digital image processing a remote sensing perspective, 3rd ed. Upper Saddle River, N.J.: Prentice Hall.

Ross SM (2007). Introduction to probability models. 9th ed, Amsterdam, Boston: Academic Press.

Schowengerdt RA (2007). Remote sensing : models and methods for image processing, 3rd ed. Oxford: Academic Press.

Sondow J, Zudilin W (2006). *E*uler's constant, q-logarithms, and formulas of Ramanujan and Gosper. Ramanujan J. 12:225-244.

Strahler AH, Jupp DLB *(*1990). Modeling bidirectional reflectance of forests and woodlands using Boolean models and geometric optics. Remot. Sens. Environ. 34:153-166.

Tsay RS, Tiao GC (1984). Consistent estimates of autoregressive parameters and extended sample autocorrelation function for stationary and nonstationary ARMA models. J. Am. Stat. Assoc. 79:84-96.

Tsay RS, Tiao GC (1985). Use of Canonical-Analysis in Time-Series Model Identification. Biometrika 72:299-315.

Whittle P (1954). On Stationary Processes in the Plane. Biometrika 41:434-449.

academicJournals

Vol. 6(11), pp. 390-397, November 2014
DOI: 10.5897/JPHE2014.0631
ISSN 2006-9723
Article Number: 3994C6E47912

http://www.academicjournals.org/JPHE

Journal of Public Health and Epidemiology

Full Length Research Paper

Epidemiology of malaria among children aged 1 to 15 years in Southeast Nigeria

Oko N. F.[1], Odikamnoro O. O.[2], Uhuo C. A.[2]*, Okereke C. N.[2], Azi S. O.[3] and Ogiji E. D.[4]

[1]Department of Biological Sciences, Evangel University, Ebonyi State, Nigeria.
[2]Department of Applied Biology, Ebonyi State University, Abakaliki, Ebonyi State, Nigeria.
[3]Department of Medical Laboratory Sciences, Ebonyi State University, Abakaliki, Ebonyi State, Nigeria.
[4]Department of Pharmacology/Therapeutics, Faculty of Basic Medicine, Ebonyi State University, Nigeria.

Received 18 February, 2014; Accepted 9 September, 2014

An epidemiological survey was conducted on prevalence of malaria among children aged 1 to 15 years in south east Nigeria. A total of 498 children were surveyed for malaria and other morbidity indicators. Out of these, 369 which include 195 (52.8%) males and 174 (47.2%) females were from experimental household and 129, including 66 (51.2%) males and 63 (48.8%) females from control household. Before the deployment of Lambdacyhalothrin-treated household items - curtains, mats and blankets, the total malaria prevalence and all the morbidity indicators examined were ($p<0.05$) high among the sexes in both the experimental households and their control. By the end of the study, there was significant ($p<0.05$) decrease in malaria prevalence and all the associated morbidity indicators among the sexes in the experimental households. The total percentage prevalence decreased from 69.7 to 39.4%, 63.2 to 33.3% and 69.2 to 23.1% for males and 77.4 to 27.6%, 63.2 to 26.3% and 50 to 28.6% for female of ages 1 to 5, 6 to 10 and 11 to 15, respectively. The mean morbidity indicators dropped from 12.9 ≡ 13 to 1.9 ≡ 2; 9 to 0.6 ≡ 1 and 6.5 ≡ 7 to 0.6 ≡ 1 in sampled children of same age bracket but in the control households, they still remain on the increase ($p < 0.05$). The least malaria prevalence was 59.1% recorded among female infants and mean morbidity indicator which remained was 6.5 ≈ 7. The prevalence of malaria was comparable by sex and age and found to be statistically not significant $p > 0.05$.

Key words: Malaria, insecticide, lambdacyhalothrin, morbidity.

INTRODUCTION

Although the overall life expectancy is pointing upwards all over the world, the situation of malaria-related mortality remains a hidden global scourge. The most common cause of hospital admission in children and in all age groups continuously reducing the population globally (Molineaux, 1988). Malaria is a mosquito-borne infectious disease of human and other animals caused by a eukaryotic protist of the genus *Plasmodium*. It is endemic in tropical and sub tropical regions, including America, Asia and Africa. It is more prevalent in sub-Saharan Africa where 85 to 90% of malaria deaths occur (Layne, 2006). Some scientist believed that one in every two

*Corresponding author. E-mail: coscusanas@gmail.com. Tel: +2348032550134.

people who have ever lived has died of malaria (Michael, 2007). According to WHO (2005), malaria causes an estimate of 250 million cases of fever annually and other morbidity indicators (Beare et al., 2006). It further estimated that 655,000 people died of malaria in 2010 (WHO, 2010). Currently, the 2012 meta-study from the University of Washington and University of Queensland found this number of deaths in 2010 to be higher with 1,238,000 people (Global Malaria Mortality, 1980 to 2010; Christopher et al., 2012). Breman (2001) argued that the precise statistics are hardly known because many cases occur in rural areas where people do not have access to hospital or means to afford health care; as a result, the majority of cases are not documented.

Malaria is present in both rural and urban areas of the countries in Africa, though the risk is lower in urban cities (Keiser et al., 2004). Provost (2011) reported that by 2010, countries with the highest death rate per 100,000 populations are Coted'Ivoire with 86.15, Angola 56.93 and Burkina Faso 50.66 all in Africa. This is attributed to consistent temperature, high humidity, significant amount of rainfall, along with stagnant waters in which mosquitoes larvae readily mature, providing them with the environment they need for continuous breeding (Prothero, 1999) and thick vegetations which prevail in African countries.

Greenwood et al. (2005) state that majority of the cases were found in children less than five years old and pregnant women. Christopher et al. (2012) found out that 90% of malaria-related deaths occur in sub-Saharan Africa, with approximately 60% of deaths being young children under the age of five. In areas of high stable transmission of malaria, the incidence of clinical malaria peaks between one and five years of age.

Moreover, the increased speed at which strains of malaria parasite that are resistant to malaria drugs have developed especially in Africa makes the perspective even more difficult. The people of this area have been under serious dilemma concerning malaria disease. Among the strategies proposed to face this worrying situation, insecticide treated bed-net has been intensively functional (Sexton, 1994). Binka et al. (1996) also reported that the introduction of insecticide treated bed-net was associated with 17 to 33% reduction in all-case child mortality, respectively.

Other research trials using insecticide treated bed nets have demonstrated reduction in morbidity and mortality (Greenwood, 1987; Alonso et al., 1991; Nevill et al., 1996; Brieger et al., 1996, 1997). Lengeler (1998) reported that between 3.5 and 6.9% lives were saved per 1000 children protected with insecticide treated bed nets per year (based on four large scale trial in Africa). Nevertheless, due to some underlying reasons: (i) bed-net normally have very fine mesh netting (1.2 to 1.5 mm) which is sufficiently small to prevent passage of mosquitoes (Gahard, 2005). This also offer protection against a small sand flies and biting midges, but in hot climate, poor ventilation through fine mesh netting is a serious disadvantage (Gahard, 2005), it also makes sleep difficult due to heat; (ii) nets are too expensive in some areas (Winch et al., 1997); (iii) if several people especially children are sharing one net, this may result in overcrowding, part of their bodies may protrude under the net during the night (Gahard, 2005). For these reasons, people started having ill feelings about using them, hence the need for an alternative method to prevent resurgence of mosquito bites and subsequent increase in malaria infection.

This work is the result of a field survey in which lambdacyhalothrin treated curtains, mats and blankets were deployed inside living household in Oruku, Enugu State, and Eastern Nigeria as alternative strategy for malaria control. The aim is to determine an alternative to insecticide treated bed-nets using lambdacyhalothrin treated household items, including curtains mats and blankets in controlling mosquitoes'' bites and to find the effect on morbidity indicators among children in Oruku.

MATERIALS AND METHODS

Study area

This study was conducted in four out of the six villages of Oruku community, Ameke, Isienu, Obinagu and Eziobodo in Udi local government area all in Enugu State. The state is located on latitude 6.5000° N and longitude 7.5000° E and has a population of 722,664 according to the 2006 Nigerian census. The mean daily temperature is 26.7°C (80.1°F) and is at its highest between March and November. Enugu State is hot all year round. Rainy season and dry seasons are the only weather periods that recurs in the state. The average annual rainfall is around 2,000 mm. There is harmattan season between December and January. It has land mass, covered by bushes, streams, rivers, stagnant water and these are features that promote insects' breeding especially mosquito.

Sample selection and data collection

A total population of 498 children including 369 (195 males and 174 females) from experimental household and 129 (66 males and 63 females) from control household was sampled for malaria and other morbidity indicators. Different sampling methods were used in selection of samples. These include random sampling method and systematic sampling method (Ali, 1996).

Structured questionnaire was administered to the selected children and/or parents of infants in face to face encounters to get information on ages, sex, and frequency of occurrence of symptoms/signs. Some teachers and head teacher of Community Primary School Oruku were also interviewed to collect data on school absenteeism. All the sampled children were also tested for malaria prevalence using blood sample collected from their index fingers. The blood was collected on slide and taken to Parasitology Research Laboratory of University of Nigeria, Nsukka for possible malaria parasite and species identification using Giemsa and Leishman's stain and data documented for both experimental and control household. This was done three times monthly. After the first malaria prevalence test, lambdacyhalothrin treated household item curtains, mats and blanket, were deployed to experimental household as a malaria control strategy. The household items were treated such that a target dose of 75 cl of 0.001 mg/L or 0.025 mg/L concentrations of lambdacyhalothrin were absorbed by each of the

Table 1. Prevalence of malaria infection according to sex of sample children in both the experimental households and their control within the various villages before deployment of treated items in Oruku, Enugu State.

Village and sex	In experimental households						In control households					
	1-5		6-10		11-15		1-5		6-10		11-15	
	No. Exam	No. Infected (%)	No. Exam	No. Infected (%)	No. Exam	No. Infected (%)	No. Exam	No. Infected (%)	No. Exam	No. Infected (%)	No. Exam	No. Infected (%)
Ameke												
Male	30	21 (70)	18	15 (83.3)	15	9 (60)	9	5 (55.6)	7	4 (57.1)	4	3 (75)
Female	39	30 (76.9)	24	18 (75)	9	6 (66.7)	12	8 (66.7)	5	4 (80)	11	8 (72.7)
Isenu												
Male	24	15 (62.5)	12	6 (50)	9	6 (66.7)	7	6 (85.7)	2	2 (66.7)	3	2 (66.7)
Female	15	15 (100)	12	6 (50)	0	-	3	1 (33.3)	2	2 (66.7)	3	2 (66.7
Obinagu												
Male	12	12 (100)	9	6 (66.7)	9	6 (66.7)	7	5 (71.4)	5	2 (40)	2	1 (50)
Female	21	15 (71.4)	9	6 (66.7)	6	3 (50)	5	4 (80)	5	4 (80)	2	2 (100)
Eziobodo												
Male	33	21 (63.6)	18	9 (50)	6	6 (100)	10	8 (80)	6	4 ((66.7)	3	2 (66.7)
Female	18	12 (66.7)	12	6 (50)	9	3 (33.3)	5	2 (40)	5	3 (60)	4	3 (75)
Total												
Male	99	69 (69.7)	57	39 (68.4)	39	84 61.2)	33	24 (72.7)	21	14 (66.7)	12	8 (66.7)
Female	93	72 (77.4)	57	39 (68.4)	24	15 (62.5)	25	15 (60)	18	13 (72.2)	20	15 (75)

χ^2=203.59, df = 9, P > 0.05, χ^2 = 71.06, P > 0.05, df=9.

control items achieved.

Statistical analysis

Data collected were analyzed according to sex of the sampled children in both experimental households and their control. Data on malaria prevalence study from sampled male and female children in both experimental households and their controls were analyzed using chi-square (χ^2) statistic. Data on the effect of treatments with local mats, curtain and blankets treated with lambdacyhalothrin, on malaria prevalence were analyzed using analysis of variance (ANOVA). Differences between treatment and effect means were detected using the least significant difference (LSD) or protected LSD after a preliminary f-test (Obi, 2002).

RESULTS

Malaria prevalence study

Before control material deployment

The prevalence of malaria infection in Oruku was investigated among children in both the experimental households and their control. The study was based on the sex of children between the ages of 1 month to 15 years. It was done before and after the deployment of the lambdacyhalothrin treated materials.

Table 1 shows the result of the study prior to the deployment of the treated items according to the sex of the sampled children in both the experimental households and their control within the various villages. The table revealed that malaria prevalence varied among the sexes in both the experimental households and their

Table 2. Prevalence of malaria infection according to sex of sampled children in both the experimental households and their control within the various villages, by the end of the study in Oruku, Enugu State.

Village and sex	In experimental households						In control households					
	1-5		6-10		11-15		1-5		6-10		11-15	
	No. Exam	No. infected (%)	No. Exam	No. infected (%)	No. Exam	No. infected (%)	No. Exam	No. infected (%)	No. Exam	No. infected (%)	No. Exam	No infected (%)
Ameke												
Male	30	9 (30)	18	3 (16.7)	15	0 (0)	8	5 (62.5)	5	5 (100)	2	2 (100)
Female	33	3 (9.1)	24	6 (55)	6	3 (50)	10	6 (60)	6	4 (66.7)	3	3 (100)
Isenu												
Male	24	12 (50)	12	6 (50)	9	6 (66.7)	6	5 (83.3)	3	2 (66.7)	3	3 (100)
Female	15	6 (40)	12	3 (25)	0	0 (0)	3	1 (33.3)	3	3 (100)	3	2 (66.7)
Obinagu												
Male	12	0 (0)	9	0 (0)	9	0 (0)	6	6 (100)	4	2 (50)	2	1 (50)
Fem	21	6 (28.6)	9	0 (0)	6	0 (0)	4	4 (100)	5	4 (80)	2	2 (100)
Eziobodo												
Male	33	18 (54.5)	15	9 (60)	6	3 (50)	8	8 (100)	3	2 (66.7)	2	1 (50)
Female	18	9 (50)	12	6 (50)	9	3 (33.3)	5	2 (40)	4	2 (50)	2	2 (100)
Total												
Male	99	39 (39.4)	54	18 (33.3)	39	9 (23.1)	28	24 (85.7)	15	11 (73.3)	9	7 (77.8)
Female	87	24(27.6)	57	15 (26.3)	21	6 (28.6)	22	13 (59.1)	18	13 (72.2)	10	9 (90)

$\chi^2 = 195.34$, $P > 0.05$, df = 9, $\chi^2 = 53.14$, $P > 0.05$; df = 9.

control. In experimental households, a highest prevalence of 100% was recorded among both male and female infants of ages 1 to 5 years in Isienu and Obinagu villages, respectively. The same 100% prevalence was noted among elderly males (11 to 15 years) in Eziobodo village. The least prevalence among all the sexes was 33.3%. It was recorded among elderly females in Eziobodo village. In control households, a 100% prevalence was also recorded among elderly females (11 to 15 years). 33.3% prevalence was also the least prevalence observed among the sampled children in the control households. It was recorded for infant females in Isienu village.

However, a chi-square analysis of this data showed that sex was not significant in the distribution of malaria infection among children examined in Oruku ($\chi^2 = 203.59$, df = 9, $P > 0.05$) ($\chi^2 = 71.06$, df = 9, $P > 0.05$).

After control material deployment

By the end of the study, the impact of the treated household items based on the sex of sampled children showed that in the experimental households, total percentage prevalence for malaria was reduced from 69.7 to 39.4%, 63.2 to 33.3 and 69.2 to 23.1% for males and 77.4 to 27.6%, 63.2 to 26.3 and 50 to 28.6% for female of ages 1 to 5, 6 to 10 and 11 to 15, respectively. 0% (zero) prevalence was recorded for infant males (1 to 5 years) in Obinagu village and for both elderly males and females (11 to 15 years) in Ameke, Obinagu and Isienu villages, respectively (Table 2). While in the control households, the

Table 3. Effects of treatments on number of reports of symptoms/signs made by sampled children of ages 1-15 years, one and two months after the deployment of protective items in the experimental households in Oruku Enugu state.

Symptom/Sign	Age groups and cumulative number of reports or frequency of occurrence								
	1 – 5 years			6 – 10 years			11 – 15 years		
	Before (n/ns)	After 1 month (n/p)	After 2 months (n/p)	Before (n/ns)	After 1 month (n/p)	After 2 months (n/p)	Before (n/ns)	After 1 month (n/p)	After 2 Months (n/p)
Rashes/Itching	19/13.8	3/84.21	3/84.21	11/11.11	0/100	0/100	2/2. /82	0/100	0/100
Headache	10/7.04	0/100	0/100	36/36.36	3/91.67	0/100	40/57.14	8/80	3/92.5
Vomiting	6/4.23	1/83.33	1/83.33	0/0	0/0	0/0	0/0	0/0	0/0
Rigor	3/2.11	2/33.33	0/100	1/1.01	0/100	0/100	0/0	0/0	0/0
Fever	38/26.76	2/94.74	2/94.74	20/20.20	3.85	1/95	13/18.31	1/92.31	1/92.31
Cough	26/18.31	5/80.77	3/88.46	6/6.06	1/83.33	1/83.33	1/1.43	1/0	0/100
Dizziness	0/0	0/0	0/0	0/0	0/0	0/0	1/1.43	0/100	0/100
Stomach ache/Cramps	10/7.04	7/30	7/30	9/9.09	3/66.67	2/77.77	8/11.27	2/75	1/87.5
Catarrh	5/3.52	0/100	0/100	0/0	0/0	0/0	1/1.43	0/100	0/100
Loss of appetite	20/14.08	8/60	5/75	13/13.13	3/76.92	2/84.62	4/5.63	1/75	1/75
Weakness	5/3.52	0/100	0/100	3/3.09	0/0	0/0	1/1.43	0/100	0/100
Mean	12.9≈13	2.6≈3	1.9≈2	9	1.2≈1	0.6≈1	6.5≈7	1.2≈1	0.6≈1
Total	142			71			71		

LSD (P=0.05) for comparing two symptoms of malaria means=1.30; LSD (P=0.05) for comparing two symptoms of malaria means=1.299; LSD (P=0.05) for comparing two symptoms of malaria means=1.21; LSD (P=0.05) for comparing two treatment means = 0.682; LSD (P=0.05) for comparing two treatment means = 0.678. N= number of infection, P= percentage reduction calculated as ns-n, mean × 100, Ns= relative importance of symptom.

least prevalence was 33.3% recorded among infant females in Isienu village. Nevertheless, sex was still not significant in the distribution of infection and reduction in prevalence is accordingly (χ^2 = 195.34, p > 0.05, df = 9) (χ^2 = 53.14, P 0.05, df = 9).

Fever among other symptoms/signs

Table 3 shows the symptoms/signs and their frequency of occurrence reported by the sampled children in experimental households and effect of lambdacyhalothrin treated household items on this frequency of occurrence, one and two months after deployment of the treated items. It was observed that rashes/itching, fever, cough, stomach ache, and loss of appetite were the most frequent malaria symptoms among children within ages 1 to 5 years. The symptoms differed significantly (P = 0.05) from each other. On the other hand, the mean number of occurrence of these symptoms within one month, for children within this age group who had these symptoms and hence an indication of having malaria infection before deployment of lambdacyhalothrin treated household items, was approximately 13 times within one month compared to 3 and 2 times in one and two months after the deployment of protective items to the study households. There was statistically significant (P = 0.05) decrease in the number of occurrence from 13 times to 2, two months after, an indication that the treated items were effective. Calculating the relative importance of the symptoms/signs in the community, it was found that fever (26.76%) was the commonest and thus the most important symptom among children of ages 1 to 5 years, while rigor (2.11%) was the least common.

Also, it was noticed that headache, fever, loss of appetite and stomach-ache, were the most frequent malaria symptoms among children within ages 6 to 10 years (Table 3). They differed significantly (P = 0.05) from each other. The mean number of occurrence of these symptoms for

Table 4. Number of reports of symptoms/signs among children of ages 1 – 15 in control households throughout the period of malaria prevalence Study in Oruku Enugu state.

Symptom/Sign	Age groups and cumulative number of reports or frequency of occurrence											
	1 – 5 years				6 – 10 years				11 – 15 years			
	Before (n/ns)	After 1 Month (n/p)	After 2 months (n/p)	Mean	Before (n/ns)	After 1 Month (n/p)	After 2 months (n/p)	Mean	Before (n/ns)	After 1 month (n/p)	After 2 months (n/p)	Mean
Rashes/ itching	17	17	20	18	13	10	13	12	1	1	3	1.67
Headache	8	9	9	8.67	20	23	24	22.33	38	38	36	37.33
Vomiting	5	4	5	4.67	0	1	0	0.33	0	0	0	0
Rigor	5	7	7	6.33	0	0	1	0.33	0	1	0	0.33
Fever	31	30	29	30	18	20	19	19	15	18	17	16.67
Cough	20	18	21	19.27	12	7	10	9.67	3	2	2	2.33
Dizziness	0	0	0	0	0	0	0	0	0	0	0	0
Stomach ache/Cramps	15	14	13	14	7	6	6	6.33	5	4	4	4.33
Catarrh	4	3	3	3.33	1	0	0	0.33	0	0	0	0
Loss of appetite	17	16	18	17	14	11	11	12	5	6	6	5.67
Weakness	8	9	8	8.33	1	0	0	0.33	2	4	3	3
Mean	11.8≈12	11.6≈12	12.9≈13		7.8≈8	7.1≈7	7.6≈8		6.3≈6	6.7≈7	6.5≈7	

LSD (P=0.05) for comparing two symptoms of malaria means=0.24 LSD (P=0.05) for comparing two symptoms of malaria means=0.43 LSD (P=0.05) for comparing two symptoms of malaria means=0. Table 3 shows that the mean morbidity indicators dropped from 12.9≡13 to 1.9≡2; 9 to 0.6≡1 and 6.5≡7 to 0.6≡1 in sampled children whiten ages 1-5, 6-10 and 11-15 in the experimental households but in the control households, they still remain on the increase($p<0.05$).

children within this age group, who had these symptoms, hence an indication of having malaria infection before deployment of protective items was 9. However, one and two months after deployment of protective items, the mean number decreased to approximately one, which was a statistically significant (P = 0.05) decrease, indicating that the protective items were effective. When the relative importance of the symptoms/signs among children of this age group in the community was calculated, headache (36.36%) was found to be the most common and thus the most important symptom, while rigor (1.01%) was the least common.

For group 11 to 15 years (Table 3), headache and fever were observed to be the most frequent malaria symptoms. These two symptoms differed (P = 0.05) from others in their frequency of occurrence. It was also noticed that the mean number of occurrence of these symptoms for children within this age group before deployment of protective items was approximately 7. One and two months after the deployment of the protective items, the number statistically (P = 0.05) decreased to approximately 1. An indication that lambdacyhalothrin treated items were effective. This is because there was no reported case of self medication or health seeking movement by the sampled children, after the treated items were deployed. For the relative importance of the symptoms and signs among this age group in the community, headache (57.14%) was the commonest and thus the most important symptom while catarrh (1.43%) was the least common.

On the other hand, a different result was recorded in the control households. Table 4 shows the frequency of occurrence of fever and other symptoms at the start of this study and throughout the study period. It was observed from analysis of data, that the frequency of fever and other symptoms was statistically (P = 0.05) high at the start of this study. It further showed that these symptoms/signs remained on the increase throughout the period of the study. For ages 1 to 5, the mean number of occurrence of these symptoms/signs within one month, was 12 at the beginning of the experiment, but statistically increased to 13 (P = 0.05) by the end of the experiment. For ages 6 to 10 and 11 to 15, the mean number of occurrence at the beginning of the experiment were 6 and 8, respectively and by

Table 5. Summary table showing the impact of lambdacyhalothrin treated household item on malaria prevalence and other morbidity indicator among the sample children in both the experimental household, their control.

Malaria prevalence and other morbidity indicators	Pre deployment results		Post deployment results		Impact	
	Experimental households	Control households	Experimental households	Control households	Experimental households	Control households
Malaria prevalence (%)	68.3	67.4	30.25	75	<38.05	>7.66
Symptom and sign						
1 – 5 years	13	12	2	13	<11	>1
6 – 10 years	9	8	1	8	<8	>0
11 – 15 years	9	6	1	6	<6	>0

LSD (P=0.05) for comparing treatment means = 4.68%. χ^2 = 145.91, P>0.05, df = 14.

the end of the study, the number remained statistically (P = 0.05) at the same 6 and 8.

Table 5 shows that an impact of <38.05% was made in experimental households post deployment of lambdacyhalothrin-treated items, while in control households impact of 7.6% was made. The table also show the impact made on morbidity indicators among children in the experimental households as <11, <8, <6 for children within ages 1 to 5, 6 to 10 and 11 to 15. However, the opposite was noted in the control household. It was >1, >0 and >0 for children of same age group. These evidence indicated that lambdacyhalothrin-treated household items were effective.

DISCUSSION

The result of this study showed that household items including curtain, mat and blanket treated with 0.01 and 0.025 mg/L concentration of lambdacyhalothrin had significant effect on malaria prevalence, fever and other symptoms and signs of malaria among both male and female children of Oruku. Prevalence of 69.7, 63.2, and 69.2% for males and 77.4, 63.2 and 50% for female of ages 1 to 5, 6 to 10 and 11 to 15 indicated that malaria infection was highly endemic in Oruku community especially among children. And reduction in prevalence from 69.7 to 39.4%, 63.2 to 33.3 and 69.2 to23.1% for males and 77.4 to 27.6%, 63.2 to 26.3% and 50 to 28.6% for female of ages 1 to 5, 6 to 10 and 11 to 15, respectively (P < 0.05) is quite encouraging. It indicated that curtains, mats and blankets treated with lambdacyhalothrin were as efficacious as other insecticide treated materials.

Many researchers have demonstrated convincingly that the use of bed-nets and curtains treated with insecticide reduces morbidity from malaria substantially. Lengeler et al. (1998) reported that insecticide treated nets and curtains now provide residents of malaria endemic area (Gambia) with an effective means of protecting themselves against malaria.

Observation was made in this study of variation in prevalence rates both in the villages, among the age groups and within the individual households. This could be attributed to house location within the community and age of individual child. Despite the fact that anopheles mosquitoes can fly substantial distances, the distance between a village or house and a breeding site may be very important in determining malaria risk. In Pikine, a suburb of Senegal, Trape et al. (1992) showed that there was a steep gradient in the prevalence of malaria between the centre and the edge of town which is adjacent to marshy areas where breeding of anopheles mosquito take place. In this study, it was found that the risk of malaria was higher among those who live near the rivers (Ameke and Obinagu villages). Also malaria prevalence is naturally higher in children of lower age groups Eneanya, (1998). In Oruku, like most rural communities in the tropics, most houses are made of mud blocks, thatch roofed without ceilings. In the households where these mud walls are cracked, they form eaves which allowed easy access for mosquitoes inside sleeping rooms (Schofield and White, 1984). It was also observed that in some households, children are left under the care of either their grandparents or their sake “Ogbo” as they call it, who lacked the knowledge of basic hygiene and as a result dirty water that should be thrown away are left in cans, cups, buckets, pots and bowels within the compounds very near the houses and in some cases, even

within the households. These are breeding sites for mosquitoes. The researcher also observed from this study that the cumulative number of symptoms/signs among these sampled children seem to be proportionally small, compared with the degree of parasite positivity. This may be attributed to the level of immunity developed by these children as a result of constant attack of malaria infection. This is in line with the report of Gerhard (2005) who observed that in many parts of Africa where malaria infection has been endemic, people are infected so frequently that they develop a certain degree of immunity and in many cases they carry malaria parasites without showing any symptoms.

The inhabitants did not complain of any adverse reaction in the course of using the treated items. Manifestations of acute or residual poisoning were not found. It was clear therefore that curtain, mat and blanket treated with graded dose of lambdacyhalothrin, control mosquito bites and consequently malaria infection. And more importantly, is well tolerated by humans. Steps should therefore be taken by the government and donor agents to produce these treated items in large quantities, for they will go a long way in getting rid of mosquitoes and save the people of Oruku in particular and Africa in general from acute and chronic problems.

CONCLUSION AND RECOMMENDATION

This study concludes that the use of insecticide treated bed net, curtains and mats with lambdacyhalothrin can serve in controlling mosquito bite thus reducing malaria infection among the experimental area. Therefore, it is suggested that there should be public health awareness on the general use of lambdacyhalothrin by individual households, because of its long term sustainability to control of mosquito bite and non-acute or residual poisonous effect to services than other mosquito control measures.

ACKNOWLEDGEMENTS

The authors wish to appreciate in a special way the effort of Professor Okafor Fabian, the kind effort of Oruku community primary schools especially the head teachers and pupils of the school. The assistance of staff of Parasitology Unit of University of Nigeria Nsukka were also kindly appreciated.

Conflict of interest

The author declared he has no conflict of interest.

REFERENCES

Ali A (1996). Population and samples. Foundation of Research in Education. Merks publishers, Awka Anambra State P 320.

Alonso PL, Lindsay SW, Armstrong JRM, Conteeh M, Hill AG, David PH, Fegan G, Francisco A, Hall AJ, Shenton FC, Cham K, Greenwood BM (1991). Effect of insecticide treated bed-nets on mortality of Gambian children. Lancet 337:1499-1502.

Binka FN, Kubaye A, Adjuik M, Smith PG (1996). Impact of permethrin Impregnated bed-nets on child mortality in Kassena-Nankana District, Ghana: Randomized controlled trial. Trop. Med. Int. Health 1:147-154

Beare NA, Taylor TE, Harding SP, Lewallen S, Molyneux ME (2006). Malaria retinopathy: A New established diagnostic signs in severe malaria. Am. J. Trop. Med. Hyg. 75(5):790-7.

Breman J (2001). The ears of the hippopotamus: Manifestation, determinants and estimates of malaria burden. Am. J. Trop. Med. Hyg. 64(1-2):1-11.

Brieger (1996, 1997). Use of impregnated mosquito net for malaria control. Bulletin of World Health Organisation, pp 69-594.

Christopher JLM, Lisa CR, Stephen SL, Kathryn GA, Kyle JF, Diana H, Nancy F, Mohsen N, Rafael L, Alan DL (2012). Global malaria mortality between 1980 and 2010:a systematic analysis. Lancet 379(9814):413-431

Greenwood BM, Bojang K, Whitty CJ, Targett GA (2005). “Malaria”. Lancent 365(9469):1487-98

Keiser J, Utzinger J, Caldas M, Smith T, Tanner M, Singer B (2004). Urbanization in sub-Saharan and implication for malaria. Am. J. Trop. Med. Hyg. 71(2):118-27

Layne SP (2006). Principles of infectious disease epidemiology. Available at: http://health.mo.gov/training/epi/Mod1StudentOutline.pdf

Lengeler C (1998). Insecticide treated bed nets and curtains for malaria control Issue 3, Oxford Uk. Available at: http://www.thecochranelibrary.com/userfiles/ccoch/file/CD000363.pdf

Michael F (2007). Stopping a global killer: the rapidly spreading disease affects more people than before but until recently, the outcry has been muted. National Geographic Magazine.

Molineaux L (1988). The epidemiology of human malaria as an explanation of its distribution, including some implications for its control In W.H. Wemsdorfer and I.J.Mc. Churchill Livingstone Publishers, Uk pp. 913-998.

Nevill CG, Some ES, Mungala VO, Mutemi W, New L, Marsh K, Lengeler C, Snow RW (1996). Insecticide-treated bed nets reduce morbidity from malaria among children on the Kenyan coast. Am. J. trop. Med. Hyg. 1:139-146

Obi IU (2002). Statistical Methods of Declining Differences Between Treatment Means and Research Methodology Issues in Laboratory and Field Experiments. AP Express Publishers Ltd Nsukka, Nigeria xiii. pp 117.

Provost C (2011). World malaria day: Which countries are the hardest hit. The Gardian Retrieved 2012-05-03. Available at: http://www.theguardian.com/global-development/datablog/2011/apr/25/world-malaria-day-data

Prothero RM (1999). Forest and people in southeast Asia. Singapore J. Trop. Geog. 20(1):76-85.

Sexton JD (1994). Impregnated bed net for malaria control: biological success and social responsibility. Am. J. Trop. Med. Hyg. 50:72-81.

WHO (2005). Guidelines for laboratory and field testing of mosquito larvicides. World Health Organization Communicable Disease Control, Prevention and Eradication. WHO Pesticide Evaluation Scheme. HO/CDS/WHOPES/GCDPP/2005.13.

WHO (2010). Guidelines for the treatment of malaria (Report) (2nd ed) 978-9-2415-4792-5 Accessed May 11, 2012.

academicJournals

Vol. 6(11), pp. 398-406, November 2014
DOI: 10.5897/JPHE2014.0660
ISSN 2006-9723
Article Number: A80EE2047913

http://www.academicjournals.org/JPHE

Journal of Public Health and Epidemiology

Full Length Research Paper

Prevalence of malnutrition among preschool children (6-59 months) in Western Province, Kenya

Isaac Kisiangani[1]*, Charles Mbakaya[2], Anzelimo Makokha[1] and Dennis Magu[1]

[1]Institute of Tropical Medicine and Infectious Diseases, Jomo Kenyatta University of agriculture and Technology, Nairobi, Kenya,
[2]Kenya Medical Research Institute, Nairobi, Kenya

Received 20 June, 2014; Accepted 8 September, 2014

Malnutrition being one of the major public health problems in developing countries, it is still unacceptably high and progress to reduce it in most regions of the world is low. In Eastern Africa region, stunting and being underweight is estimated at 48 and 36% and are expected to increase over the next decade. There is limited information available on the prevalence of malnutrition in this area. This study determined nutritional status, and examined correlates of stunting among the children. This was a cross-sectional study undertaken among 125 preschoolers in western province, drawn from 37 clusters. For each cluster a total of 10 households were selected using systematic simple random sampling. Data were collected on nutritional status, socioeconomic status, food consumption and current malaria infection status. The prevalence of stunting (Z-scores for height for age [HAZ] <-2), wasting (Z-scores for weight for height [WHZ] < -2) and being underweight (Z-scores for weight for age [WAZ] < -2) was 28.9, 1.7 and 6.6%, respectively. Stunting was associated with poverty (OR=4.29, 95% CI: 1.06-17.36, p= 0.037) and lack of consumption of solid foods that include ripe mangoes, pawpaw and guavas (OR=3.15, 95% CI: 1.11-8.94, p=0.025), fish (OR=4.1, 95% CI: 1.15-14.61, p=0.021) and eggs (OR=4.42, 95% CI: 0.97-20.08, p=0.039). Child growth is a good indicator of nutritional status of both the individual and the community. The study demonstrates a high prevalence of stunting. Given the acute and long term consequences of malnutrition, interventions aimed at reducing child malnutrition in such a population should focus on all children less than 5 years of age.

Key words: Stunting, underweight, wasting, preschool children.

INTRODUCTION

Malnutrition is a public health problem which is still unacceptably high and progress to reduce it in most regions of the world is slow as shown in the fourth report on global nutrition (Administrative Committee on Coordination/Sub-Committee on Nutrition (ACC/SCN), 2000). In the year 2000, it was estimated that 182 million pre-school children which was one third of children less than five years old in developing countries were stunted and approximately 27% were estimated to be underweight (World health Organization (WHO), 1995).

*Corresponding author. E-mail: kisianganiisaac@gmail.com.

The overall trend in nutritional status in developing countries over the last 20 years is one of improvement, whereas Eastern Africa region (which includes Kenya) is the only region where the trend has been in the opposite direction. The prevalence of stunting and being underweight among pre-school children in this region are estimated at 48 and 36% and are expected to increase further over the next decade (ACC/SCN, 2000).

In Kenya, malnutrition is still a serious public health problem (United States Agency for International Development (USAID), 2006) and the situation has been worsening despite the numerous acitivities geared toward improving food and nutrition security. The Kenya Demographic Health Survey findings of 2008 showed that 35% of Kenyan children of under-five years of age were stunted which was an increase in the national stunting rates of children from 30% in 2003, with the highest prevalence between the ages of 18 to 35 months. At the sub-national level, western province recorded at 34.2% (Central Bureau of Statistics, 2009).

The main problems contributing to childhood malnutrition include inadequate household food security, inadequate care giving capacity, and an unhealthy environment predisposing young children to infections (MOH-GOK, 2006). Malnutrition has devastating effects on any population as it increases mortality and morbidity rates, diminishes the cognitive abilities of children and lowers their educational attainment, reduces labour productivity and reduces the quality of life of all affected (Wekesa et al., 2006). Children are more vulnerable to infection and their rapid rate of growth is easily affected by poor nutrition, hence their nutritional status measurements are a good indicator of overall community health (Ngugi and Nyariki, 2006).

The most commonly collected indicators of nutritional status are anthropometric measurements of children under five years of age. Children are more vulnerable to infection and their rapid rate of growth is easily affected by poor nutrition, thus measures of children's nutritional status are a good barometer of overall community health (Ngugi and Nyariki, 2006). The aim of this study was to determine the nutritional status, dietary patterns, socioeconomic and malaria infection of the children.

Methodology

Study site

This study was carried out in Western Province of Kenya, outside Nairobi, West of the Eastern Rift Valley and is inhabited mainly by the Luhya people. It harbours 3,358,776 inhabitants within an area of 8,361 km². The main economic activity is farming with maize as the staple food and some animal husbandry (a few heads of cattle and goats or chicken). Other activity includes quarrying for construction materials.

Study population

The study population consisted of preschool children aged between 6 and 59 months. The inclusion of the study subjects was based on consenting parents/guardians of children aged 6 to 59 months and without physical disability that would affect height measurement but those who had physical disability were excluded from the study.

Study design and sampling procedure

This study was a cross-sectional study that used a two-stage stratified cluster sample. The households were clustered using National Sample Survey and Evaluation Programme (NASSEP IV). The province was stratified into rural and urban enumeration areas (EAs). The first stage involved selection of primary sampling units (PSUs) which were the EAs using probability proportional to measure of size (PPMOS) method. The second stage involved the selection of households and EAs were selected with a basis of one measure of size (MOS) defined as the ultimate cluster with an average of 100 households and constituted of one (or more) EAs. The household and structure were listed through a quick count, amalgamation/segmentation of EAs to form clusters, physical numbering of the structure of the dwelling unit.

The sample was selected using a stratified two-stage cluster design consisting of 37 clusters, 18 in the urban and 19 in the rural areas. For each cluster a total of 10 households were selected using systematic simple random sampling.

Data collection

A structured and pretested questionnaire was used to record data. It captured demographic, socioeconomic, anthropometric measurements, knowledge and dietary intake on children aged 6 to 59 months.

Anthropometric measurements were recorded: height and weight were measured among children who were in light clothing to determine their nutritional status. The weight measurement was taken using a Seca scale (Hanson mode) to the nearest 0.1 kg and height/length portable wooden constructed scale calibrated for height measurement to the nearest 0.1 cm. Height for age (stunting), weight for age (underweight) and weight for height were calculated using ≤ 2D National Center for Health Statistics (NCHS) reference data. The height for age Z-score (HAZ) of <-2 was classified as stunted and Z-score cut off point of <-2 standard deviations (SD) was used to classify low weight for age, low height for age and low weight for height

Malaria rapid diagnostic kits (RDKs) were used at the household for malaria test using blood collected in EDTA tubes. The RDKs used were *Plasmodium falciparum* only (HRP2) to capture *P. falciparum* malaria. Thick blood smears was prepared, stained with Giemsa stain and allowed to dry and observed under a microscope using oil immersion objectives (×100). The presence or absence of malaria was reported as any parasitaemic detected in blood smear.

Dietary intakes of the study participants were assessed by means of food variety scores in the previous 24-h. Parents/Guardians were interviewed by a face-to-face method. They were asked to recall all foods and beverages they consumed by their children during the preceding 24-h. To assist subjects and their parents to recall accurately, household utensils were used.

Statistical analysis

The data was coded and double entered into a computer database using Ms-Access and Ms-Excel and analysis was performed using Statistical Package for Social Sciences (SPSS). In order to maintain the assumption of an equal probability sample, weighting was used to adjust for unequal cluster size due to variation in the number of absentees or refusals between clusters. Chi-square test was used

Table 1. Demographic, malaria status and socioeconomic characteristics of the study subjects.

Variable	n=125	%
Age in months		
6-11 months	5	4
12-23 months	18	14.4
24-35 months	37	29.6
36-47 months	36	28.8
48-59 months	29	23.2
Sex		
Male	72	57.6
Female	53	42.4
Residence		
Rural	82	65.6
Urban	43	34.4
Malaria status		
Positive	7	6.7
Negative	30	93.3
Not tested	2	
Main Material of the floor of the house		
Earth/Sand	36	28.8
Dung	54	43.2
Cement	35	28
Main Material of the roof of the house		
Grass/Thatch/Makuti/Dung /Mud	12	9.6
Corrugated iron (Mabati)	111	88.8
Asbestos sheet	2	1.6
Main material of the (inside) walls of the house		
Dirt/Mud/Dung	87	69.6
Bamboo with mud/ Stone with mud	4	3.2
Cement	30	24
Bricks	3	2.4
Cement blocks	1	0.8
Household ownership		
Clock/Watch	36	28.8
Electricity	13	10.4
Radio	97	77.6
Television	30	24
Mobile telephone	91	72.8
Fixed telephone	2	1.6
Refrigerator	7	5.6
Solar panel	4	3.2
Type of fuel used for cooking		
LPG/Natural gas	5	4
Charcoal	28	22.4

Table 1. Cont'd.

Wood	91	72.8
Other	1	0.8
Where cooking is usually done		
In the house	41	32.8
In a separate building.	78	62.4
Outdoors	6	4.8
Number of rooms used for sleeping		
One	57	45.6
Two	47	37.6
Three	16	12.8
Four	5	4
Wealth index		
First quintile	17	13.6
Second quintile	57	45.6
Third quintile	31	24.8
Fourth quintile	15	12
Fifth quintile	5	4

for the relationship between variables. The cut offs used to define stunting, wasting and underweight were those recommended by the World Health Organization, that is, less than two Z-scores were considered to be stunted, wasted and underweight. The relationship of various predictors, with stunting at the individual level was analysed by doing cross tabulations using the Chi-squared test for significance of associations and P-values <0.05 were considered statistically significant.

Ethical clearance

Ethical clearance was sought from scientific steering committee (SSC) and ethical review committee (ERC) of Kenya Medical Research Institute (KEMRI) for approval. Prior consent was sought from parents/guardians of the preschoolers who participated in the study. During the interview privacy and confidentiality was observed.

RESULTS

Characteristics of the study participants

A total of 125 preschoolers aged 6 to 59 months were enrolled in the study and consisted of males 72 (57.6%) and 53 (42.4%) females with a mean age of 35± (10 SD) ranging between 6 and 59 months. A high proportion (29.6%) was aged between 24 and 35 months. The majority (65.6%) of the participants resided in rural areas and a substantive proportion (34.4%) in urban areas. The wealth was defined by the type of house, roofing material and number of sleeping rooms. The study findings indicated that the main material of the (inside) walls of the house was mud (69.6%) and main house roofing materials was corrugated iron (88.8%). The commonly used source of energy for cooking was wood as reported by 72.8% of the participants. The other sources of energy for cooking were liquefied petroleum gas (LPG)/natural gas (4%), charcoal (22.4%) and others (0.8%). The prevalence of malaria among the preschool children was 6.7%. The economic status for each household was determined by means of a wealth index, which was a generic of all the social economic characteristics. Going by the wealth index scale, the bulk of the population (45.6%) were in the second quintile. The minority of the population were in the fifth quintile (4%) as shown in Table 1.

Consumption of solid foods in the previous 24 h by the children

A high proportion (59.2%) of the children consumed bread, rice, noodles or other food made from grains which are carbohydrates rich food sources than vitamin A rich and protein rich foods sources as shown in Table 2.

Nutritional status among children (6-59 months)

The results indicate high prevalence of stunting (height for age ≤ 2D, 28.9%) but wasting was low (weight for height Z-scores ≤ 2 SD, 1.7%) and being underweight (Z-scores for weight for age [WAZ] < -2) was 6.6%.

Table 2. Children consumption of solid foods in the previous 24 h.

Variable	n=125	%
Any brand of commercially fortified baby food for example, Cerelac	1	0.8
Bread, rice, noodles, or other food made from grains	74	59.2
Pumpkin, yellow yams, butternut, carrot, squash or sweet potatoes that are yellow or orange inside	27	21.6
Ripe mango, pawpaw, guavas	36	28.8
Any other fruits or vegetables	57	45.6
Liver, kidney, heart and other organ meats (offals)	6	4.8
Any meat such as beef, pork, lamb, goat, chicken or duck	23	18.4
Eggs	21	16.8
Fresh or dried fish, shell fish or other seafood	32	25.6
Any food made from beans, peas, lentils or nuts	58	46.4
Sour milk, cheese, yoghurt or other food made from milk	5	4.0
Any other solid, semisolid, or soft food	114	91.2

Bivariate analysis

The demographic characteristics were of age in months, sex and residence that were not significantly associated with stunting. Using children of aged 48 to 59 months as the reference, males in all the age groups were at a higher risk of stunting than females (34.7%, OR=2.29, 95% CI: 0.99-5.31, p=0.051). The risk of stunting decreased with age increase among the subjects, progressively lowering with each age group. Living either in a rural or urban set up had no effect with the children being stunted. There was no association between stunting and malaria infection. Using fourth/fifth quintiles as the reference for the relationship between stunting and socioeconomic characteristics, first quintile of the wealth index was significantly associated with stunting (OR=4.29, 95% CI: 1.06-17.36, p=0.037) as shown in Table 3.

The association between stunting and consumption of solid foods in the previous 24 h was analysed as presented in Table 4. Three of the seven foods were identified to be significantly associated with stunting. The foods include ripe mangoes, pawpaw and guavas (OR=3.15, 95% CI: 1.11 to 8.94, p=0.025), fresh/fried fish (OR=4.1, 95% CI: 1.15 to 14.61, p=0.021) and eggs (OR=4.42, 95% CI: 0.97 to 20.08, p=0.039). Children not consuming these three foods are likely to be stunted.

DISCUSSION

Stunting is usually an indication of long term deprivation of nutrients in children and it remains a problem of greater magnitude than underweight or wasting. The Kenyan children aged between 6 and 59 months from both urban and rural areas of intense malaria transmission in western province, 28.9, 6.6 and 1.7% of the children were stunted, underweight and wasted, respectively. The stunting finding concurs with those of the 2008 KDHS with the highest prevalence being between 18 and 35 months. According to the World Health Organization classification of prevalence ranges of stunting, this level is classified as high (WHO, 1995). This is a more accurate reflection of nutritional deficiencies and illness that occur during the critical periods for growth and development in early life (UNICEF, 2009). The study examined the various predictors of stunting among the children of 6 to 59 months.

Poverty is associated with inadequate food and poor sanitation and hygiene that lead to increased infections and stunting in children. There was a significant relationship between household wealth and stunting, with children from poorer households being more likely to suffer from stunting. This finding concurs with previous studies regarding wealth status of child's household and stunting (Christiaensen and Alderman, 2004; Girma and Genebo, 2002; Glewwe et al., 2002). This relationship could be explained by the fact that rich people are able to afford good living conditions that may improve the child's health including nutrition (Obeng, 2003). The efforts to reduce stunting depend on reducing poverty and raising peoples' living standards by improving the quality of homes, hygiene and sanitation. This has prompted UNICEF to come up with a social protection programmes focused on the most disadvantaged children helping them and their families by increasing the quality and quantity of food for children through cash or voucher transfer schemes, price subsidies and improving food storage for lean seasons and periods in crisis.

The increased risk of under-nutrition as children reach their second year in life may be due to interactive effects. During this period children are weaned from the breast and mothers do lose their ability to produce enough milk to meet the nutritional demand of a growing infant (Chavez et al., 2000). The child's age was found not a significant determinant of stunting. The finding differs with those of Ghana which showed that, stunting was high among children of this age. This situation has been

Table 3. Association between stunting and malaria status, demographic and socioeconomic characteristics.

Variable	Stunted (n=35)		Normal (n=90)		OR	95% CI		p value
	n	%	n	%		Lower	Upper	
Age in months								
6-11 months	3	60.00	2	40.00	5.75	0.78	42.58	0.065
12-23 months	8	44.40	10	55.60	3.07	0.84	11.17	0.083
24-35 months	11	29.80	26	70.20	1.62	0.52	5.08	0.404
36-47 months	7	19.40	29	80.60	0.93	0.27	3.13	0.902
48-59 months	6	20.70	23	79.30	REF	-	-	-
Sex								
Male	25	34.70	47	65.30	2.29	0.99	5.31	0.073
Female	10	18.90	43	81.10	REF	-	-	-
Residence								
Rural	19	23.20	63	76.80	0.53	0.22	1.28	0.156
Urban	16	37.20	27	62.80	REF	-	-	-
Malaria status								
Positive	3	42.90	4	57.10	1.7	0.36	8.07	0.5
Negative	30	30.60	68	69.40	REF	-	-	-
Not tested	2		18					
Wealth index								
1st quintile	10	58.80	**7**	41.20	4.29	1.06	17.36	**0.037**
2nd quintile	10	17.50	47	82.50	0.64	0.19	2.16	0.525
3rd quintile	10	32.30	21	67.70	1.43	0.4	5.04	0.579
4/5th quintile	5	25.00	15	75.00	REF	-	-	-

attributed to the fact that these children have already been introduced to complementary feeding (Ghana Statistical Service, 2009).

Micronutrients such as vitamins are obtained from consumption of fruits mostly seasonal. Foods containing vitamins A, C and E have shown to have protective effects on young children. Maize is a staple crop commonly grown and consumed by most children. Unfortunately, they lack important nutrients for child growth. The key risk factors for vitamin A deficiency are a diet low in sources of Vitamin A (that is, dairy products, eggs, fruits and vegetables). Findings from the current study, revealed a significant association between stunting and vitamin A food sources, that is, ripe mangoes, pawpaws, guavas and eggs, by comparing stunted and non-stunted children.

Presence of infection has a negative impact on utilization of nutrients. Certain types of parasities can cause anemia. Malnutrition increases one's susceptibility to and severity of infections and is thus the most important risk factor for illness and death in developing countries. Malaria has enormous impact on the quality of life and likelihood of survival in this vulnerable age group in malaria endemic areas. There is evidence to support that malaria plays part in decreased nutritional status. In this study, malaria outcome does not relate to low height for age z-scores, an indicator of achieved height and long term nutritional status. These findings concur with longitudinal study findings where it found that stunted children had a lower incidence of clinical malaria episodes than not stunted children (Genton et al., 1999). This findings contradict a longitudinal study in Gambia where stunting at the start of transmission season was associated with increased incidence of malaria (Deen et al., 2002).

Deficiency of proteins in diet is seen in stunted children and this deficiency might have a role in the retardation of growth in height (Ibrahim et al., 2002). This study finding shows an association between stunting and fish. Thus animal sourced foods are good sources of nutrients that are required for growth and also of micronutrients that support the immune system. This concurs with a study that was conducted by Dror and Allen (2011) reported that consuming animal sourced foods not only decreased stunting but also improved other anthropometric indices toward the reduction of morbidity and mortality of undernourished children. Educating parents and care-givers about the importance of improving child feeding

Table 4. Association between stunting and consumption of solid foods in the previous 24 h.

Variable	Stunted (n=35)		Normal (n=90)		OR	95% CI		p value
	n	%	n	%		Lower	Upper	
Bread, rice, noodles, or other food made from grains								
No	12	23.50	39	76.50	0.68	0.3	1.54	0.355
Yes	23	31.10	51	68.90	REF	-	-	-
Pumpkin, yellow yams, butternut, carrot, squash or sweet potatoes that are yellow or orange inside								
No	29	29.60	69	70.40	1.47	0.54	4.02	0.450
Yes	6	22.20	21	77.80	REF	-	-	-
Ripe mango, pawpaw, guavas								
No	30	28.30	59	71.70	3.15	1.11	8.94	0.025
Yes	5	13.90	31	86.10	REF	-	-	-
Any other fruits or vegetables								
No	20	29.40	48	70.60	1.17	0.53	2.56	0.701
Yes	15	26.30	42	73.70	REF			
Liver, kidney, heart and other organ meats (offal)								
No	34	28.60	85	71.40	2.00	0.23	17.76	0.526
Yes	1	16.70	5	83.30	REF	-	-	-
Any meat such as beef, pork, lamb, goat, chicken or duck								
No	29	28.40	73	71.60	1.13	0.4	3.14	0.821
Yes	6	26.10	17	73.90	REF	-	-	-
Eggs								
No	33	31.70	71	68.30	4.42	0.97	20.08	0.039
Yes	7	26.90	19	73.10	REF	-	-	-
Fresh or dried fish, shell fish or other seafood								
No	32	33.00	65	67.00	4.1	1.15	14.61	0.021
Yes	3	13.80	25	86.20	REF	-	-	-
Any food made from beans, peas, lentils or nuts								
No	18	26.90	49	73.10	0.89	0.41	1.94	0.762
Yes	17	29.30	41	70.70	REF	-	-	-

Table 4. Cont'd.

Sour milk, cheese, yoghurt or other food made from milk								
No	32	26.70	88	73.30	0.24	0.04	1.52	0.104
Yes	3	60.00	2	40.00	REF	-	-	-
Any other solid, semisolid, or soft food								
No	2	18.20	9	81.80	0.57	0.12	2.78	0.482
Yes	32	28.10	82	71.90	REF	-	-	-

feeding practices with diverse diet and animal sourced food is a critical public health intervention.

The nutrition surveys are prone to technical error of anthropometric measurements which could result in misclassification of the children's nutritional status. However, minimization of biases was addressed through appropriate study procedures, standardization of anthropometric measurements, appropriate training of researchers and close supervision of fields activities.

CONCLUSION AND RECOMMENDATION

The child growth and monitoring is a good indicator of nutritional status of both the individual and the community. The study demonstrated a high prevalence of stunting among the preschool children. Given the acute and long term consequences of malnutrition, interventions aimed at reducing child malnutrition in such a population should focus on all children less than 5 years of age. To improve the nutritional status of the children by improving their intake of vitamin A food sources and putting in place mechanisms to improve cost of living of the people in western province.

ACKNOWLEDGEMENTS

The authors wish to thank the Jomo Kenyatta University of Agriculture and Technology (JKUAT), Kenya Medical Research Institute (KEMRI), and all who participated in the study. My gratitude goes to Dr. Kombe for giving me the chance to undertake this research. The authors also thank Moses Mwangi for statistical advice and assistance.

Competing Interests

The authors declare no competing interests.

REFERENCES

ACC/SCN (2000). Fourth Report on the World Nutrition Situation. Geneva: ACC/SCN in collaboration with IFPRI.

Central Bureau of Statistics (Kenya) (2009). Ministry of Health (Kenya), ORC Macro: Kenya Demographic and Health Survey 2008. Calverton, MD: CBS, MOH and ORC Macro.

Chavez A, Martinez C, Soberanes B, (2000). The effect of malnutrition on human development: A 24-year study of well-nourished and malnourished children living in a poor Mexican village. In: Goodman A, Dufour D, Pelto G (eds), Nutritional Anthropology: Biocultural Perspectives on Food and Nutrition. Mayfield Publishing, San Francisco pp 234-68.

Christiaensen L, Alderman H (2004). Child malnutrition in Ethiopia: can maternal knowledge augment the role of income? Econ. Dev. Cult. Change 52(2):287-312.

Deen JL, Walraven GE, von Seidlein L (2002). Increased risk for malaria in chronically malnourished children under 5 years of age in rural Gambia. J. Trop. Pediatr. 48:78-83

Dror DK, Allen LH (2011). The importance of milk and other animal-source foods for children in low-income countries. Food Nutr. Bull. 6:227-243.

Genton B, Al-Yaman F, Ginny M, Taraika J, Alpers MP (1999). Relation of anthropometry to malaria morbidity and immunity in Papua New Guinean children. Am. J. Clin. Nutr. 68:734-741.

Ghana Statistical Service (GSS) (2009). Noguchi Memorial Institute for Medical Research (NMIMR), ICF Macro: Ghana Demographic and Health Survey 2008. Calverton, Maryland: GSS, NMIMR, and ORC Macro.

Girma W, Genebo T (2002). Determinants of nutritional status of women and children in Ethiopia. ORC Macro: Calverton, Maryland, USA.

Glewwe P, Koch S, Nguyen BL (2002). Child nutrition, economic growth, and the provision of healthcare services in Vietnam in the 1990s. World Bank Working Paper. Available at: http://elibrary.worldbank.org/doi/pdf/10.1596/1813-9450-2776.

Ibrahim SA, Abd el-Maksoud A, Nassar MF (2002). Nutritional stunting in Egypt: which nutrient is responsible? East Mediterr. Health J. 8:272-80.

MOH-GOK (2006). National guidelines for Diagnosis, treatment and prevention of Malaria for health workers in kenya.

Ngugi RK, Nyariki DM (2006). Rural livelihoods in the arid and semi-arid environments of Kenya: Sustainable alternatives and challenges. Agric. Hum. Value.22:65-71.

Obeng C (2003). Impart of childhood poverty on health and development. Healthy Gen. 4(1):1-12.

UNICEF (2009). Tracking progress on child and maternal nutrition, UNICEF, New York.

USAID (2006). Understanding nutrition data and the causes of malnutrition in Kenya. A special report by the Famine Early Warning Systems Network (FEWS NET).

Wekesa M, Karani I, Waruhiu S (2006). Emergency interventions in the arid and semi-aridareas of northern Kenya. Humanitarian Exchange Magazine. 35: November. Available at: http://www.odihpn.org/humanitarian-exchange-magazine/issue-35/emergency-interventions-in-the-arid-and-semi-arid-areas-of-northern-kenya.

WHO (1995). Physical Status: The Use of and Interpretation of Anthropometry. Geneva: World Health Organization.

academicJournals

Vol. 6(11), pp. 407-416, November 2014
DOI: 10.5897/JPHE2014.0643
ISSN 2006-9723
Article Number: 5E03E5D47916

http://www.academicjournals.org/JPHE

Journal of Public Health and Epidemiology

Full Length Research Paper

Evaluation of measles surveillance systems in Afghanistan-2010

Jawad Mofleh[1]* and Jamil Ansari[2]

[1] Associate Director for Science, Eastern Mediterranean Public Health Network, Amman, Jordan.
[2]Faculty Member, Field Epidemiology and Laboratory Training Program, National Institute of Health, Islamabad, Pakistan.

Received 24 April, 2014; Accepted 12 September, 2014

Measles is a leading cause of death among children under five years world-wide. In Afghanistan, measles claimed 35,000 lives in 2001. Despite reported measles vaccination coverage of 75%, the number of outbreaks was increasing in 2008. The systems involved in measles surveillance in Afghanistan include: Health Management Information System (HMIS), Disease Early Warning System (DEWS), and the Expanded Program on Immunization (EPI). These three systems were evaluated to identify their strengths and weaknesses and formulate recommendations. A qualitative study based on the CDC updated guidelines for evaluating public health surveillance systems was conducted. A detailed checklist was developed and used during the interview with the candidates to collect information about the system attributes. Data were collected from representatives of all mapped stakeholders through face-to-face interviews, telephone, and email. System attributes were assessed and scored for description and comparison on a Likert scale from 1 to 10. The average of scores was obtained to determine the overall ranking. World Health Organization (WHO) estimates for measles cases in the county (2008) was used to calculate sensitivity and predictive values. HMIS scored well for acceptability, cost effectiveness, representativeness, but had poor timeliness and flexibility. The sensitivity of EPI, HIMS and DEWS were 40, 34 and 20%, respectively and predictive value positive (PVP) of the system EPI, HMIS, DEWS were 69, 61 and 22%, respectively. EPI scored well for data quality, representativeness, and stability, but poorly in flexibility, timeliness and cost effectiveness. DEWS had good data quality, timeliness and flexibility, but weak stability. None of the systems has up to the mark attributes, and none of these systems can provide all necessary information to the health system alone. Systems are fragmented and serve different objectives. Lack of integration limits utilization of generated data for policy and planning. Measles surveillance through EPI should be strengthened and integrated with DEWS and HMIS to enhance cases detection and timely response.

Key words: Measles, measles surveillance evaluation, surveillance system, Afghanistan.

INTRODUCTION

Modern public health needs information to decide and act. Surveillance is the system which collects information for public health action. In other words, public health surveillance is the ongoing, systematic collection, analysis, interpretation, and dissemination of data regarding health-related event used to reduce morbidity

and mortality by improving public health (Centers for Disease Control and Prevention [CDC], 2001). Design, objectives, purpose, mode of operandi of each surveillance systems is different. Hence, to ensure quality of data provided by surveillance system, effectiveness, efficiency and usefulness of the surveillance system, should be evaluated periodically.

Measles is a highly contagious self-limiting viral disease (Okonko et al., 2009) that can lead to fatal complications. It is transmitted via droplets from the nose, mouth or throat of infected persons. Initial symptoms, which usually appear 8 to 12 days after infection, include high fever, runny nose, bloodshot eyes, and tiny white spots on the inside of the mouth. Several days later, a rash develops, starting on the face and upper neck and gradually spreading downwards (WHO Health Topics, 2014).

There is no specific treatment for measles (PubMed Health, 2012) and most people recover within 2 to 3 weeks. However, particularly in malnourished children and people with reduced immunity; measles can cause serious complications, including blindness, encephalitis, severe diarrhea, ear infection and pneumonia. Measles can be prevented by immunization (WHO Health Topics, 2014). Measles is a widespread killer, ranked number fifth in 2012. Globally, 139,300 deaths were reported due to measles only in 2012 (WHO Media Center, 2013). A highly effective vaccine has been available since the 1960s. Despite this, measles remains the leading cause of vaccine-preventable deaths in the world, accounting for over 40% of the 1.4 million annual deaths due to vaccine-preventable diseases (UNICEF-WHO, 2005).

The fourth Millennium Development Goal (MDG 4) is to reduce the under-five mortality rate by two-thirds between 1990 and 2015. As per World Health Organization, globally 344,276 reported cases of measles and 139,300 deaths were reported in 2010 (WHO Immunization Surveillance assessment and monitoring, 2012), which was equal to 430 deaths per day due to measles. However, numbers of deaths due to measles has significantly reduced but as per 2010 data 18 children are dying per hour from measles, a vaccine preventable disease (WHO Media Center, 2013). Number of deaths dropped by 74% since 2000, number of cases and deaths significantly decreased since the revolution of the vaccine discovery in 1960s. More than 95% of measles deaths occur in countries with low gross domestic product (GDP) and weak health systems (WHO Media Center, 2013). World Health Statistics (2012) report reads that only 65% of the countries reached measles vaccination coverage of equal or more than 90% (WHO Global Health Observatory (GHO), 2012).

Inequalities in access to vaccines within countries mean that death and disability from measles is concentrated primarily among the poorest, most marginalized and remote people. Failure to deliver at least one dose of measles vaccine to all infants remains the primary reason for high measles mortality.

Measles killed 30,000 to 35,000 of Afghan children annually till 2003 (MMWR, 2003; Gaafar et al., 2003); number of cases of measles reduced to 3,013 in 2011 (WHO RD Report, 2011), 2787 in 2012 (WHO Vaccine-Preventable Diseases: Monitoring System, 2013) and 1,822 deaths reported in 2008 (Black et al., 2010).

In order to reduce the number of measles cases, Ministry of Health Afghanistan with support of national and international partners conducted successive rounds of measles catch-up and follow-up immunization campaigns in the year 2001 to 2002 (for children of 6 months to 12 years old) and 2003 (for children of 9 months to 5 years old), in 2006 to 2007 (for children of 9 to 59 months) and in 2009 (for children of 9 to 36 months). Also in November 2012, WHO reported that a significant reduction in the number of cases of measles, after four months from vaccination of six million children aged 9 months to 10 years in Afghanistan (Measles and Rubella Initiatives, 2012).

Current data claims that still two percent of under five years children deaths are attributed to measles in Afghanistan, with a similar report of one percent at the regional and global level. The country has the third highest number of measles cases per hundred thousand population at the regional level, after Iraq and Qatar (WHO World Health Statistics, 2012a). Case fatality of measles in developing countries is between 3 and 5%, but in some localities it may reach 10 to 30% (Heyman, 2008).

A timely surveillance and rapid case detection for measles followed by rapid outbreak response is key for control and elimination of measles and reducing number of cases, complications and related mortality (WHO Position, 2009). Disease Early Warning System (DEWS) in Afghanistan, established in December 2006, detected 17 outbreaks of measles in 2007, 42 outbreaks of measles in 2008, 54 outbreaks of measles in 2009, 131 outbreaks of measles in 2010 (Ministry of Public Health Afghanistan, Diseases Early Warning System Annaul report, 2011, 2012), 147 outbreaks of measles in 2011 and 213 outbreaks of measles in 2012(Ministry of Public Health Afghanistan, Diseases Early Warning System Annaul Report 2012, 2013). DEWS data shows that the number of outbreaks of measles increased by more than100% from 2009 to 2010. Forty two per cent (N=190) of all outbreaks detected in 2009 were measles, and most of these outbreaks occurred in the provinces with high reported coverage of measles vaccination.

*Corresponding author. E-mail: jmofleh@yahoo.com. Tel: +962795826582.

Objectives

The objectives of this study were to conduct in depth review of the existing measles surveillance systems in Afghanistan; highlight the strengths and weaknesses of these surveillance systems; and provide constructive recommendations based on the findings for improvement of measles surveillance systems in Afghanistan.

METHODOLOGY

This is a qualitative study based on CDC's updated guidelines for Evaluating Public Health Surveillance Systems conducted (CDC, 2001). The guideline includes some main steps: engage the stakeholders in evaluation; describe the surveillance system to be evaluated; focus on the evaluation design; gather credible evidence regarding the performance of the surveillance system; justify and state conclusions and make recommendations; ensure the use of evaluation findings and share lessons learned.

The team has conducted mapping of all measles elimination partners at the country level. The team has met or communicate with the stakeholders individually/study subjects and the structured checklist was applied.

Field work of this evaluation started mid-November 2009 and was completed by the beginning of January 2010.

This evaluation was conducted at the national and provincial levels. Stakeholders for each of the surveillance systems were mapped and contacted.

Measles related documents, reports, policies and strategies of Ministry of Public Health (MOPH) and other stakeholders at the national, regional and global levels were reviewed.

The team located and found main stakeholders of measles surveillance system, contact information and addresses obtained and they were contacted through relevant means and channels. Major stakeholders of measles were: World Health Organization (WHO): Provide technical and financial support; United Nation's Children Fund (UNICEF): Provide financial support to measles immunization; Expanded Program on Immunization (EPI): Main planner and implementer of immunization activities and overall responsible/owner of measles surveillance activities at the national and provincial level; Disease Early Warning System (DEWS): Responsible for outbreak detection and response with the assistance of EPI and Control of Communicable Disease Department; Health Information Management System (HMIS); Policy and Planning Directorate of MOPH; Central Public Health Laboratory (CPHL); Non-Governmental Organizations (NGO): Implementers of basic package of health services and essential package of health services.

All measles reporting sites were located at the public health facilities and limited number of medical doctors-mainly paediatricians are working as AFP and measles focal point. Stakeholders were contacted and discussions were carried-out by telephone, email and also in-person.

Team ranked all attributes on a Likert scale of 1 to 10, while 1 to 5 were considered to be poor performance on that specific attribute, 6 to 7 fair and more than 7 considered as good performance. An average was obtained to see that the system is ranked higher.

Existing measles surveillance systems and description

At the time of study, there are three measles surveillance systems in the country: Health Management Information System (HMIS); Expanded Program for Immunization (EPI); and Disease Early Warning System (DEWS).

This information were sourced from registration book of health facilities; in addition to the fact that DEWS and EPI collect the case counts which are reported during outbreaks and develop line lists.

Health management information system is a passive surveillance system, with coverage of 82% designed to collect service information from health facilities throughout the country, the system is based in the Ministry of Health Facilities fully integrated in the health system of the country. Medical doctors at the outpatient department are responsible for tallying of the cases. Monthly aggregated report, along with other morbidities and mortality reports are shared with the provincial level. HMIS has provincial and regional offices which are linked to their central office. Monthly reports are transmitted from health facilities to district levels and from district level to provincial levels. Aggregated data is shared from provincial level to national level on quarterly basis which is analyzed and disseminated at the end of fourth month at the national level.

HMIS collected information are used at strategic level. The system has a direct support from Ministry of Health and Management Science for Health (MSH). Data flow charts of HMIS are as shown in Figure 1.

Expanded Program on Immunization's measles surveillance system is a case based active and passive surveillance system and they detect all cases and outbreaks. Their goal is to reduce the number of cases of measles to one case per million populations by 2015. This rate was 63 per million in 2011; the system is kept in EPI office in MOPH strongly supported by World Health Organization. Focal points at the health facility level notify the upper level as soon as the suspected case is recorded. Monthly aggregated report is shared with the EPI office at the provincial level, which will be transmitted to regional and national level during the coming month. Outbreak investigation and response is triggered based on the district data at the district level. Collected information were used at the strategic and operational levels. Figure 2 shows the data flow chart of the EPI Measles surveillance data.

Disease Early Warning System is a sentinel based surveillance system. The mixture of active and pass surveillance systems, established in 2006 had more than 200 sentinel sites at the time of the study. Their coverage was 10% of governmental health facilities at the time of the study. The system had full technical support of WHO and financial support of USAID. Measles is reported immediately by focal points and the focal points collect the blood specimen and send it to provincial level. Aggregated reports are shared with the provincial and regional level end of the week and national level produce the weekly report at the beginning of the coming week. Collected information were used at the strategic and operational levels. Figure 3 shows the data flow chart of DEWS.

RESULTS

System attributes

Simplicity

All systems use the registration book of the health facilities as the source of information; DEWS and EPI also use outbreak line-list for data collection. Registration at the health facility level takes very short time; records are not digital and retrieval of these records at the health facility level is very difficult. Aggregate reports are transmitted to the higher level monthly in HIMS and EPI surveillance systems and weekly in the DEWS. Health care workers provide the same aggregated data to

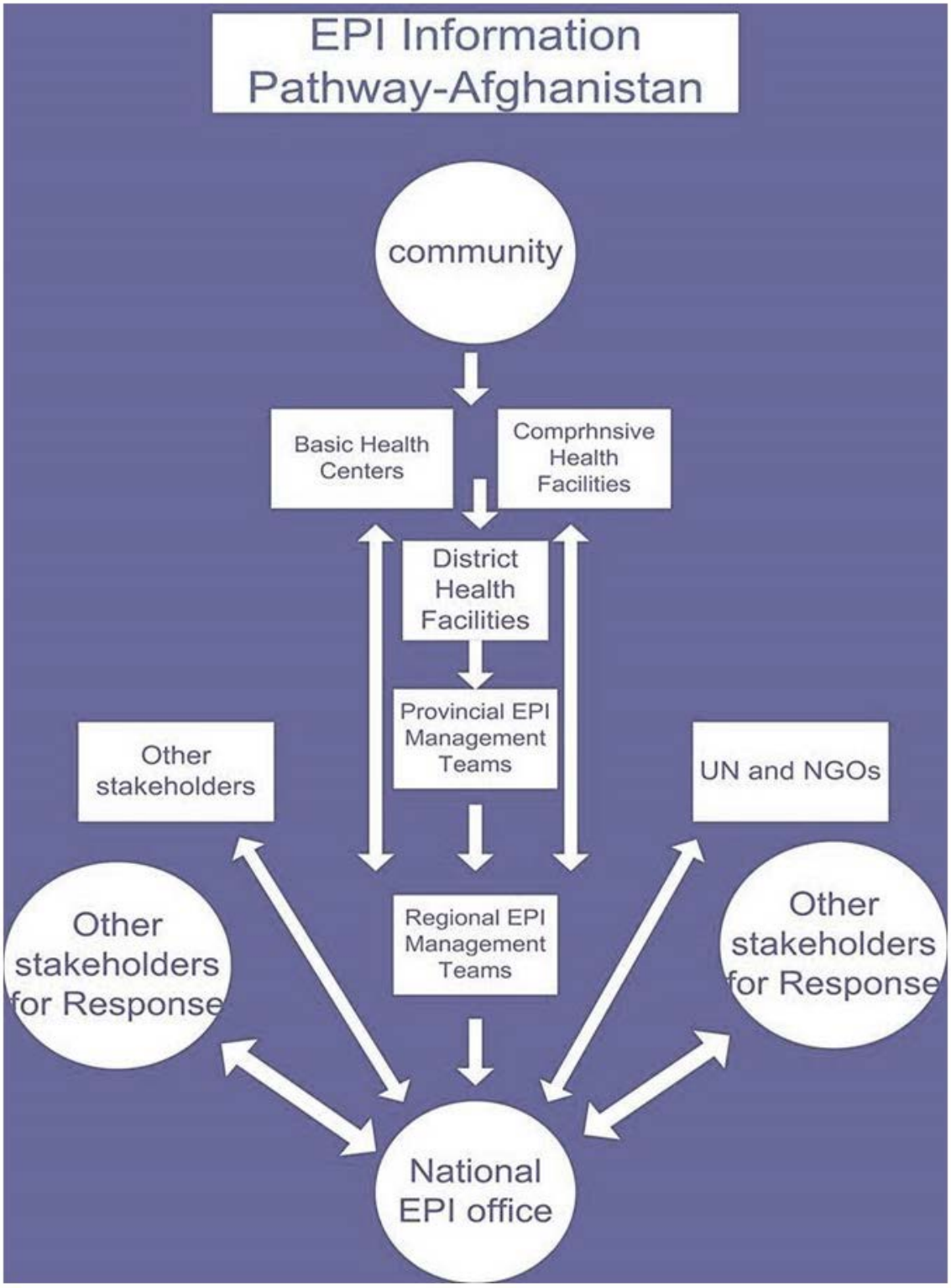

Figure 1. Flow chart of HMIS data.

different surveillance systems while EPI and DEWS use their focal points to collect blood specimens and arrange response at the health facility/district level.

1. Flexibility: HMIS and EPI surveillance systems are very rigid and needs at least six months to bring necessary changes and the DEWS takes a week.

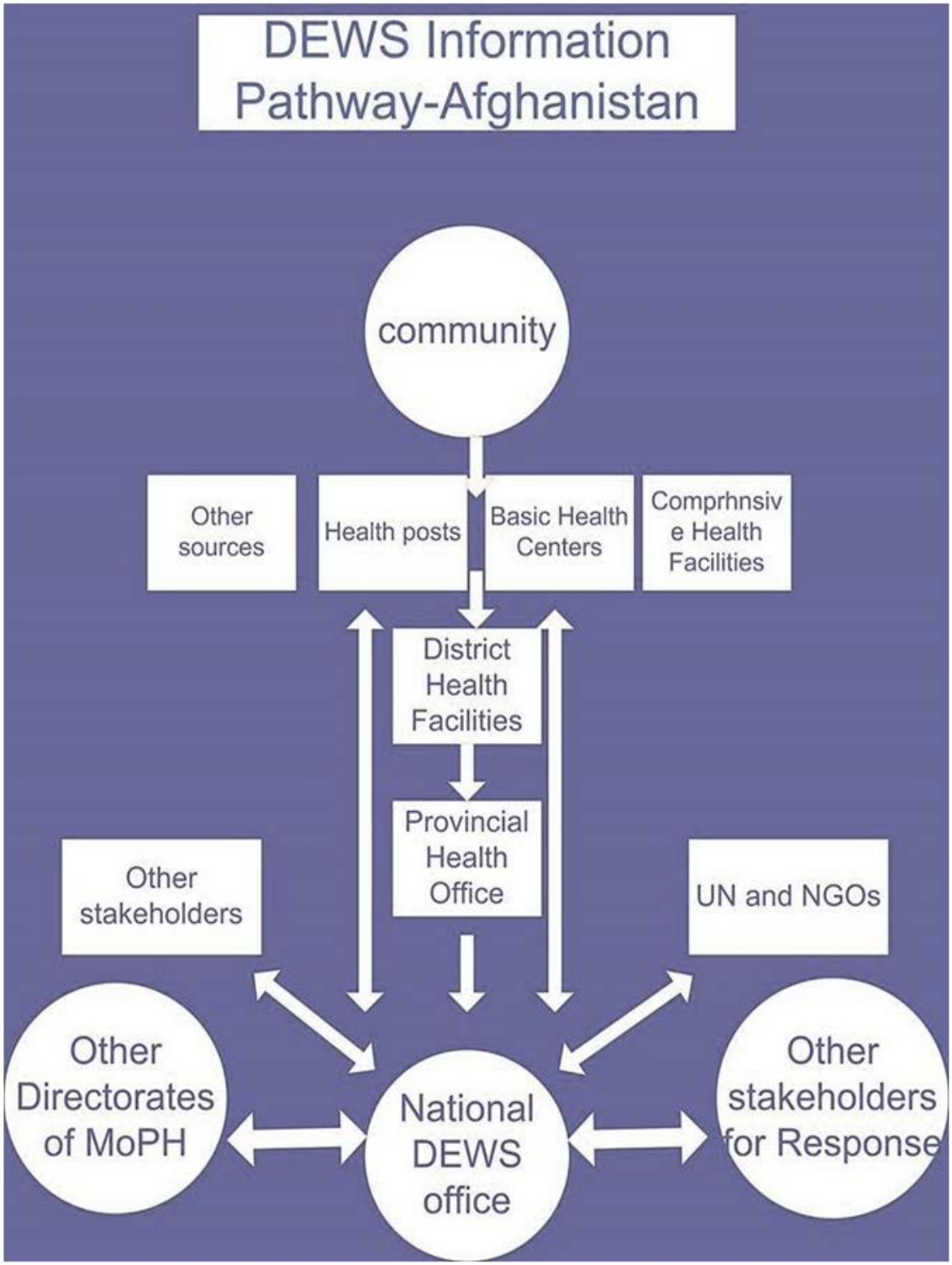

Figure 2. Flow chart of the EPI measles surveillance data.

2. Data quality: Completeness is 95% in HMIS and EPI systems and 97% in DEWS. EPI has a problem with denominator of their data, which is a national level issue. Reported values at the national and throughout the systems are matching with the provincial reported figures; use of case definition is the best throughout the systems

Figure 3. Data flow chart of DEWS.

data management starts from health care facility, forms are all readable and clearly charted and graphed at the health facility level. Hence, the data quality is very good throughout the systems.

3. Acceptability: All systems are well accepted in the government settings. Reporting to HMIS and EPI headquarters are official obligation; however, all system pays an extra incentive to the focal points, while DEWS pays the highest incentive.

4. Sensitivity: Measles surveillance systems in Afghanistan use the WHO standard case definition for measles, in which a clinical case is (A) any person with fever and maculopapular rash (that is, non vesicular), and cough, coryza (that is, runny nose) or conjunctivitis (that is, red eyes); or (B) any person in whom a clinical health worker suspects measles infection and a confirmed case of measles which is a WHO certified laboratory, confirmed the presence of measles specific IgM antibodies in the blood specimen of the case.

HIMS is not directly linked for central public health laboratory, while the other two are directly linked. As per available data in 2008, HMIS reported 13 cases of suspected measles against each laboratory confirmed case of measles, while this ratio reduced to 4.5:1 in 2009. DEWS and EPI are sharing the same source of information from health facilities and laboratory. DEWS is covering 10% of the total governmental health facilities at the national level and EPI measles surveillance is covering all government health facilities, while DEWS reported equal to 58% of the measles cases reported by

HMIS. DEWS reports measles cases recorded in the health facility and outbreak cases. In order to calculate the sensitivity, one needs the total expected number of cases as well. As this information is not available at the national level and the incidence and prevalence rates which are reported are based on the number of detected cases at the national level, the team used prevalence of measles in 2008 at the EMR region and also Nepal (outside the region) and standardized for rate. Afghanistan obtained calculations were cross checked using the standardized expected rate of measles in Afghanistan. The sensitivity of each system based on the available data is HMIS 20, DEWS 34 and EPI 40%.

(A) Sensitivity of EPI measles surveillance system: Sensitivity of the EPI measles surveillance system is calculated using the prescribed formula of the updated guideline for evaluation of surveillance systems which is A/A+C, where A is true positive cases and C is false negative cases and A+C is the total number of positive cases (true and false). EPI measles surveillance detected 1023, laboratory confirmed cases among a total 2524 cases so the sensitivity rate is calculated as:
Sensitivity (%)=1023/2524×100=40.
(B) Sensitivity of HMIS measles surveillance system: Sensitivity of the HMIS measles surveillance was calculate as per the aforementioned formula, where 1,023 confirmed measles cases reported amongst 5,232 suspected, probable and confirmed cases: Sensitivity (%)=1023/5232×100=20.
(C) Sensitivity of DEWS measles surveillance system, 2008 data: The same formula was applied, DEWS reported 1165 confirmed measles cases, 3380 were suspected, probable and confirmed in year 2008, so the sensitivity is SE (%)=1165/3380×100=34.

5. Predictive value positive (PVP): In 2008, HMIS reported 5232 suspected cases, DEWS detected 3380 suspected cases and EPI reported 2529 suspected cases of measles. 1165 specimens collected from routine EPI and outbreak investigation tested positive for measles in the same year.
In order to calculate the PVP, one needs the total expected number of cases at the national level, as this information is not available at the national level and the incidence and prevalence rates which are reported are based on the number of detected cases at the national level; the team used prevalence of measles in 2008 at the EMR region and also Nepal (outside the region) and standardized the rate for Afghanistan. The information obtained from this standardization was cross checked with expected rate of measles in Afghanistan. The PVP of EPI is 69%, DEWS is 61% and HMIS is 58%.

(A) PVP of EPI measles surveillance system is calculated as per the guideline. PVP is represented by A/(A+B), where A is true positive cases and B is false positive cases. In 2008, EPI report 1023 laboratory positive cases, where 1475 cases (suspected, probable and confirmed) were detected.
PVP (%) =1023/1475×100= 69

(B) PVP of HMIS measles surveillance system is calculated as PVP for the HMIS measles surveillance system as the aforementioned formula. Total number true for positive cases (Laboratory Confirmed Cases) reported in 2008 were, 1023 cases, over 1762 detected cases in the same year.
PVP (%)=1023/1762×100=58

(C) PVP of DEWS measles surveillance system is calculated as PVP of the DEWS measles surveillance calculated as per the prescribed formula of the guideline. The same detected 1165 were true for positive cases (Laboratory Confirmed Cases) in the year 2008 with over 1904 all detected cases (suspected, probable and Confirmed), so the PVP is 61%.
PVP =1165/1904×100= 61%

(D) Representativeness: HIMS covers 82% of all governmental health facilities at the time of study. Studies reveal that only 30% of all cases are consulted in the government health facility and the rest is absorbed by private health sector (Ministry of Public Health Afghanistan AHS, 2006, 2006). DEWS at the time of study covered around 10% of the total health facilities at the national level. Representativeness in terms of person and time cannot be calculated as the population for catchment area of each health facility is not available. While each type of health facility is established to serve certain number of population. Available health facilities that provide reports to HMIS office covers 82% of the population at the time of study, so it is estimated that 82% of population are covered under HMIS, while this coverage is 10% for DEWS.

(E) Timeliness: Source of routine data for all systems is registration book of health facilities. The data is collected on tally sheets from the clinics on daily basis. The collected information is compiled and then transferred to provincial level offices of each system. Frequency of this data transmission for DEWS and EPI is weekly and for the HMIS is at the end of each month. National office of DEWS received the information at the end of the week, EPI end of month and HMIS at the end of quarter. Timely transmission of reports to central level is 80% (total number of reports received divided by total number of expected reports multiplied by 100) in HMIS and almost 100% for DEWS and EPI.

(F) Stability: The most stable surveillance system for measles is HMIS. They enjoy being part of the organogram of ministry. The system receives regular funding from government of Afghanistan and also HMIS measles surveillance system receives external financial and technical support from USAID and MSH. EPI

Table 2. Ranking of surveillance attributes.

Attribute	HMIS	EPI	DEWS
Acceptability	9	8	8
cost effectiveness	8	6	7
Data quality	8	9	9
Flexibility	5	5	9
PVP	5	7	6
Representativeness	9	9	7
Sensitivity	5	8	7
Simplicity	6	8	8
Stability	8	9	5
Timeliness	3	5	9
Average	6.6	7.3	7.5

surveillance system is part of the organogram of the Ministry of Public Health. The system has enough financial and technical resources through WHO, GAVI and global fund, plus all necessary equipment and infrastructure to manage and run the system. DEWS is a newly established system, they were not part of MOPH organogram, while they have access to operating fund and infrastructure through WHO.

(G) Usefulness: HMIS is the only routine data collection system that provides information to MOPH and other stakeholders for long term planning evaluation of Basic Package of Health Services implementers' performance and to justify the requested fund for implementation of MOPH activities from donors. DEWS produce actionable information on a weekly basis. Good to mention that there is no clear demarcation between DEWS and EPI surveillance at the grass root level, all focal points and surveillance workers are working together to detect and respond to the cases and outbreaks of measles, so the use of information obtained is the same at the grass root level. Summary of surveillance comments are as shown in Table 1.

Conclusion

Health system management needs three types of information from surveillance systems, operational information, strategic information and tactical information, each category of information for different level of management. The three surveillance systems that were evaluated cannot produce all these information about measles at the same time; however, HMIS can provide strategic and tactical information for the mid to high level managers of MOPH. DEWS and EPI can provide operational or actionable information to the low to mid-level managers of MOPH.

When the purpose and objectives of each surveillance system were compared with the required attributes and their strengths, with the type of the data provided in short or long terms, the systems serve their purposes. HMIS as a system that tend to produce longer term data should have better attributes of data quality, acceptability, PVP, representativeness and stability. While EPI with an objective to detect all cases of measles should have superior attributes of sensitivity, PVP, acceptability and timeliness. The DEWS with an overall goal of outbreak detection should have better attributes of flexibility, timeliness, stability, sensitivity and PVP. HMIS is good in data quality, acceptability, representativeness and stability, while EPI is good in sensitivity and acceptability and DEWS is good in flexibility and timeliness. PVP is poor in HMIS and fair in EPI and DEWS systems. EPI is poor in timeliness and DEWS is poor in stability. Table 2 shows the surveillance components ranking.

As per available information and documents collaboration between these three measles, surveillance systems are very limited at the national level; however, DEWS and EPI are closely working together at the district and provincial levels, and for reverse cold chain they are using the same infrastructure. Also, level of collaboration between HMIS and National Public Health Laboratory (CPHL) is very low, while DEWS and EPI has a better collaboration with CPHL, which is mainly due to the need of outbreak detection and case based surveillance.

Main strength of the Measles Surveillance Systems (DEWS and EPI) is that they are designed to detect and respond to the outbreak. They are using the same platform for outbreak detection and response, and these surveillance systems are linked with action, meaning investigation and response to the outbreaks. There are some functional integrations at the district level and the terms and responsibilities of each system is clear, while there are some functional overlaps at the national level and two different units are handling the same issues. Also both surveillance systems have an active surveillance component, while working separately as per the organogram and policies of the Ministry of Public Health; this increases the cost of the outbreak investigation and increase the time of response coordination.

These three surveillance systems for measles are working on three different objectives and report to three different general directorates, while the overall objective or goal of the program for ministry and people of Afghanistan is the same, measles elimination.

Data management and data integration between these three systems were almost not performed, which causes differences in the level of measles vaccination coverage, number of cases and outbreaks.

Measles is a notifiable disease under HMIS; health care workers should report the disease to Ministry of Health in the first 48 h after detection. Most of the health care workers do not have a direct link with the ministry of public health and they are following the usual chain of communication to notify relevant unit of ministry of health;

Table 1. Summary of surveillance components.

Component	HMIS	DEWS	EPI
Population under surveillance	82% of all health facilities, which cover 82% of population of Afghanistan	10% of the health facilities	Coverage is at the level of HMIS because all sites based in the government health facilities
Time period of data collection	Quarterly	Weekly	Monthly
Data collection	Count	Count and line list	Counts and line list
Reporting source of data	Registration book of health facilities	Registration book of health facilities and outbreak line list	Registration books of health facilities
Data management	Health facilities, provincial, national	Health facilities, provincial, national	Health facilities, Provincial, National
Data analysis	Health facilities, provincial, national	Health facilities, provincial, national	Health facilities, Provincial, National
Information dissemination	National	Health facilities, provincial, national	Provincial
Patient privacy, data confidentiality	Patient names and other personal identifiers remain in the registration book of health facilities and the counts are shared with the concerned people.	Detailed information kept in database, identifiers not shared except team for treatment of cases	-
Compliance with record management system	NA	NA	NA

which is time consuming. Sometimes, health care professionals use their mobiles to contact people at the central level or they forward the information to the provincial health directorate and from there they send the information to ministry of health through Radio CODAN System, which is a wireless radio system. Hence, this is a lengthy process. Also HMIS is not directly linked with the national laboratory to obtain information about result of the specimens collected by other systems and they are not collecting information about the confirmed cases of measles.

Sensitive case definition for the suspected cases used in surveillance system, causes a wide range of PVP among surveillance systems.

All of the HMIS reporting sites are government health facilities; also the same is right in case of EPI and DEWS surveillance systems. So these systems do not capture number of measles cases that are recorded in the private health sector. Studies revealed that only 30% of all the cases are absorbed in the public health sector and the rest are taken care of by providing the health sector.

Based on these findings, the evaluation team recommended the following point:

(1) Measles surveillance cell: Establish or assign one coordinating office, owner for the measles surveillance systems at the national level. This unit should compile all the relevant data, reconcile with those relevant and share with all stakeholders. Finally, this unit should transcribe the data into actionable information and make sure the information is pushed through to decision makers.

(2) Functional integration: These surveillance systems should work much closer with each other at the national and provincial levels. Ministry of health should develop an operational platform for all of these surveillance activities which can be strongly linked with confirmatory entities and also build the capacity for investigation and response to outbreaks of measles. Functional integration of these systems will reduce the cost of these surveillance systems by distribution of task, information dissemination throughout the systems and all levels, increase data quality, timeliness of information and provide stronger tool for decision makers at all levels on the other functional integration will increase their chance for sustainability and reduce the chance for fragmentation.

(3) Central database e-reporting system: Establish a central database or e-reporting for measles case that let the health care providers and surveillance officers to obtain information about suspected, probable and confirmed cases of measles, can facilitate information sharing horizontally and vertically.

(4) Ministry of health should include private sector in the health information management systems of the ministry; as a major part of information is not

coming to ministry of health.

Limitation

Priority of the stakeholders for other diseases and outbreaks, such as H1N1, this study was conducted at the time that H1N1/2009 was the first priority to the country.

ACKNOWLEDGEMENT

The authors acknowledge the time and efforts of all individuals and entities that assisted to conduct this study and prepare this paper.

REFERENCES

Gaafar T, Moshni E, Lievano F (2003). The Challenge of Achieving Measles Elimination in the Eastern Mediterranean Region by 2010. *187*(Supplement I):164-71. Retrieved November 28, 2012

Okonko I, Nkang A, Udeze A (2009, August). Review Global Eradication of Measles: A highly contagious and vaccine preventable disease-What went wrong in Africa? J. Cell Animal Biol. *3*(8), 119-140.

Black R, Cousens S, Johnson H (2010, May 12). Global, regional, and national causes of child mortality in. online. Retrieved 2013, from http://www.who.int/immunization_monitoring/diseases/Lancet_2010_withAppendix.pdf

CDC (2001). *Mortality and Morbidity Weekly Report.* CDC. Atlanta: Centers for Disease Control and Prevention (CDC). Retrieved 2012

Heyman D (2008). *Control of Communicable Disease Manual* (19th ed.). (D. Heymman, Ed.) APHA press.

Ministry of Public Health Afghanistan. (2006). *Afghanistan Health Survey.* Kabul Afghanistan: Ministry of Public Health. Retrieved 2012, from http://www.independentadvocate.org/downloads/afghanistan-health-survey-2006.pdf

Ministry of Public Health Afghanistan. (2012). *Diseases Early Warning System Annaul report 2011.* Ministry of Health Afghanistan. Retrieved July 09, 2013, from http://moph.gov.af/Content/Media/Documents/DEWSAnnualReport2011181201314522879553325325.pdf

Ministry of Public Health Afghanistan. (2013). *Diseases Early Warning System Annaul Report 2012.* Ministry of Health Afghanistan. Retrieved July 9, 2013, from http://moph.gov.af/Content/Media/Documents/AR_2012_FinaldraftFORPRINT306201310244669553325325.pdf

MMWR (2003). *Nationwide Measles vaccination campaign for children 6month-12 years Afghansitan 2002.* CDC. Atalnta: CDC. Retrieved 2012, from http://www.cdc.gov/mmwr/preview/mmwrhtml/mm5216a3.htm

PubMed Health (2012, August 1). *PubMed Health Measles*. Retrieved 2012, from Measles: http://www.ncbi.nlm.nih.gov/pubmedhealth/PMH0002536/

UNICEF-WHO. (2005). *WHO-Immunization.* Retrieved 2012, from Immunization_ WHO/UNICEF Joint statement-Global Plan for reducing Measles Mortality 2006-2010: http://www.who.int/immunization_delivery/adc/measles/Measles%20Global%20Plan_Eng.pdf

WHO (2009). *Position Paper.* WHO. Geneva: WHO. Retrieved 2013, from http://www.who.int/wer/2009/wer8435.pdf

WHO (2011). *RD Report.* Cairo Egypt: WHO, EMR. Retrieved April 2013, from http://applications.emro.who.int/docs/rd_annual_report_2011_country_statistics_en_14587.pdf

WHO (2012, June 13). *Global Health Observatory (GHO)*. (WHO) Retrieved 2012, from Global Health Statistics: http://www.who.int/gho/publications/world_health_statistics/2012/en/

WHO (2012, October 16). *Immunization surveillance, assessment and monitoring*. (WHO) Retrieved 2012, from Measles: http://www.who.int/immunization_monitoring/diseases/measles/en/index.html

WHO (2012). *World Health Statistics.* World Health Organization. Retrieved July 11, 2013

WHO (2013, February). *Media Center*. (WHO) Retrieved 2013, from Factsheet 286: http://www.who.int/mediacentre/factsheets/fs286/en/

WHO (2013, May 27). *Vaccine-preventable diseases: monitoring system*. (World Health Organization) Retrieved July 9, 2013, from World Health Organization: Immunization surveillance, assessment and monitoring: http://apps.who.int/immunization_monitoring/globalsummary/incidences?c=AFG

WHO (2014). *Health topics*. (WHO) Retrieved 2012, from Health Topics-Measles: http://www.who.int/topics/measles/en/

Journal of Public Health and Epidemiology

Related Journals Published by Academic Journals

Journal of Diabetes and Endocrinology
Journal of Medical Genetics and Genomics
Journal of Medical Laboratory and Diagnosis
Journal of Physiology and Pathophysiology
Medical Practice and Reviews
Research in Pharmaceutical Biotechnology

academicJournals